MECHANISMS OF PATHOLOGY IN CHAGAS DISEASE PROGRESSION

A DISSERTATION
SUBMITTED ON 3/24/2023
TO THE DEPARTMENT OF TROPICAL MEDICINE
IN FULFILLMENT OF THE REQUIREMENTS OF THE SCHOOL OF PUBLIC HEALTH AND TROPICAL MEDICINE
OF TULANE UNIVERSITY
FOR THE DEGREE
OF
DOCTOR OF PHILOSOPHY
BY

Hans G Desale **APPROVED:**

Eric Dumonteil, PhD (chair) **Date**

Claudia Herrera 4/12/2023

Claudia Herrera, PhD **Date**

Pierre Buekens

Digitally signed by Pierre Buekens
Date: 2023.04.13 12:16:07 -05'00'

Pierre Buekens, PhD **Date**

I. Table of Contents

II. Figures and Tables

Figures

Tables

III. Dissertation Abstract

Chagas disease is a neglected tropical disease with an estimated annual burden of $627.46 million in health-care costs and 806,170 DALYs[2], which at its worst, symptomology manifests as organomegaly or cardiomyopathy. Caused by infections of the protozoan parasite *Trypanosoma cruzi*, how and why certain hosts progress to severe disease remains unresolved. Recent studies suggest that both parasite traits[3] and a host immune response that balances parasite elimination with pathogenic inflammation[4] influence disease progression; however, these mechanisms have not been fully explored or validated, particularly in natural infections.

Using the transcriptome data from peripheral blood mononuclear cells (PBMCs) taken from chronically naturally infected rhesus monkeys, we were able to create a holistic framework the host immune response during chronic infection, describing the expression of key T_H1 and T_H2 cytokines as well as important immune cell trafficking and activation markers that were necessary for parasite control. We further dissected this response, determining infected hosts that could control parasitemia had a balanced T_H1/T_H2 profile: with overexpression of IFNγ, IL-6, and IL-24 gene expression and downregulated CCL22 gene expression whereas infected hosts with rising parasitemia maintained a purely T_H1 response. Additionally, through multivariate analysis of gene expression, we identified biomarkers and parasite traits associated with the host ability to control parasite, serving as potential new prognostic tools for Chagas disease progression. Alongside this work, we performed an

Epigenome-Wide Association Study (EWAS) to compare the DNA methylation patterns of cord blood cells from uninfected children born to Chagasic and uninfected mothers, uncovering altered cell composition and methylated genes associated with development in uninfected children born to Chagasic mothers.

Collectively, we were able to describe the host-parasite relationship through a holistic integration of genetic data taken from naturally infected hosts. This work provides the foundation to build new tools and therapeutics for chronic Chagas disease, as well as the ability to identify those most at risk for severe disease.

IV. Acknowledgements

I wish to acknowledge the following funding sources which have both supported myself and the research within:

- “Congenital Transmission of Lineages I and II of Trypanosoma cruzi” (PI: Buekens) NIH/NIAID (R01AI083563)
- “Short-course Benznidazole Treatment to Reduce Trypanosoma cruzi Parasitic Load in Women of Reproductive Age: A Non-inferiority Randomized Controlled Trial” (PIs: Buekens and Cafferata) NIH/NICHD (R01HD095857)

V. Background and Significance

Chagas disease is a neglected tropical disease with an estimated annual burden of $627.46 million in health-care costs and 806,170 DALYs[2] due to its complex pathology. Caused by infections of the protozoan parasite *Trypanosoma cruzi*, Chagas disease can manifest in a variety of pathologies: transient high parasitemia acute infections characterized by non-specific symptoms, long lasting asymptomatic periods, chronic inflammation from low parasitemia infections resulting in severe cardiac pathology, even congenital infections resulting in neonatal pathology. While the pathologies of Chagas disease are documented, many of the mechanisms of pathogenesis are still not known, leaving gaps in the knowledge of what to target when beginning research for new medications or treatments. There is an *urgent need* to fill these gaps to understand how and why parasite infection develops into symptomatic Chagas disease.

Our *long-term goal* is to identify the important molecular drivers of *T. cruzi* pathogenesis during infection. Our *overall objective* is to describe the relationships between parasite load, parasite diversity, and maternal infection with Chagas disease progression using systems bioinformatic techniques that characterize and measure these connections between host immune responses and parasite dynamics, under a *central hypothesis* that these genetic associations can help explain some mechanisms of pathogenesis. The rationale for the proposed research is that by applying computationally intensive techniques, we can incorporate large amounts of

genomic information into a comprehensive picture of the biological interactions of interest during natural infections, overcoming current obstacles in the field.

Current Chagas drugs have questionable efficacy[5] alongside severe side effects[5] and are contraindicated during pregnancy[5], and new therapeutic avenues and prognostic tools are necessary. The proposed studies are expected to provide insights into the mechanisms of Chagasic disease pathology, knowledge that can serve as the foundation for research developing novel diagnostics, treatment protocols, and medications.

VI. Specific Aims

Aim 1: Validate the Current Paradigm of PBMC response During Chronic T. cruzi Infection from a Holistic Perspective

We hypothesize that monkeys with chronic *T. cruzi* infection will have downregulated genes related to T-cell function, antigen presentation, and T_H2 immune response activation compared to uninfected monkeys. To achieve this aim, we propose the use of bulk RNA-sequencing of peripheral blood mononuclear cells (PBMCs) taken from naturally infected monkeys. The current understanding of the host immune response to chronic *T.* cruzi infection is incomplete as it is built from studies targeting the effects of individual immune markers often using experimental infection models, thereby missing the cumulative effect of the immune response or lacking generalization to real world infections. By comparing the transcriptome of PBMCs taken from naturally chronically infected monkeys and uninfected monkeys, we can objectively interrogate the functional gene activities of these immune cells; validating current knowledge, identifying new cellular processes and immune activation molecules, and contextualizing this information within the holistic immune response to chronic *T.cruzi* infection. This will shed light on the role of PBMCs within the context of host-parasite interaction.

Aim 2A: Identify Biomarkers Associated with Controlling Parasitemia

We hypothesize that monkeys chronically *T. cruzi* infected with stable parasitemia will have different biomarkers compared to monkeys chronically *T. cruzi* infected with increasing parasitemia. To achieve this aim, using the transcriptome data generated in Aim 1, we will identify biomarkers. We will correlate these markers to chronically infected monkeys with increasing parasitemia and chronically infected monkeys with stable parasitemia to identify the predictive nature of the markers on host parasitemia control. Blood parasitemia is an important predictor of disease progression[3]; however, parasitemia during chronic *T. cruzi* infection can be too low to detect and current tools detecting anti-*T. cruzi* antibodies require that the infection persist to measure the change in parasitemia over time. Therefore, there is a need for new host biomarkers that can predict parasitemia control as a potential prognostic indicator for Chagas disease progression.

Aim 2B: Characterize the Immune Response of Infected Monkeys with Parasite Diversity

We hypothesize that monkeys with 2 or less *T. cruzi* DTUs will have a skewed inflammatory response whereas monkeys with multiple *T. cruzi* DTUs will have a balanced inflammatory response. To achieve this aim, we will compare the transcriptome data generated in Aim 1 between monkeys infected with high parasite DTU diversity and monkeys infected with low parasite DTU diversity. Parasitemia control has been associated

with parasite diversity, monkeys infected with high parasite genotype diversity tend to control parasitemia better than monkeys infected with low parasite genotype diversity,[3] yet the mechanisms of why this occurs are not fully understood. By characterizing the immune response associated with parasite diversity, we can shed light on these mechanisms and attempt to decipher what host immune responses are affected by parasite traits during infection.

Aim 3: Compare the DNA Methylation Patterns of Children Born to T. cruzi Infected and Uninfected Mothers

We hypothesize that children born to Chagasic mothers will have differentially methylated genes compared to those born to uninfected mothers. To achieve this aim, we propose an Epigenome-Wide Association Study (EWAS) using DNA extracted from human cord blood samples collected during live delivery of children born to Chagasic or non-Chagasic mothers as determined by PCR and serology. Prenatal experiences can influence health trajectories and contribute to adult health outcomes, including obesity, cancer, cardiovascular and metabolic diseases, asthma, and osteoporosis[6-8]. Prenatal exposures to infectious agents are associated with neurodevelopmental brain disorders, including schizophrenia[9,10], autism[11,12], and bipolar disorder[13,14]. Epigenetics have been suggested as a source of this pathology through alerted DNA methylation of developmental genes in patients exposed to infectious agents *in utero.* Maternal infections with multiple bacteria[15],

rubella virus[15], and Zika virus[16] can result in differential DNA methylation patterns in newborns compared to those born to uninfected mothers. This study would be the first of its kind to investigate the epigenetic effects of in utero *T. cruzi* exposure and can serve as the foundation for future work understanding congenital Chagas disease pathology.

VII. Introduction

Chagas Disease Overview

Chagas Disease (CD), also known as American trypanosomiasis, is caused by the protozoan parasite *Trypanosoma cruzi* (*T. cruzi, Figure 1*)[17]. The natural history of CD is described in three stages: an acute stage characterized by flu-like non-specific symptoms, an indeterminate asymptomatic stage often lasting many decades, an a final chronic stage with serious cardiac (e.g., cardiomyopathy) and gastrointestinal (e.g., megaesophagus and megacolon) morbidities, and the main cause of disability and death[18]. Transmission of the parasite to susceptible hosts can occur through multiple pathways: vertically from mother to child, through contact with contaminated food or drink, blood transfusion or organ transplantation from infected donors, laboratory accidents, and primarily through infected arthropod vectors[18-20].

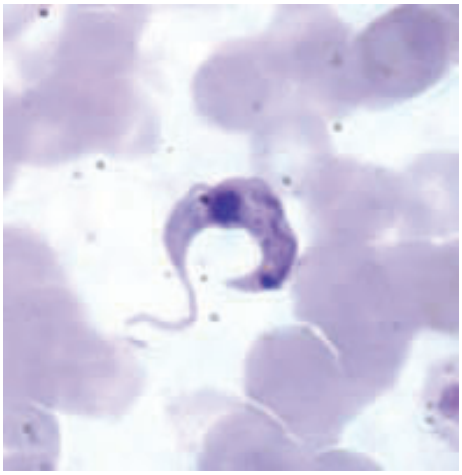

Figure 1: Trypanosoma cruzi in blood.

Trypanosoma cruzi (T. cruzi), the protozoan parasite responsible for causing Chagas disease, shown among red blood cells

Epidemiology

An estimated 8-10 million people are infected with *T. cruzi* worldwide[21-23], with a near 6 million cases in Latin America[21,22].

Approximately 90 to 100 million people are at risk of infection in Latin America[24-26]. Infections of *T. cruzi* cause 56,000 new cases of CD per year[22,25,27] and 12,000 deaths per year[24,27]. In the United States, it is estimated that 240,000 to 350,000 people are infected with *T. cruzi*[21,23,28].

Due to the chronic nature of CD, untreated infection can have devasting effects on individual and population morbidity[18,24]. Globally, CD is associated with nearly 800,000 disability-adjusted life-years (DALYs)[24], the economic impact of which can be astounding[24]. Economic models suggest that CD accounts for $6-8 million US dollars a year in health care costs in Latin America alone[20,24].

Vector-Borne Transmission

Currently, 157 arthropod species[29] in the Order: Hemiptera, Family: Reduviidae, Subfamily: Triatominae[30] have been identified as potential vectors of *T. cruzi*[31]. Both sexes of triatomines and their nymphs are hematophagous[32,33], becoming infected after feeding on infected mammalian hosts[34]. After replicating in the vector digestive system, the parasite is passed through the fecal material along with the waste products from the blood meal.[17,34] Susceptible hosts become infected when the parasite enters through the triatomine bite wound[17], mucosal membranes[17], ingestion of contaminated food or drink, or the placental barrier[35] during vertical transmission. Triatomines are opportunistic feeders[33], nearly all members of the mammalian order have been identified as susceptible hosts for *T. cruzi*[36,37]. Many species of

triatomines have become adapted to living with humans[18]. Of these, insects belonging to the *Triatoma*, *Rhodnius,* and *Panstrongylus* genera are the most important vectors of human *T. cruzi* transmission[38,39]. *Triatoma infestans* is considered to be the main vector of CD in South America[20,32], *Rhodnius prolixus* and *Triatoma dimidiata* in Central America[20]. In the United States, *Triatoma gerstaeckeri* and *Triatoma sanguisuga*[34] in the southern US and *Triatoma protracta* in the western US are the predominant vector species. The campaign to eliminate urban *T. cruzi* transmission by targeting domestic Triatomine species through indoor insecticide spraying, education campaigns, and improved construction has been generally successful in stopping vector-borne transmission in certain areas of the Americas[20,26,36]. However, eliminating one species can lead to an ecological niche for a new species[24], and the parasite still resides in sylvatic transmission cycles in rural areas[24], among more forest animal reservoirs[36,37]. Coupled with human encroachment into wildlife habitats, vector-borne transmission remains a threat of parasite transmission. Additionally, with human migratory movements, globalization[18,36,40], and congenital transmission, cases of CD are now spreading into traditionally non-endemic areas.

T. cruzi Diversity

The *T. cruzi* genome is described as diploid and highly polymorphic[41] resulting in a variable genome length by parasite strain due to aneuploidies and gene copy number differences[42]. This structure

is likely due to minimal sexual reproduction during the parasite life cycle[41]. With the advancement of molecular and next generation sequencing (NGS) technologies and markers, characterization of *T. cruzi* strains revealed that the parasite heterogeneity was much larger than thought, leading to the current consensus nomenclature using discrete typing units (DTUs) to identify parasite clades[36]. These DTUs are known as TcI-TcVI and TcBat, each with their own epidemiological features and pathogenicity[36,43]. Most recently, intra-DTU diversity has also been described within the TcI clade, suggesting that the true nature of parasite diversity has yet to be truly elucidated[37]. This is further evidenced by the appearance of genetically distinct strains within clades[44,45].

These DTUs tend to keep to general geographic regions although these ranges are expanding based on the spread of the vector and human movement. TcI has the widest distribution, infections of which have been detected throughout North, Central, and South America[43]. TcIV tends to have a widespread distribution much like TcI, but is much more restricted from the northern area of South America up to North America[46,47]. TcII, TcIII, TcV, and TcVI have been limited to sporadic reports in the United States[33,48-55], Panama[56], Mexico[57-64], Belize[45], and Honduras[58]. TcBat is less well studied, but has been reported in infections from Colombia[65], Guatemala[66], Brazil[67], and Panama[68].

Chagas Disease Pathology

Acute CD symptoms are largely mild in immunocompetent persons[25], mostly non-specific flu-like symptoms similar to other febrile diseases. Rarely, patients may manifest acute myocarditis, pericardial effusion, and/or meningoencephalitis[21] or the Romana's sign (swelling occurring near the eye). The parasite typically transforms between life stages during this phase of disease, entering host cells as metacyclic trypomastigotes, then transforming into intracellular amastigote parasites that multiply through clonal fission, finally exiting the cell as trypomastigotes which can be taken up by vectors or passed vertically. Whether or not the parasite has a tropism for specific tissues is widely debated[69]; however, the pathology does tend to manifest with cardiac or gastrointestinal symptoms. Mechanisms of cell invasion are still unclear; it is likely that the parasite makes use of cell surface and adhesion molecules such as TuMUC for internalization[70].

Left untreated, most patients can control the acute infection and enter an indeterminate phase of CD. This stage is characterized by an absence of symptoms in spite of detectable infection by serology[71], although parasitemia is generally very low. Most of those infected in endemic areas are in the indeterminate stage of CD, nearly 40% of these patients staying infected for years[21,72] while untreated. Because of the lack of pathology, patients in this stage of CD can live without knowing they are infected, and their life expectancy is like those without CD[21,71,72].

Eventually, patients evolve from the indeterminate to chronic form of CD. This stage is characterized by severe symptomology complemented by varying levels of parasitemia depending on the tissue that is sampled and degree of parasite reactivation. Most estimates suggest that 20-30% of patients will develop chronic CD[21,23,25,73-76], often decades after the initial infection[21,25,73,75]. Clinical symptoms are generally grouped into cardiac, digestive, or neurological symptoms based on which organs are involved[21,75], with cardiac pathology being the most important clinical aspect due to the fatality and frequency of onset[23,25,74]. Indeed, cardiac chronic CD accounts for 25-40% of the chronic CD cases[25,73], while only 6% of chronic CD patients develop digestive symptoms (megaesophagus, megacolon, etc) and 3% develop peripheral nerve damage[73,74]. Direct nerve damage by the parasite has been documented as a cause of cardiac disfunction[77], likely in conjunction with antineuronal autoimmune reactions[77].

Studying the natural course of chronic CD development in humans is very difficult due to the very long time between infection and chronic disease, challenges diagnosing infection particularly during the indeterminate phase, and that acute infections are treated upon discovery thereby not allowing the chronic phase to develop[78].

The suggested paradigm is that the chronic CD pathogenesis occurs through damage from inflammation composed of a non-functional immune response against any remaining parasites leftover from the

indeterminate stage[78]. Samples taken post-mortem from chronic CD animals found mild inflammation in cardiac tissue[79-82]. This has been shown in animal models. Increasing the parasite burden in animal models increases cardiac inflammation[83-85], which can be attenuated with treatment to decrease the parasite load[86-88]. Canine models of chronic infection found small foci of mild chronic myocarditis, with interstitial edema, early fibrosis, and infiltration by lymphocytes, macrophages, and plasma cells[89]. Chagas myocarditis is often characterized by inflammation driven fibrosis in heart tissue[78]. It is important to note that the inflammation may occur completely independent to the geographic or temporal state of the parasite[81], as the inflammatory response cascade may already be in place even after the parasite has been cleared, and experiments have shown that cardiac damage can still occur without cardiac parasitism[81].

The mechanisms of chronic CD damage are still being debated, although there is some combination of the parasite driven damage and the host immune response.

Immune Response to T. cruzi Infection

Overall, *T. cruzi* infections elicit inflammatory responses like other eukaryotic parasites Leishmania[90-92], Plasmodium[93], and *Toxoplasma gondii*[94]; modulating antigen presenting cells (APC), dysregulation of stimulatory molecules, and impairing immune cell functions.

An important mechanism of host evasion is the parasite attack on the complement system[95]. *In vitro* experiments have found parasite strains evading complement driven lysis[96] through changing surface molecules resulting in inefficient complement binding[97]. Additional studies have even found that the parasite can use complement to enhance its ability to invade host cells[98].

Diseased tissue samples commonly have areas of immune cell inflammation composed primarily of T cells and macrophages, with a few eosinophils, natural killer cells, dendritic cells, granulocytes, plasma cells, and mast cells[78]. Heart tissue from diseased patients specifically found a predominance of $CD8^+$ T cells[78,99,100], as well as populations of $CD4^+$ T cells and macrophages[101-103]. This suggests the importance of peripheral blood mononuclear cells (PBMCs) in the host response to *T. cruzi* infection.

Because the parasite multiplies intracellularly, phagocytic immune cells can be a double-edged sword. While necessary for parasite clearance, macrophages can serve as sites of parasite growth after phagocytosis[101,104]. The parasite escapes the phagolysosome, manipulating the host cell cytoplasm through lysosome mobilization, cytoskeleton rearrangements, membrane repair and elevation of Ca^{2+} and cAMP[105]. Extracellular vesicles produced by these infected macrophages contain newly replicated parasite and are more infective than parasite alone, capable of infecting new cells more efficiently[105].

Understanding parasite persistence during chronic CD necessitates understanding this relationship between the phagocytic cells and parasite growth.

Among the lymphocytic PBMC response, it appears that patients with a balanced $T_H1/T_H2/T_H17$ immune response fare better than those with response skewed toward one T cell subtype[78,106,107], particularly in the ability to control parasite burden without tissue damage. This is unsurprising, as it is likely the combination of stimulatory and inhibitory molecules secreted is critical to maintain the necessary balance[95,108,109], and any skew will cause a pathogenic inflammatory response, immune exhaustion[110,111], or both. Key cytokines associated with severe Chagas disease have been identified, primarily produced by monocytes and T cells[112,113] and follow this pattern of balanced cytokine profiles among patients with better disease outcomes[4] (*Figure 2)*. Patients in the indeterminate phase of infection produce higher circulating IL-4, IL-10, IL-17, and IL-13 compared to increased TNFα, IL-12, IL-6, CCL2, IL-2, and IFNγ found in patients with chronic Chagas cardiomyopathy both in serum and cardiac tissue[4,78,99,100,111-133].

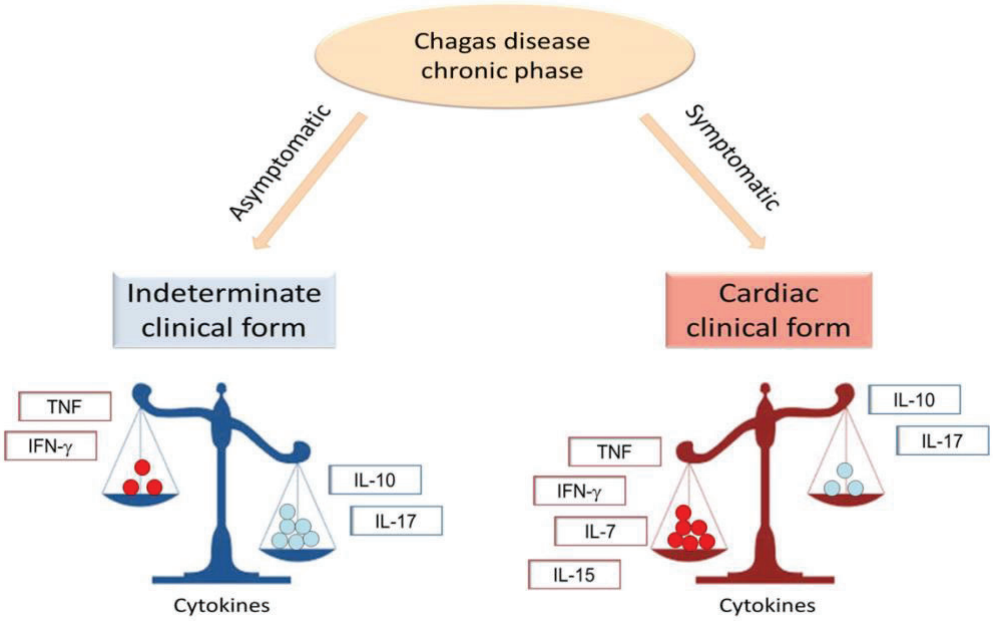

Figure 2: Cartoon representation of important cytokine expression during different forms of chronic Chagas disease[1].

A tip in the balance of T_H1 (red bubbles) or T_H2/T_H17 (blue bubbles) cytokine expression can skew the disease progression from indeterminate (blue scale) to cardiac (red scale) form of disease.[1]

A closer look at these identified cytokines presents a logical story of immune function balancing parasite killing with systemic regulation in patients with healthier disease pathology[134]. The additional T_H2/T_H17 response among patients in the indeterminate phase is primarily anti-inflammatory[134]: IL-10[135], IL-4[78,99,100,111,129,130], IL-13[131], TGFβ[136], and IL-17[4,137,138], likely acting to reign in the proinflammatory T_H1 parasite killing response: TNFα, IL-12, IL-6, CCL2, IL-2, and IFNγ[134]. This is not to downplay the importance of this T_H1 response. For example, mice deficient in proinflammatory IL-6[139-141] production developed higher parasitemia and had increased mortality compared to wild type mice[142-144]. Similarly the expression of IL-12 is linked to the control of

parasitemia[143-145], serving as the catalyst for the production of additional pro-inflammatory cytokines TNFα and IFNγ[146]. Curiously, IL-12 production is one of many pathways the parasite uses for evasion. The parasite inhibits infected macrophage and dendritic cell IL-12 production, leading to reduced lymphocyte activation and proliferation[147]. The protective immunity and T cell activation effects of IFNγ are well documented among *T. cruzi* infections[4,112,148,149]. Perhaps more interesting, the effects of IFNγ also offer insight into the importance of a balanced immune response.

It is crucial to note that none of these cytokines act alone, the immune system is a vast network of feedback loops and signaling agents. While it is clear that too much of a pro-inflammatory T_H1 response result in poorer outcomes and tissue damage in Chagasic patients, an excessive T_H2 response can also leave the patient vulnerable. Increased IL-10 levels in mice have been associated with susceptibility of *T. cruzi* infection[150], likely through inhibition of IFNγ production[151]. Consistently it has been shown that both IFNγ and IL-17 driven responses are essential to control infection[138] illustrating their push/pull dynamic on immune activity. Any therapeutic or vaccine against *T. cruzi* infection will have to consider this necessary $T_H1/T_H2/T_H17$ balance.

Maternal Infections

It is estimated that globally, 1.7 million women of reproductive age are infected with *T. cruzi*[152]*. T. cruzi* can be passed vertically during pregnancy and nearly 5% of infected pregnant women transmit the parasite vertically[153]. In Latin America alone, nearly 8700 infants are born with congenital Chagas disease each year[154]. Considering these numbers, coupled with the inability to treat infections during pregnancy[154], there is a considerable need to understand the pathology an infection during pregnancy can have on both the mother and the developing fetus to address the health risks.

Maternal bacterial, viral, and parasite infections have been linked to abnormal fetal development and poor birth outcomes[155]. Known as the "TORCH" pathogens, infections with Toxoplasma gondii, other agents (syphilis, varicella-zoster, parvovirus B19, Zika virus), Rubella, Cytomegalovirus, and Herpes simplex virus can cause complications such as miscarriage, abortion, and intrauterine fetal growth restrictions.[155] Congenital infections resulting from maternal TORCH infections can result in post birth complications such as hearing loss, developmental delays, and/or blindness.[156] Maternal infections with Zika virus have famously been linked to microcephaly in newborns.[157] Severe TORCH infections have resulted in maternal and/or fetal mortality.[155] Non-TORCH parasites such as malaria is also associated with pregnancy complications including fetal growth restriction, low birth weight, preterm

birth, and miscarriage.[155] It has been suggested that the maternal immune response to infections may also be pathogenic to the developing fetus, cytokine storms during pregnancy have been linked to onset of autism and other neurodevelopmental disorders.[157]

Maternal infections with *T. cruzi* have been associated with low birth weight, low Apgar scores, hepatosplenomegaly, respiratory distress syndrome, myocarditis, and meningoencephalitis[158]. Even if no pathology presents at birth, congenitally infected children are at risk of developing digestive, neurological, and cardiomyopathy as they develop into adulthood[158-161].

VIII. Aim 1: Compare the Gene Signatures of PBMCs from Chronically Infected and Uninfected Rhesus Monkeys

Background

The immune response to *T. cruzi* infection has been studied to understand and discover mechanisms of pathogenesis, parasite host evasion, diagnostic biomarkers, and therapeutic targets against Chagas disease. Hosts that can control parasite burden without overloading the immune response tend to have better disease outcomes. It is understood that this occurs through a balanced $T_H1/T_H2/T_H17$ response, offsetting the necessary immune cell activation and proliferation with regulatory elements to not cause inflammatory tissue damage or immune system exhaustion due to a skewed immune response. However, this paradigm has been identified through targeted identification of specific molecules using experimental infection models, making generalization difficult.

The major issue plaguing current research is the fragmented approach to studying the immune response and parasite control. Because the immune system is a complex network of feedback loops, researching a singular mechanism in isolation is impossible[78]. Results can be difficult to generalize between host species[99,101]. It can be nearly impossible to contextualize multiple studies of the effects of single cytokines into a cohesive framework[99,101]. This limitation is exacerbated by the methods used: the literature is dominated by experiments that require prior knowledge of a target for study. Genetically manipulated animals must have a gene or cell line to knock-out or manipulate to study

the resulting effects, and it is impossible to know the full systemic ramifications even minor genetic manipulations may have. Immunofluorescent detection techniques such as flow cytometry can only measure a limited number of cell populations or biomolecules at one time.

Because of this, the pathogenic effects of chronic parasite infection are pieced together using this fragmented information. This approach can result in the demanding task of trying to puzzle together a comprehensive picture of the host response using piecemeal information, potentially missing key components of the host immune response. These missing components could be potential novel therapeutic or diagnostic targets or fill in gaps in our current knowledge of the host response during *T. cruzi* infection. Methods that can explore the immune response in an integrative manner can be useful for placing fragmented knowledge into the appropriate context of the overall immune response. Transcriptomics have offered insights at the gene expression level[162] through a non-targeted identification of the functional components of a complex gene network[163].

By comparing the gene signatures of PBMCs taken from naturally *T. cruzi* infected and non-infected monkeys it is possible to create a holistic framework of the immune response during natural chronic infection. By using naturally infected monkeys, we eliminate many of the biases associated with experimental infections, such as the necessity to

use *T. cruzi* strains that can be cultured, confounding the results when applied to real-world infections.[164] With this holistic framework we will identify key molecules and pathways differentially regulated during infection, validating or amending the current paradigm of the cumulative immune response to chronic *T. cruzi* in the context of a natural infection.

Methods

Samples

Samples were selected from a cohort of 50 naturally infected rhesus macaques (*Macaca mulatta*) held in captivity at the Tulane National Primate Research Center in Covington, LA, USA. Animals were on average 11 years old. Animals had been infected between 3-7 years, on average 5 years, as determined by serology. Those infected were placed in the cases group, while those uninfected were control group monkeys. Whole blood was collected in tubes containing EDTA-K2 during routine veterinary appointments. All methods were approved by the Tulane University Office of Research and Tulane University Institutional Animal Care & Use Committee.

Sample Size/Power

Sample size was calculated using the R package RNASeqPower[165] which uses Monte Carlo simulations to estimate alpha and beta significance based on user provided sample data. Assuming an average depth of count for each gene of 50 based on preliminary data, a coefficient of variation within groups equal to .2[165], and an alpha

significance of 0.05, groups of 5 or 6 monkeys will have an 80% power to detect a difference in gene expression with a minimum fold change of 1.5.

For comparing infected vs non-infected monkeys, we were able to achieve groups of 11 controls and 18 cases. Samples had an average read count of 343. Under these parameters with an alpha significance of 0.05 we estimate a 99% power to detect a difference in gene expression with a minimum fold change of 1.5.

PBMC Purification

PBMCs were isolated from whole blood undercentrifugation with a Ficoll-Paque™ (Millipore-Sigma, Inc) solution using manufacturers conditions. PBMCs were pipetted off and washed with RPMI and PBS, then stored at -80°C in Cryostor™ (Biolife Solutions, Inc) media until use.

RNA Extraction/Sequencing

Frozen PBMCs were thawed and assessed for viability through counting via hemocytometer using trypan blue dye. Thawed PBMCs with at least 90% viability were used for RNA extraction. RNA was extracted using the PerfectPure RNA Cultured Cell Kit™ (5 Prime, Inc.) as per manufacturer's instructions. Total RNA was sequenced using the Illumina MiSeq platform, which has an error rate of 0.473%[166].

Differentially Expressed Gene Calling

Reads were mapped to the rhesus macaque mmul10 reference genome (RefSeq assembly accession: GCF_003339765.1) using the

STAR (Spliced Transcripts Alignment to a Reference)[167] package under default conditions. Quality mapped read counts were batch adjusted using the R package ComBat-seq[168]. Read counts were normalized and differentially expressed genes (DEGs) called using DESeq2[169] under the apeglm[170] shrinkage estimator to reduce noise. Significant genes were called at a significance alpha of 0.05 adjusted for multiple testing using the Benjamini-Hochberg false discovery rate method and a fold change of 1.5 was set to maximize functional relevance. Principle component analysis (PCA) was performed through the DESeq2 package.

Data Analysis

Data analysis and visualization was performed using R version 4.2.1[171].

Pathway analysis of up and down regulated DEGs were performed using both the clusterProfiler[172] R package and the ShinyGO[173] webapp to query the Gene Ontology[174,175] and Kyoto Encyclopedia of Genes and Genomes[176] databases using over-representation analysis under a false-discovery rate cutoff < 0.05. Two query algorithms and two pathway databases were used to provide confidence in the physiological relevance of significant DEGs; only pathways shared between the two search algorithm results were considered relevant. Functional pathways were visualized using the Pathview[177] R package.

Multivariate analysis was performed using the MADE4 package[178] which is specifically built to perform supervised dimension reduction and

between group analysis using gene read count data. Between Group Analysis (BGA) is a supervised PCA method seeking to ordinate groups rather than individual samples.[178]

Results

Samples

In total, the transcriptomes of PBMCs taken from 29 monkeys were sequenced (**Table 1**). There were 11 uninfected monkeys and 18 T. cruzi infected monkeys as determined by qPCR and serology. Infected monkeys had been chronically infected for minimum 35 months and maximum 89 months. There were no observable difference could be found in mean age nor sex distribution between uninfected and infected groups.

Over the 29 samples, 4-29 million reads were sequenced through Illumina sequencing. Reads were filtered for quality and mapped to the MMUL10 reference genome with an average 80% unique mapped reads. Batch-adjusted, filtered read counts were used to call differentially expressed genes between sample groups.

Table 1: Table of Monkey Samples Used for Aim 1

Monkey ID	Age (Months)	Sex	Infection Group	Months Infected
HA67	14	Female	Infected	35
IN54	12	Female	Infected	82
IP64	12	Female	Infected	89
JC08	11	Female	Infected	63
JM46	10	Male	Infected	77
JN64	10	Female	Infected	72
LL64	5	Female	Infected	57
KP37	8	Male	Infected	77

EP36	18	Female	Infected	85
GI52	15	Female	Infected	75
KA90	9	Female	Infected	81
KC05	9	Female	Infected	81
KL57	6	Female	Infected	81
HN75	14	Female	Infected	59
JL71	11	Male	Infected	82
JT42	10	Female	Infected	81
MD12	4	Female	Infected	34
ED57	19	Female	Infected	75
AG23			Uninfected	0
HD69			Uninfected	0
ID59			Uninfected	0
JN58			Uninfected	0
KC78			Uninfected	0
KK63			Uninfected	0
KL72			Uninfected	0
KR83			Uninfected	0
LB83			Uninfected	0
LD53			Uninfected	0
ME13			Uninfected	0

Differential Gene Expression

To observe how well chronic *T. cruzi* infection could explain differences in PBMC gene expression, PCA plots were used to visualize the overall gene expression profile of PBMCs from uninfected and infected monkeys (**Figure 4**). Clear clustering could be seen between chronically *T. cruzi* infected and uninfected monkeys, indicating that

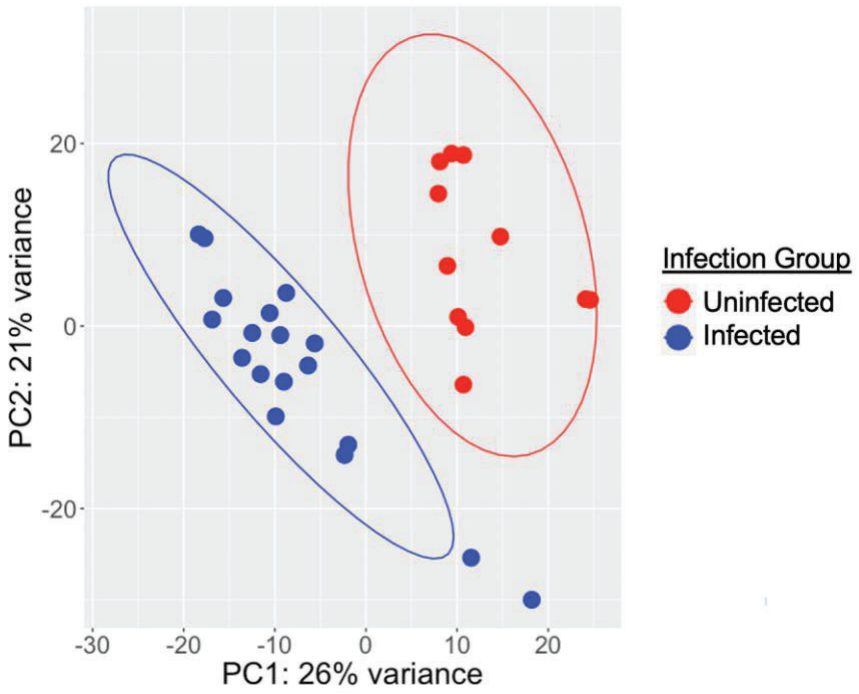

Figure 3: Principal Component Analysis (PCA) Plot between uninfected monkeys (red) and infected monkeys (blue)

PCA plot showed strong clustering of infected monkeys and uninfected monkeys. Normalized, adjusted read counts were used as the inputs to visualize how well *T. cruzi* infection could explain variation between the samples.

chronic *T. cruzi* infection could explain some of the variation in gene expression seen between samples.

Gene read counts were filtered for genes with low counts or outliers. Of the 28065 genes that passed filtering, 5794 were significantly differentially expressed between uninfected and infected groups (adjusted p-value < 0.05). To provide confidence in the functional relevance of these genes, significant genes were further categorized into downregulated and upregulated genes if there was a mean expression fold change greater than 1.5 between the sample groups. Under this classification, 1468 genes were called significantly upregulated, and 1160

genes were called significantly downregulated between uninfected and infected monkeys. Volcano plot was used to visualize the distribution of significant genes in the context of all gene (**Figure 5**). Individual gene expression difference was visualized using a heatmap (**Figure 6**). Not only was there clear clustering between sample groups as seen before, but genes clustered well into groups of upregulated and downregulated genes, further providing evidence of a different gene profile found among PBMCs taken from chronically infected monkeys compared to those uninfected.

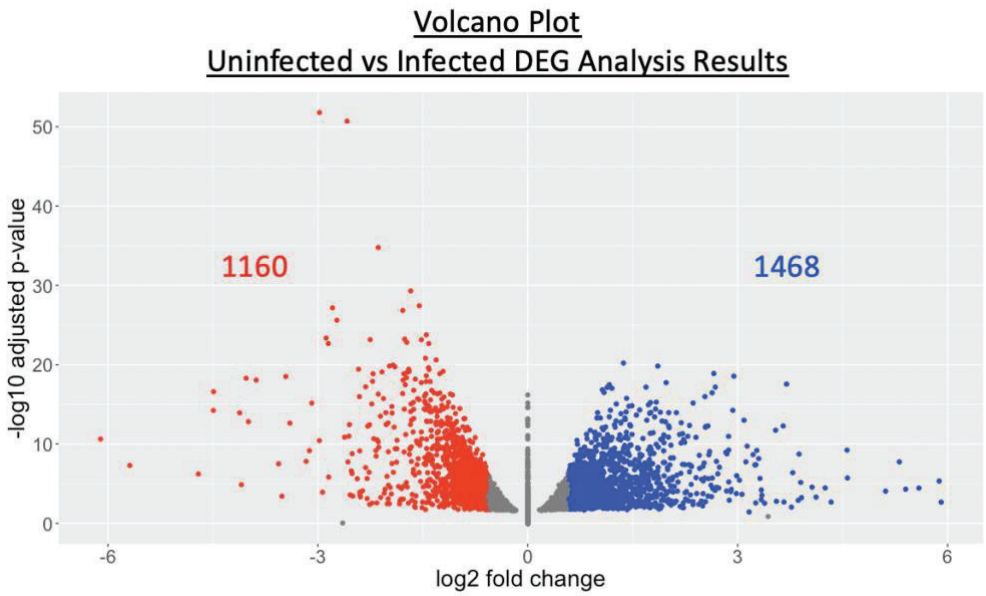

Figure 4: Volcano plot of the distribution of the differential gene expression analysis results between uninfected and infected monkeys.

Between uninfected and infected monkeys, 2628 genes had significant differential expression using an alpha = 0.05. Using a fold change cutoff of 1.5, of the 2628 genes, 1468 genes were upregulated (blue) and 1160 genes were downregulated (red).

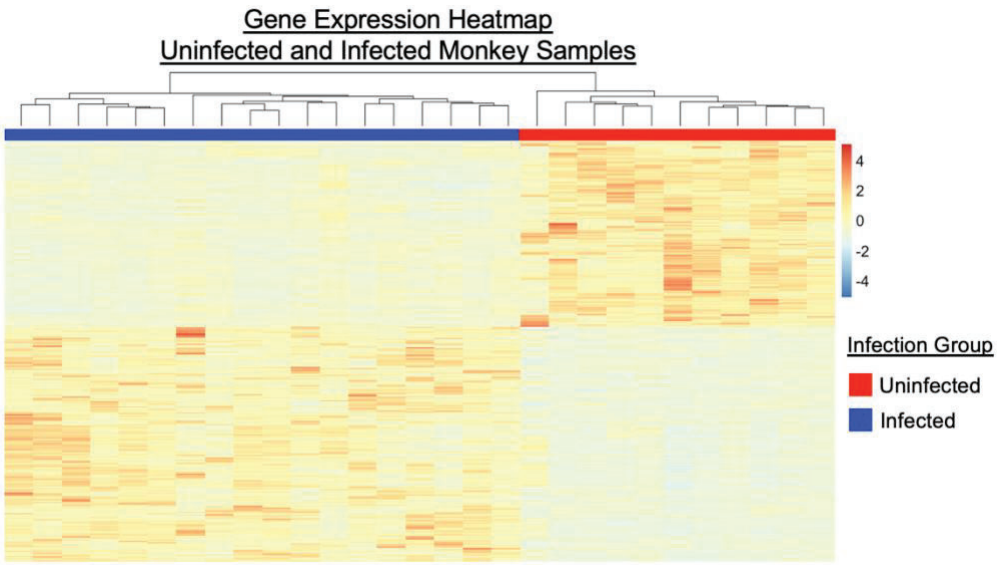

Figure 5: Comparative gene expression between infected (blue) and uninfected (red) monkeys.

Clear groupings of overexpressed (red/orange) and underexpressed (white/blue) genes were seen between sample groups when visualized using a heatmap

Pathway Analysis

To further explore the function of the significant DEGs, upregulated and downregulated genes were queried using over-representation analysis. Among infected monkeys, the platelet activation and hematopoietic cell lineage pathways were over-represented by upregulated DEGs. Many more relevant downregulated pathways were found in infected monkeys (**Table 2**). Predictably, these included immune system pathways concerning cytokine production and signaling, $T_H1/T_H2/T_H17$ cell activation, and immune cell differentiation. In addition, pathways suggested an overall dysregulation of cell processes in infected monkeys, including responding to external stressors and regulation of the cell cycle. The tolerance induction pathway was downregulated, perhaps

indicating a systemic compensatory mechanism to immune exhaustion due to chronic infection.

Table 2: Pathways over-enriched from genes differentially downregulated in infected monkeys compared to uninfected monkeys

Name	GO/KEGG ID	FDR p-value
apoptotic signaling pathway	GO:0097190	0.0043
B cell activation	GO:0016071	0.0031
cell surface receptor signaling pathway involved in heart development	GO:0030099	0.0177
cellular response to biotic stimulus	GO:0043066	0.0161
cellular response to chemical stress	GO:0001818	0.0310
cellular response to external stimulus	GO:0043069	0.0266
cellular response to extracellular stimulus	GO:0050867	0.0437
cellular response to hydrogen peroxide	GO:0008284	0.0437
cellular response to lipid	GO:0022409	0.0326
cellular response to lipopolysaccharide	GO:0002639	0.0310
cellular response to oxidative stress	GO:1902533	0.0098
cellular response to oxygen-containing compound	GO:0002696	0.0235
Chagas disease	mcc05142	0.0251

cytokine production	GO:1903039	0.0306
Cytokine-cytokine receptor interaction	mcc04060	0.0191
ER-nucleus signaling pathway	GO:0051251	0.0437
establishment of protein localization to organelle	GO:0042113	0.0282
hematopoietic or lymphoid organ development	GO:0061311	0.0043
hemopoiesis	GO:0071216	0.0046
I-kappaB kinase/NF-kappaB signaling	GO:0050870	0.0331
immune system development	GO:0062197	0.0018
inflammatory response	GO:0050865	0.0096
leukocyte activation	GO:0071496	0.0018
leukocyte cell-cell adhesion	GO:0031668	0.0012
leukocyte differentiation	GO:0070301	0.0088
lymphocyte activation	GO:0071396	0.0012
lymphocyte differentiation	GO:0071222	0.0031
mononuclear cell differentiation	GO:0034599	0.0031
mRNA metabolic process	GO:1901701	0.0312
myeloid cell differentiation	GO:0001816	0.0177
negative regulation of apoptotic process	GO:0022407	0.0412
negative regulation of cytokine production	GO:0051090	0.0306

negative regulation of programmed cell death	GO:0002637	0.0306
NF-kappa B signaling pathway	mcc04064	0.0251
positive regulation of cell activation	GO:0006984	0.0047
positive regulation of cell population proliferation	GO:2001242	0.0306
positive regulation of cell-cell adhesion	GO:0072594	0.0057
positive regulation of immunoglobulin p roduction	GO:0002694	0.0177
positive regulation of intracellular signal transduction	GO:1903037	0.0101
positive regulation of leukocyte activation	GO:0048534	0.0043
positive regulation of leukocyte cell-cell adhesion	GO:0030097	0.0019
positive regulation of lymphocyte activation	GO:0007249	0.0036
positive regulation of T cell activation	GO:0002520	0.0046
regulation of cell activation	GO:0006954	0.0018
regulation of cell-cell adhesion	GO:0045321	0.0018
regulation of DNA-binding transcription factor activity	GO:0051249	0.0161
regulation of immunoglobulin	GO:0045589	0.0241

production		
regulation of intrinsic apoptotic signaling pathway	GO:0050863	0.0310
regulation of leukocyte activation	GO:0007159	0.0018
regulation of leukocyte cell-cell adhesion	GO:0002521	0.0012
regulation of lymphocyte activation	GO:0046649	0.0018
regulation of regulatory T cell differentiation	GO:0045066	0.0177
regulation of T cell activation	GO:0030098	0.0012
regulatory T cell differentiation	GO:0032496	0.0235
response to lipopolysaccharide	GO:0010243	0.0375
response to organonitrogen compound	GO:0006979	0.0327
response to oxidative stress	GO:1901652	0.0397
response to peptide	GO:0042110	0.0415
T cell activation	GO:1903131	0.0022
Th1 and Th2 cell differentiation	mcc04658	0.0251
TNF signaling pathway	mcc04668	0.0028
vasculogenesis	GO:0001570	0.0268

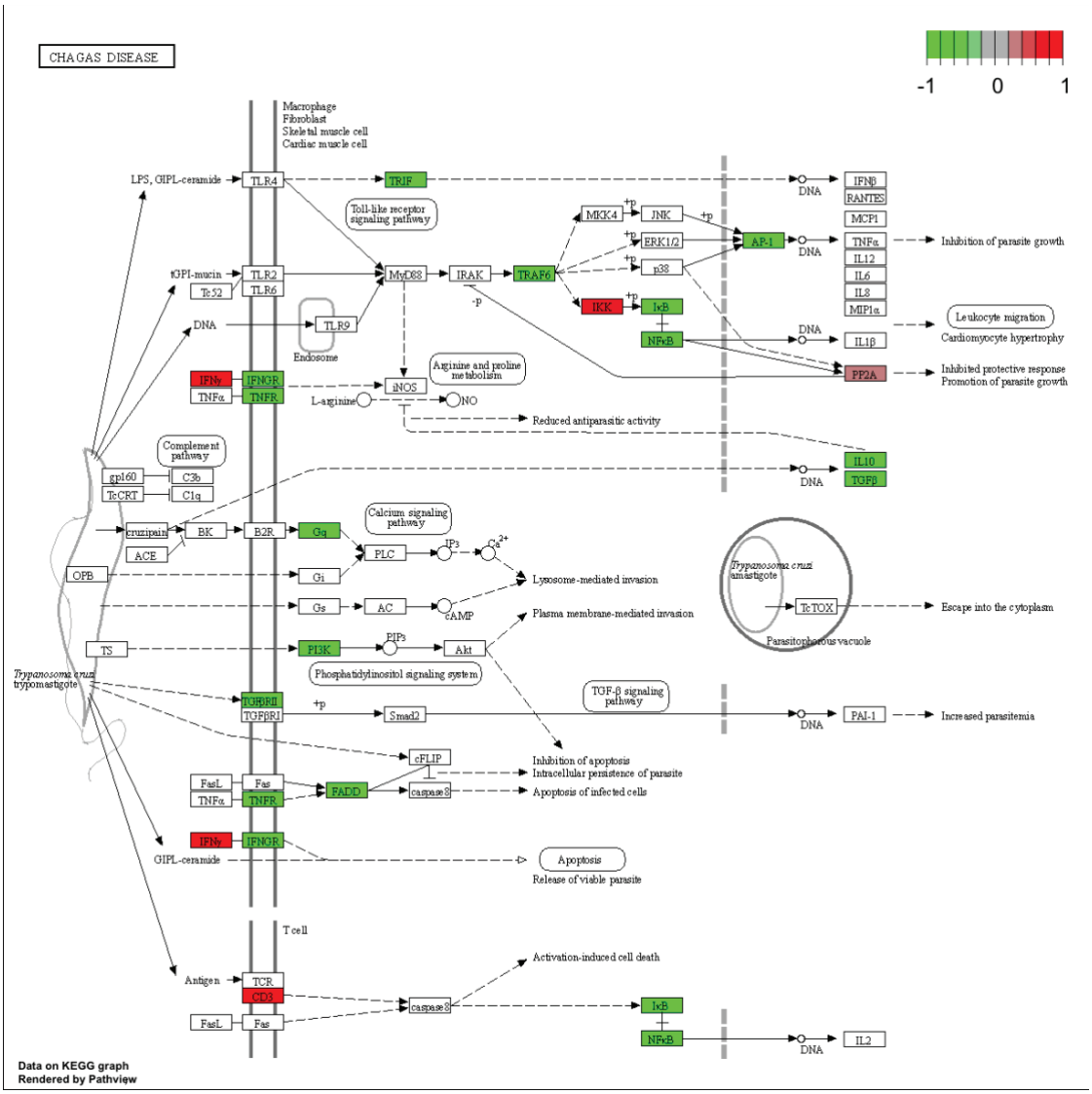

Figure 6: The KEGG Chagas disease pathway with differentially expressed genes between uninfected monkeys and infected monkeys.

Differentially expressed genes called from DESeq2 were queried in the KEGG database Chagas Disease Pathway. Genes upregulated in infected monkeys are highlighted in red. Genes downregulated in infected monkeys are highlighted in green.

The Chagas disease pathway (KEGG ID: mcc05142) in the KEGG database was downregulated, providing evidence that this method could identify appropriate pathways reasonably to contextualize the functional relevance of the genes during *T. cruzi* infection (**Figure 7**). Within this pathway, genes related to cytokine signaling: IFN-γ, TNF, IL-10, TGF,

and Activator protein 1 were found among those differentially expressed in infected monkeys, as well as genes related to NF-κB signaling.

$T_H1/T_H2/T_H17$ Activation

Building off the current paradigm that chronic *T. cruzi* infections results in downregulation of genes associated with T_H pathway dysregulation, the differential expression of cytokine, chemokine, and CD marker genes were specifically analyzed to better characterize which molecules were affecting the $T_H1/T_H2/T_H17$ response and which cells were activated or inhibited during infection.

Of the 62 genes associated with cytokine expression, 29 passed low count and outlier filters. To view the expression of these genes in the context of $T_H1/T_H2/T_H17$ response, the fold change in gene expression between chronically infected monkeys and uninfected monkeys was graphed using radar plots (**Figure 8**). Significant DEGs included upregulated T_H1 cytokine IFN-γ as well as IL-15 and downregulated TGFβ1 and the T_H2 cytokine IL-10 in infected monkeys.

Of the 41 genes associated with chemokine expression, 34 passed low count and outlier filters. To view the expression of these genes in the context of immune cell attraction, the fold change in gene expression between chronically infected monkeys and uninfected monkeys was graphed using radar plots (**Figure 9**). Two DEGs were

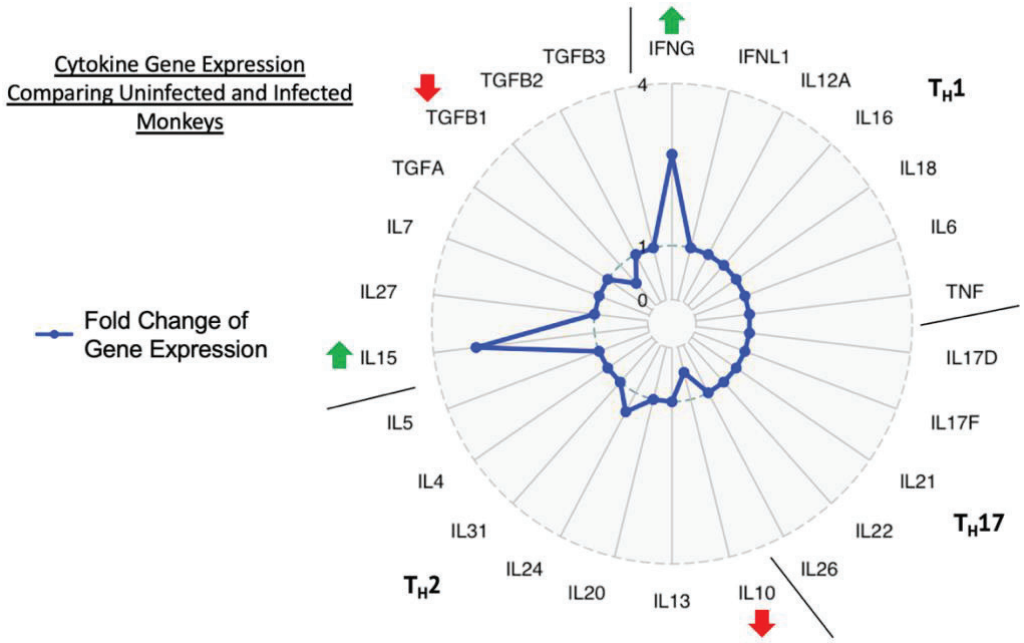

Figure 7: Fold change of cytokine gene expression (blue) between infected and uninfected monkeys.

Fold change of cytokine gene expression visualized using a radar plot to compare the response between infected and uninfected monkeys. Arrows indicate genes that were significantly different in expression as called by DESeq2 analysis. Arrows are colored to indicate the direction of expression change in infected monkeys compared to uninfected monkeys: up (green) or down (red).

significant: upregulated CXCL10 in infected monkeys associated with T-cell attraction and downregulated CCL22 in infected monkeys, associated with T-cell and macrophage/monocyte attraction.

Of the 72 genes associated with CD marker expression, 70 passed low count and outlier filters. To view the expression of these genes in the context of immune cell activation, the fold change of gene expression was visualized using radar plot (**Figure 10**). 14 genes were significantly differentially expressed. Of these 14, 10 were downregulated in infected monkeys: CD9, CD44, CD68, CD70, CD82, CD83, CD93, CD276 and two T cell activation markers CD28 and CD7. Four genes were upregulated in infected monkeys: CD1A, CD1C, CD101 and CD244.

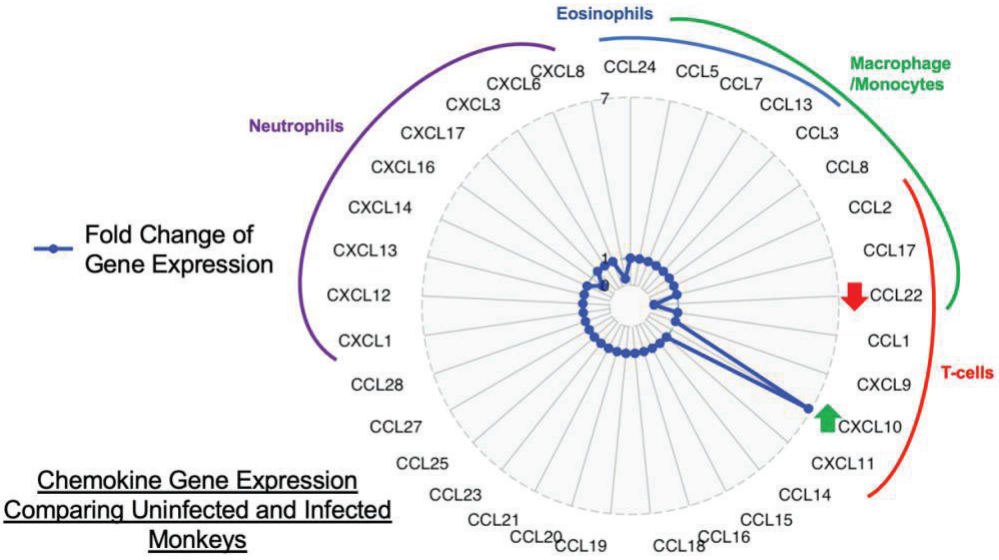

Figure 8: Fold change in chemokine gene expression between infected and uninfected monkeys.

Fold change in chemokine gene expression visualized using a radar plot to compare the response between infected and uninfected monkeys. Arrows indicate genes that were significantly different in expression as called by DESeq2 analysis. Arrows are colored to indicate the direction of expression change in infected monkeys compared to uninfected monkeys: up (green) or down (red).

Having identified immune markers differentially expressed between infected monkeys and uninfected, multivariate analysis was used to identify which immune markers were predictive of chronic infection. Between group analysis of gene expression between samples revealed strong separation of chronically infected monkeys and uninfected monkeys along the main BGA discrimination axis (**Figure 11A**). The main BGA discrimination axis provides coordinate data associated with sample clustering. By overlaying this coordinate data of the samples over the clustering of gene expression, genes found at the ends of the main BGA discrimination axis represents genes most associated with groups: infected or uninfected samples (**Figure 11B**). The top 20 genes associated with infected monkeys were identified along

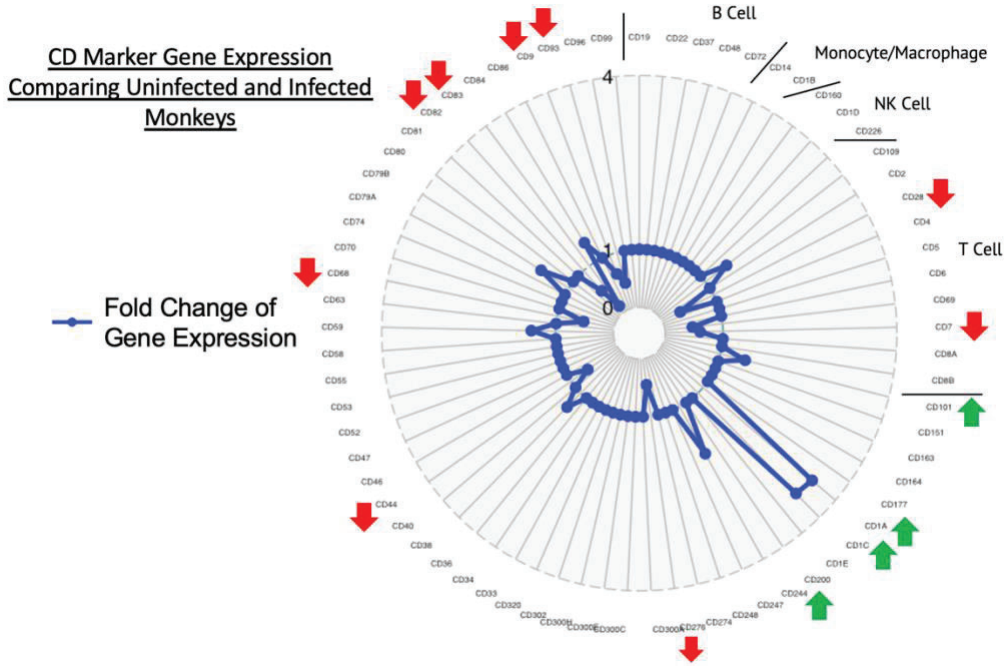

Figure 9: Fold change of CD marker gene expression between infected monkeys and uninfected monkeys.

Fold change of CD marker gene expression were visualized using a radar plot to compare the response between infected monkeys and uninfected monkeys. Arrows indicate genes that were significantly different in expression as called by DESeq2 analysis. Arrows are colored to indicate the direction of expression change in infected monkeys compared to uninfected monkeys: up (green) or down (red).

this main BGA discrimination axis (**Figure 12**). Upregulation of pro-inflammatory CXCL10, IFN-γ, and IL-15, alongside CD markers CD40LG, CD1A, CD1C, CD244, CD101, CD226, and CD59 was most associated with infected monkeys. IFNγ and CXCL10 enhance T_H1 immunity. IL-15 is expressed by a wide range of cells, including phagocytic immune cells, activating T and natural killer cells. Downregulation of IL-1B, CXCL8, TGFβ1, and CXCL16, alongside CD markers CD83, CD93, CD28, CD82, CD70, and CD9 were most associated with infected monkeys. TGFβ1 is an anti-inflammatory cytokine, as well as an important T_H2 enhancer. IL-1B is a pro-inflammatory cytokine and a major activator of the host fever response. CXCL8, also known as IL-8, is an important chemoattractant for neutrophils and is produced by an endothelial cells at sites of

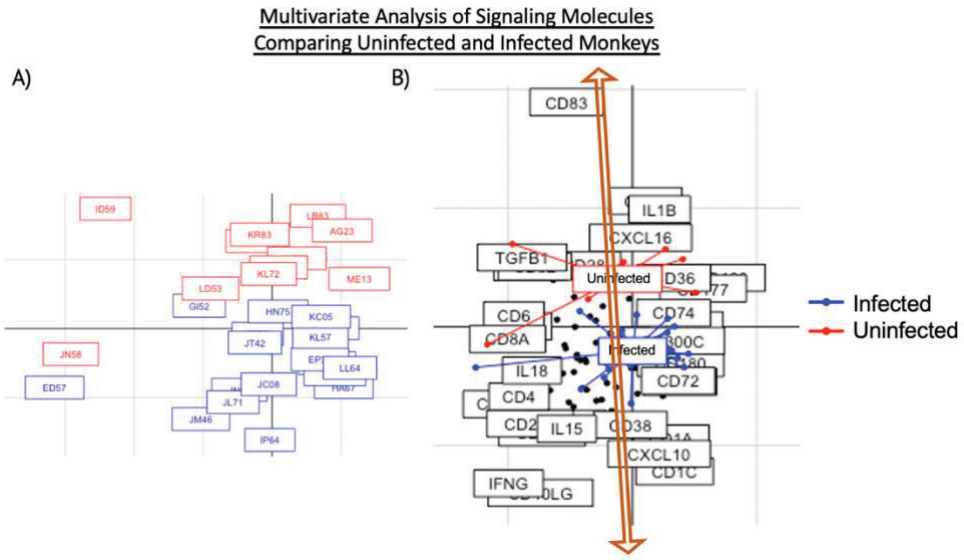

Figure 10: Between group analysis of cytokine, chemokine, and CD marker gene expression counts between infected monkeys (blue) and uninfected monkeys (red).

Between group analysis showing the separation of cytokine, chemokine, and CD marker gene expression on the BGA discrimination axis along one line of differentiation: infected vs uninfected (A). By overlaying sample clustering and gene clustering from BGA analysis, genes most associated with infected or uninfected status were determined (B). Black dots represent individual genes, colored dots and lines represent monkey samples, and the BGA discrimination axis is colored orange.

infection. CD28 is a marker found on T cells, acting with T-cell receptors to stimulate IL-6 expression from activated T cells.

Discussion

We used of bulk RNA-sequencing of peripheral blood mononuclear cells (PBMCs) taken from naturally infected monkeys to validate the current paradigm of PBMC response during chronic *T. cruzi* Infection from a holistic perspective.

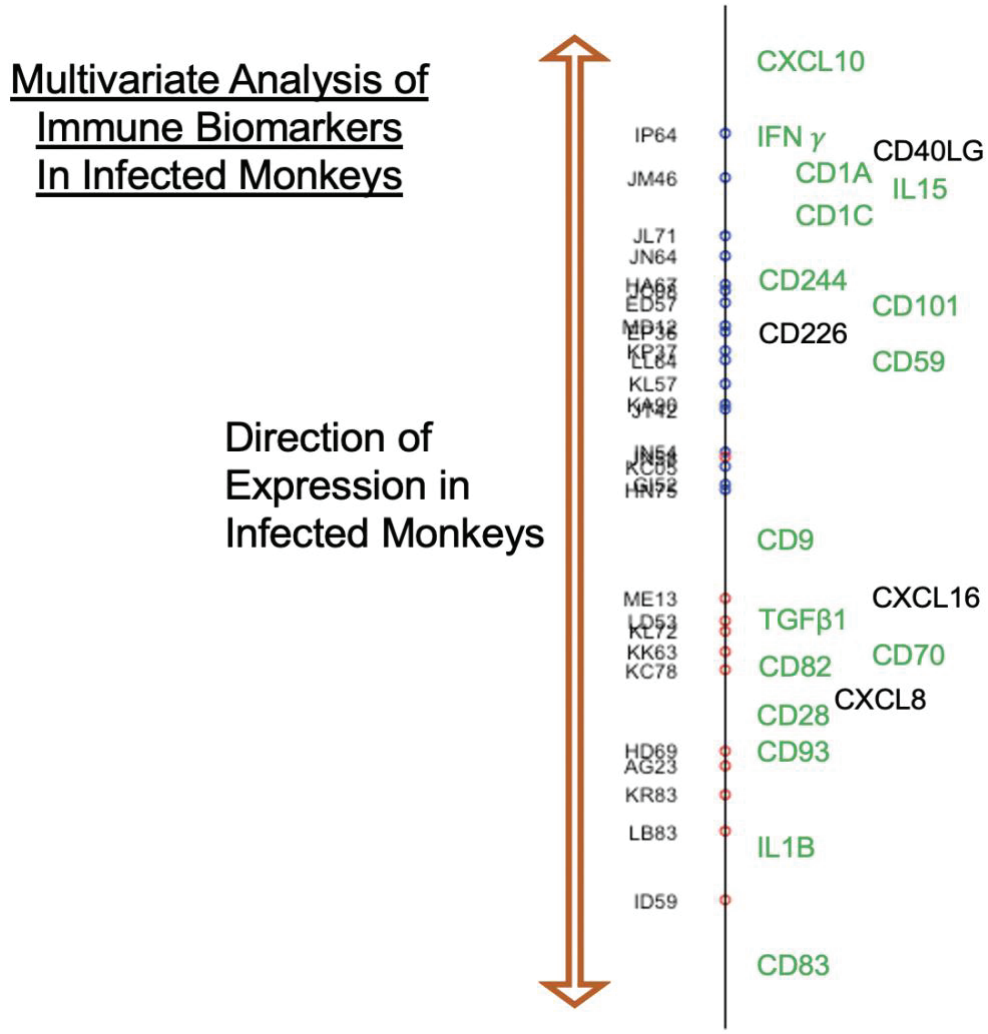

Figure 11: Ordination plot of the top 20 immune biomarker gene expression most likely to predict infected monkeys

Ordination plot showing the top 20 cytokines, chemokines, and CD marker genes most likely to predict infected monkeys along the main BGA discrimination axis. Genes colored in green were found significant by DESeq2 analysis as well. Genes at the top of the arrow are associated with upregulated in infected monkeys, while genes toward the bottom are associated with downregulation in monkeys.

We were able to confirm that the immune response was consistent with current literature: naturally infected monkeys had an increased pro-inflammatory T_H1 response and a decreased T_H2 anti-inflammatory response. Evidence for this pro-inflammatory response appeared to be driven by cytokines and chemokines gene expression upregulation: IFNγ, IL-15, and CXCL10 in infected monkeys. The T_H2 response was lost through a downregulation of IL-10, TGFβ1, and CCL22 gene expression in infected monkeys. No genes associated with T_H17 cytokine expression were differentially expressed; however, cytokines such as TGFβ1 can stimulate T_H17 cell differentiation, suggesting that the T_H17 response in infected monkeys may be downregulated as well.

TGFβ1 was the most expressed gene of any of the cytokines and chemokine genes in both infected and uninfected monkeys. Indeed, it is unsurprising that both TGFβ1 and IFNγ would be differentially expressed in infected monkeys, as the importance of both in determining Chagas disease progression has been well documented in the literature[179]. IL-15 had a large fold change in gene expression between infected and uninfected monkeys, suggesting this pro-inflammatory cytokine plays a highly important role during infection. IL-15 has a wide range of pro-inflammatory functions, primarily stimulating T, B, and natural killer cell responses as well as inducing IFNγ expression. As both IL-15 and CXCL10 enhance IFNγ expression, both may serve as therapeutic targets by tangentially inhibiting IFNγ response to stop pathogenetic inflammation without directly inhibiting IFNγ expression necessary for parasite clearance. Our suggestion that IL-15 and CXCL10 are major

molecules during Chagas disease progression has been frequently been shown: increased IL-15 and CXCL10 expression in serum has previously been associated with cardiac Chagas disease[1], whereas co-expression of IL-15 with vaccine delivery was shown to improve anti-trypanosomic vaccine effectiveness in mice[180]. We were also able to confirm the importance of IL-10. Reduction of the T_H2 cytokine IL-10 has consistently been shown to be associated with *T. cruzi* infection[179]. IL-10 could potentially be another lucrative therapeutic target, as its functions can counter-act IFNγ inflammation, without eliminating the IFNγ expression necessary for parasite clearance. Indeed, the ratio of IL-10/IFNγ expression has correlated well with chronic cardiac Chagas disease progression, future studies may seek to test this in experimental models.

Noteworthy in this study was the upregulation of CCL22 gene expression in infected monkeys. CCL22 is primarily expressed by dendritic cells and macrophages. CCL22 is an important ligand of CCR4. CCR4 has been extensively studied as a drug target because CCR4 is predominately expressed by T_H2 cell types including T_{reg} cells. CCR4 expression was associated with severe disease and has been explored as a marker of Chagas disease progression[181], but ligands of CCR4 have yet to be explored as therapeutic targets despite precedence in other diseases[182].

Many cytokines previously associated with Chagas disease progression were not significant in this study. Surprisingly there was no significant difference in gene expression in IL-12 and TNFα expression between infected and uninfected monkeys as previous studies have suggested these cytokines are

upregulated during *T. cruzi* infection[179], although IL-12 did appear to be downregulated and TNFα upregulated in infected monkeys, just not to a level that achieved significance. Previously reported cytokines that were associated with parasite burden control: IL-13, IL-6, and IL-2[179,183], did not have significantly differentially expressed genes between infected and uninfected monkeys, although these genes were filtered out from differential gene expression calling due to low read counts. No genes associated with IL-17 expression were significantly differentially expressed between infected and uninfected monkeys, nor were any IL-17 variants, although IL-17 expression has been associated with better parasite control in Chagasic mice[184]. IL-17A, IL-17B, and IL-17C were filtered out due to low read counts. IL-17F appeared to be downregulated in infected monkeys; however, this change was not large enough to pass our fold change cutoff of 1.5. Neither IL-21, IL-22, or IL-26 were differentially expressed in infected monkeys compared to uninfected monkeys. It is important to consider that gene expression serves as the starting point of the immune system response. Because signaling molecules in the immune system work in a network, single cytokine gene expression could result in an immune cascade produced from non-PBMC sources. Therefore, experiments measuring serum and tissue level cytokines could reflect the final stage of the response, whereas gene expression of cytokine and chemokine expression serves as the starting line.

There appeared to be a downregulation of T cell response, suggested by the downregulation of CD7 and CD28, alongside important intracellular function

pathways related to protein expression and packaging, cell cycle regulation, and energy metabolism. These pathways were indicative of an inability of the cells to respond to infection, as many pathways related to stress response were downregulated. This suggests that the T cells responding to infection are expressed, but not functional, likely resulting in some form of immune exhaustion. Indeed, gene expression of programmed cell death 1 ligand 2, killer cell lectin like receptor G1, and CD244, markers of immune tolerance were upregulated in infected monkeys. Interestingly, no other specific immune cell markers were differentially expressed, and of those CD markers that were, most had ubiquitous functions or were non-specific cell activators. Focusing on the downregulated CD markers found in infected monkeys, $CD28^-$ T cells have been found reduced in Chagasic patients and this reduction was associated with disease progression and cardiac symptoms[185,186]. $CD28^+$ T cells are important for IL-10 and TGFβ1 production; therefore, it is unsurprising that these cells would be important for Chagas disease control with their importance in maintaining the T_H2 response. $CD7^+$ T cells have not been investigated in relation to Chagas disease and may serve as an effective marker of infection.

In conclusion, we were able holistically describe the immune response in naturally infected monkeys. Through this framework, we validated the current understanding that chronic *T. cruzi* infection results in an immune response skewed toward T_H1 responses, with downregulated T_H2 cytokines and no expression of T_H17 activators. This response appears to be driven by very specific cytokine expression: downregulation of anti-inflammatory TGFβ1 and

IL-10 alongside upregulation of pro-inflammatory IFNγ and IL-15. T-cells appear to be highly trafficked through upregulated CXCL10 expression in infected monkeys, although T cell function appears to be downregulated.

IX. Aim 2A: Identify Immune Biomarkers Associated with Parasite Burden Control

Background

Most estimates suggest that 20-30% of patients will develop chronic Chagas disease[21,23,25,73-76] after infection, suggesting there may be differences in the host response that determine the course of disease. Because parasite burden has also been linked to disease severity, it stands to reason that disease severity is dependent on the host ability to control parasitemia. For this reason, current treatments focus on using anti-trypanosomic compounds, aiming to clear the parasite from infected hosts. In addition to their high toxicity, these drugs must also be balanced with treating any associated tissue damage or inflammatory symptoms. Therefore, there is a compelling reason to target treatment at those at risk of severe disease.

Biomarkers of parasitemia control could potentially serve as drug targets or diagnostic tools[187,188]. Current tools focus on parasite antigens as identifiers of infection; however, because parasitemia can be undetectable during chronic infection, host biomarkers of parasitemia control are necessary.

Immune biomarkers have been explored as biomarkers, but only for treatment effectiveness[189]. Prothrombotic markers such as endogenous thrombin potential and sP-selectin were upregulated in infected patients but reduced after treatment with benznidazole[187]. IFNγ, IL-12, IL-10, and CD40L have been studied as markers correlated with

disease progression[187,190], but have been studied in isolation and only as markers of treatment effectiveness. There is a need for markers that can identify patients at risk of severe disease pre-treatment.

There is evidence that parasite burden correlates with Chagas disease progression.[3] By comparing the transcriptomes of PBMCs taken from chronically infected monkeys with stable parasitemia over time and chronically infected monkeys with rising parasitemia over time, we can identify molecules associated with parasitemia control. These molecules can provide the foundation for functional biomarker studies by identifying which molecules to target for measurement in serum or blood. These biomarkers can serve as prognostic tools of disease progression, allowing for targeted anti-trypanosomic treatment to those high risk for severe disease.

Methods

Samples

The same samples from Aim 1 were used for Aim 2. All sample collections and handling were performed as described previously.

Parasitemia Measurement

Monkey blood samples were mixed with equal volumes of 6M guanidine-HCl 0.2 M EDTA shortly following collection and stored at 4ºC. DNA was extracted from 300 µL of blood/guanidine mixtures using the QIAamp DNA Blood Mini Kit (QIAGEN, Hilden, Germany). Quantitative real-time PCR (qPCR) was performed according to a previously

proposed methodology, using the duplex TaqMan system targeting the 195 bp region of *T. cruzi* satellite DNA. The qPCR reactions were carried out at a final volume of 20 µL containing 5 µL DNA from each sample, 750 µM of the two primers, and 50 µM of the TaqMan probe. The FastStart Universal Probe Master Rox Kit (Roche, Basel, Switzerland) was used, and the Techne PrimePro 48 Real-Time PCR detection system (Bibby Scientific, Staffordshire, UK) was used for amplification. A standard curve was obtained by extracting DNA from serially diluted epimastigote forms of the WB1 strain (DTU TcI), with a detection limit of 0.01 parasites/mL. Positive, negative, and reagent internal controls will be used for all qPCR reactions. Parasitemia of samples will be back calculated to the standard curve line using Techne ProStudy Software (Bibby Scientific, Staffordshire, UK).

Genotyping

The hypervariable intergenic region of the mini exon gene was PCR-amplified as per previously described protocols[55] from extracted DNA. PCR products were purified using an Invitrogen PureLink Quick PCR Purification Kit (Thermo Fisher Scientific, NY, USA) and sequenced using MiSeq Illumina sequencing. Reads were filtered using fastp program, a FASTQ preprocessor for quality control, adapter trimming, quality filtering, and per-read quality pruning.[191] Sequence reads were mapped to *T. cruzi* mini-exon reference sequences representing all parasite DTUs (H1 TcI [EF576846], Tu18 TcII [AY367125], M5631 TcIII

[AY367126], 92122102r TcIV [AY367124], SC43 TcV [AY367127], CL TcVI [U57984], and TCC2477 TcBat [KT305884]) using the BWA MEM mapper algorithm. Only sequences representing at least 1% of the reads were used to determine DTU within samples.

Sample Size/Power

Sample size was calculated as in Aim 1. Comparing uninfected, controller, and progressor groups we were also able to achieve a 99% power using at minimum 9 samples per group.

Transcriptome Analysis

PBMC handling, RNA extraction, DEG calling, and data analysis was performed as described in Aim 1.

Pathway/Biomarker Analysis

Pathway analysis was performed as described in Aim 1. Potential molecular biomarkers were found by querying the SPRomeDB, a free online database of human classical secretory proteins.

Results

Samples

Parasitemia over time of chronically infected monkeys used in Aim 1 had been previously quantified.[3] Monkeys had been infected for 4.1 ± 0.3 years at the start of the follow-up, with infections ranging from 1 to 6 years.[3] On average, monkeys were infected with 8.1 ± 1.5 parasite eq./ml of blood over 24-30 months of follow up as measured by qPCR.[3] Parasitemia changes measured over time revealed two groups of

infected monkeys: those with a slow decrease in parasitemia over time, called “Controllers”, and those with an increase in parasitemia over time, called “Progressors”.[3]

Table 3: Monkey Samples Used for Aim 2A

Monkey ID	Age	Sex	Infection Group	Infection Status
HA67	14	F	Infected	Controller
IN54	12	F	Infected	Controller
IP64	12	F	Infected	Controller
JC08	11	F	Infected	Controller
JM46	10	M	Infected	Controller
JN64	10	F	Infected	Controller
LL64	5	F	Infected	Controller
KP37	8	M	Infected	Controller
HN75	14	F	Infected	Controller
EP36	18	F	Infected	Progressor
GI52	15	F	Infected	Progressor
KA90	9	F	Infected	Progressor
KC05	9	F	Infected	Progressor
KL57	6	F	Infected	Progressor
JL71	11	M	Infected	Progressor
JT42	10	F	Infected	Progressor
MD12	4	F	Infected	Progressor
ED57	19	F	Infected	Progressor
AG23			Uninfected	Uninfected
HD69			Uninfected	Uninfected
ID59			Uninfected	Uninfected
JN58			Uninfected	Uninfected
KC78			Uninfected	Uninfected
KK63			Uninfected	Uninfected
KL72			Uninfected	Uninfected
KR83			Uninfected	Uninfected
LB83			Uninfected	Uninfected
LD53			Uninfected	Uninfected
ME13			Uninfected	Uninfected

Differential Gene Expression

PCA was used to visualize sample similarly by adjusted read count data (**Figure 13**). As expected, controllers and progressors clustered separately from uninfected samples. Controller samples clustered tightly; however, progressor samples displayed larger

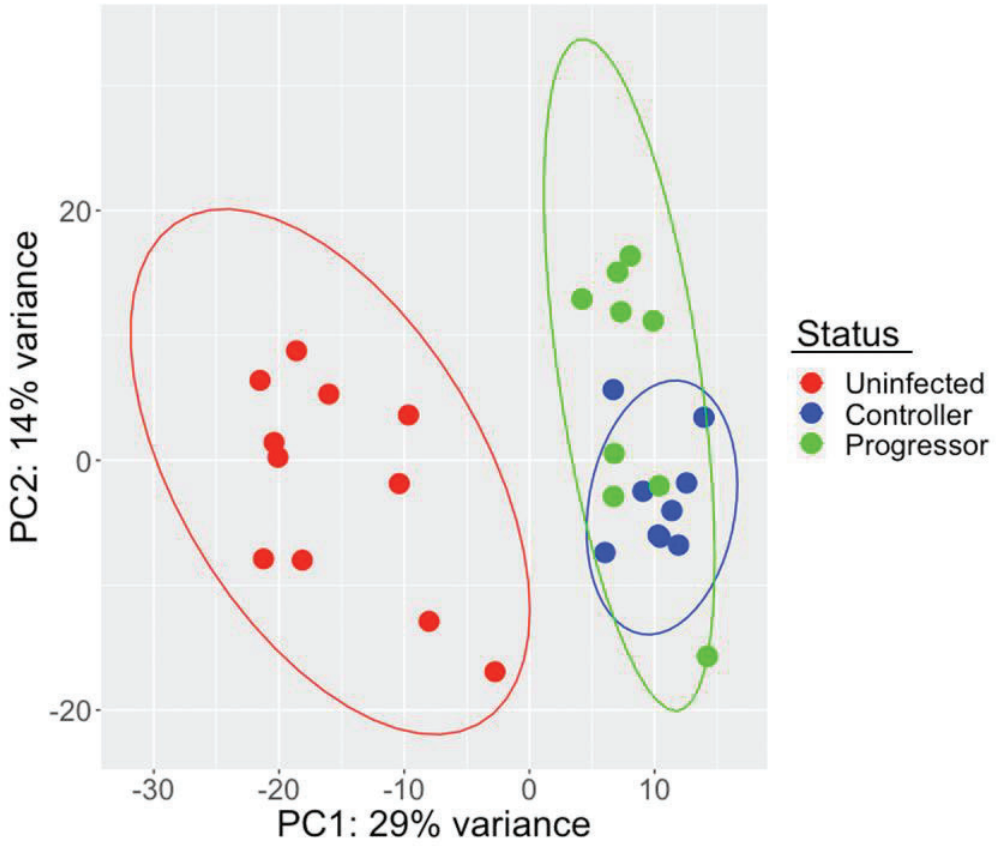

Figure 12: PCA of samples categorized as uninfected (Red), infected with controlled parasitemia (Controller, Blue), and infected with rising parasitemia (Progressor, Green)

Adjusted, normalized read counts from samples showed clear separation between uninfected (red) and infected monkeys. Categorized by infection status, those that could control parasitemia (Controllers, blue) clustered tightly while those with rising parasitemia (Progressors, green) showed heterogeneity within their group but remained separate from uninfected.

heterogeneity. The tight clustering of controller samples suggested an immune response specific to monkeys able to control parasite burden.

Differential expression was determined using uninfected monkeys as the comparison baseline group. After filtering and Q/C, 28076 genes remained for differential expression analysis. Controllers had 1349 genes upregulated and 912 genes downregulated compared to uninfected monkeys. Volcano plots were used to visualize this distribution (**Figure 14**). Progressors followed a similar pattern, 1231 upregulated and 985 downregulated genes compared to uninfected monkeys, against visualized by volcano plot (**Figure 15**).

Pathway Analysis

Significant DEGs were queried for functional pathway analysis. By comparing pathways over-enriched in controllers or progressors to the ones found in all infected monkeys in Aim 1, it was possible to identify immune responses relevant to controlling parasitemia, while clarifying those generally found during chronic infection.

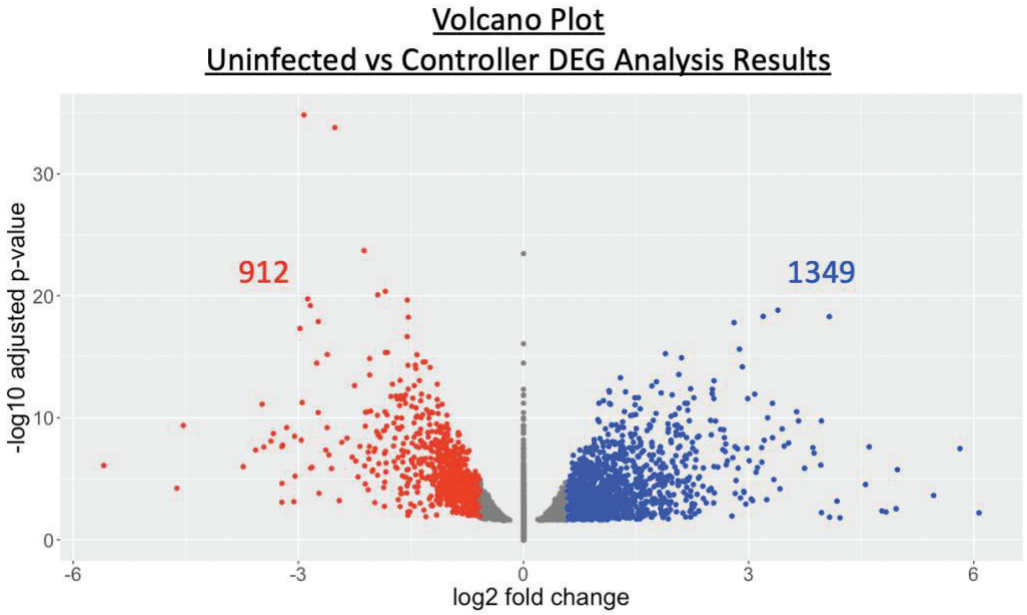

Figure 13: Volcano plot of the distribution of the differential gene expression analysis results between uninfected and infected monkeys that could control parasitemia.

Between uninfected and infected monkeys that could control parasitemia, 2216 genes had significant differential expression using an alpha = 0.05. Using a fold change cutoff of 1.5, of the 2216 genes, 1231 genes were upregulated (blue) and 985 genes were downregulated (red).

No upregulated pathways were found through this analysis method.

Comparatively, a substantial number of pathways were downregulated unique to infected monkeys that could control parasitemia and infected monkeys with rising parasitemia.

Unique pathways were found in controller monkeys (**Table 4)**. The IL-4 production pathway was specifically downregulated. In addition, T-cell differentiation pathways were specifically downregulated in controller monkeys compared to general lymphocyte activation found among all infected monkeys. Perhaps surprisingly, this included the T_H17 differentiation pathway.

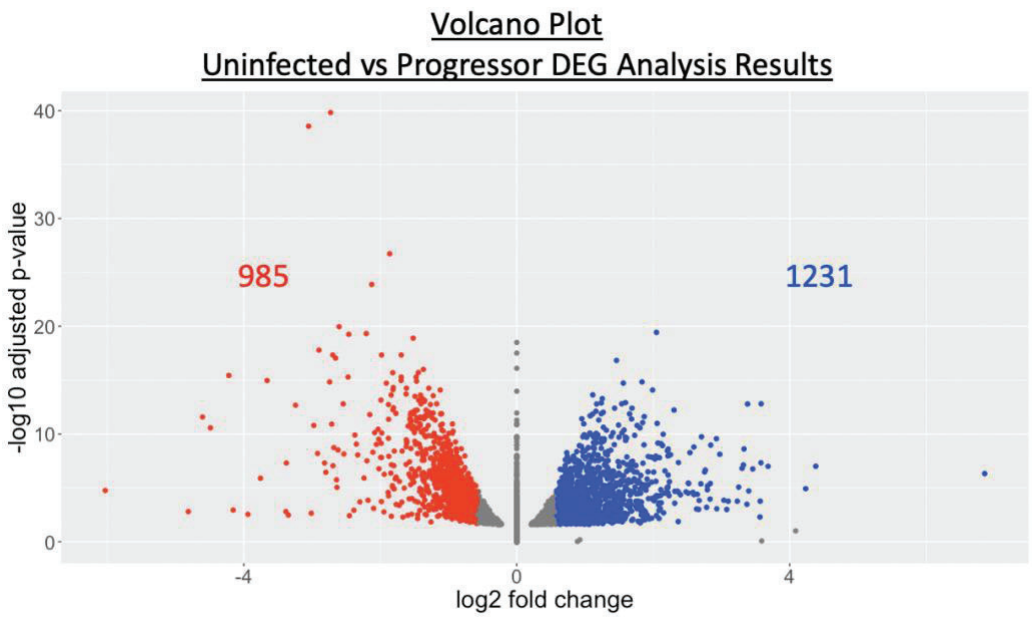

Figure 14: Volcano plot of the distribution of the differential gene expression analysis results between uninfected and infected monkeys with rising parasitemia.

Between uninfected and infected monkeys that could control parasitemia, 2261 genes had significant differential expression using an alpha = 0.05. Using a fold change cutoff of 1.5, of the 2261 genes, 1349 genes were upregulated (blue) and 912 genes were downregulated (red).

Table 4: Pathways over-enriched from genes differentially downregulated in infected monkeys that can control parasitemia compared to uninfected monkeys

Name	GO/KEGG ID	FDR p-value
alpha-beta T cell activation	GO:0046631	0.007
alpha-beta T cell differentiation	GO:0046632	0.008
cardiac ventricle morphogenesis	GO:0003208	0.016
cell activation	GO:0001775	0.002
cell-cell adhesion	GO:0098609	0.012

HIF-1 signaling pathway	mcc04066	0.003
immune effector process	GO:0002252	0.044
interleukin-4 production	GO:0032633	0.013
myeloid leukocyte differentiation	GO:0002573	0.032
outflow tract morphogenesis	GO:0003151	0.026
positive regulation of cell adhesion	GO:0045785	0.023
positive regulation of gene expression	GO:0010628	0.010
positive regulation of hemopoiesis	GO:1903708	0.006
positive regulation of immune system process	GO:0002684	0.041
positive regulation of leukocyte differentiation	GO:1902107	0.006
positive regulation of lymphocyte differentiation	GO:0045621	0.007
positive regulation of myeloid cell differentiation	GO:0045639	0.032
positive regulation of T cell differentiation	GO:0045582	0.009
regulation of cell adhesion	GO:0030155	0.015
regulation of cytokine production	GO:0001817	0.028
regulation of hemopoiesis	GO:1903706	0.002
regulation of interleukin-4 production	GO:0032673	0.013
regulation of leukocyte differentiation	GO:1902105	0.013
regulation of lymphocyte differentiation	GO:0045619	0.005
regulation of myeloid cell differentiation	GO:0045637	0.023
regulation of T cell differentiation	GO:0045580	0.003
response to lipid	GO:0033993	0.020
response to nitrogen compound	GO:1901698	0.023

response to oxygen-containing compound	GO:1901700	0.005
T cell differentiation	GO:0030217	0.022
Th17 cell differentiation	mcc04659	0.022
tissue remodeling	GO:0048771	0.034
viral life cycle	GO:0019058	0.040
viral process	GO:0016032	0.014

Among downregulated pathways found in progressor monkeys (**Table 5**), IFN-γ production was downregulated. In addition, progressor monkeys had downregulation of tolerance induction and regulation of apoptosis, suggesting a systemic compensatory mechanism to deal with non-functioning immune cells among these samples fighting rising parasite burden. Regulation of leukocyte, lymphocyte, mononuclear, and T cell proliferation pathways were all downregulated in progressor monkeys.

Table 5: Pathways over-enriched from genes differentially downregulated in infected monkeys with rising parasitemia compared to uninfected monkeys

Name	GO/KEGG ID	FDR p-value
adaptive immune response based on somatic recombination of immune receptors built from immunoglobulin superfamily domains	GO:0002460	0.024
endoplasmic reticulum unfolded protein response	GO:0030968	0.033
interferon-gamma production	GO:0032609	0.027
intrinsic apoptotic signaling pathway	GO:0097193	0.009

lymphocyte proliferation	GO:0046651	0.031
mononuclear cell proliferation	GO:0032943	0.031
positive regulation of apoptotic process	GO:0043065	0.004
positive regulation of cell death	GO:0010942	0.011
positive regulation of interferon-gamma production	GO:0032729	0.022
positive regulation of leukocyte mediated immunity	GO:0002705	0.039
positive regulation of programmed cell death	GO:0043068	0.005
protein catabolic process	GO:0030163	0.028
protein import	GO:0017038	0.028
receptor catabolic process	GO:0032801	0.024
regulation of interferon-gamma production	GO:0032649	0.027
regulation of leukocyte proliferation	GO:0070663	0.039
regulation of lymphocyte proliferation	GO:0050670	0.028
regulation of mononuclear cell proliferation	GO:0032944	0.028
regulation of T cell proliferation	GO:0042129	0.043
response to endoplasmic reticulum stress	GO:0034976	0.031
RNA processing	GO:0006396	0.014
T cell proliferation	GO:0042098	0.027
tolerance induction	GO:0002507	0.032

Identification of Immune Biomarkers Associated with Parasitemia Control

Differentially expressed cytokine, chemokine, and CD marker genes were identified for each comparison: uninfected vs controller and uninfected vs progressor (**Figure 16**). These immune biomarkers were surveyed because they represent potential low hanging fruit: cytokine, chemokines, and CD markers can be measured in blood and can serve as accessible prognostic indicators of what hosts can control parasitemia.

Among upregulated genes associated with immune biomarker expression, controller monkeys had a balanced T_H1/T_H2 profile: genes for IFNγ, IL-6, and IL-24 expression all were upregulated in controller

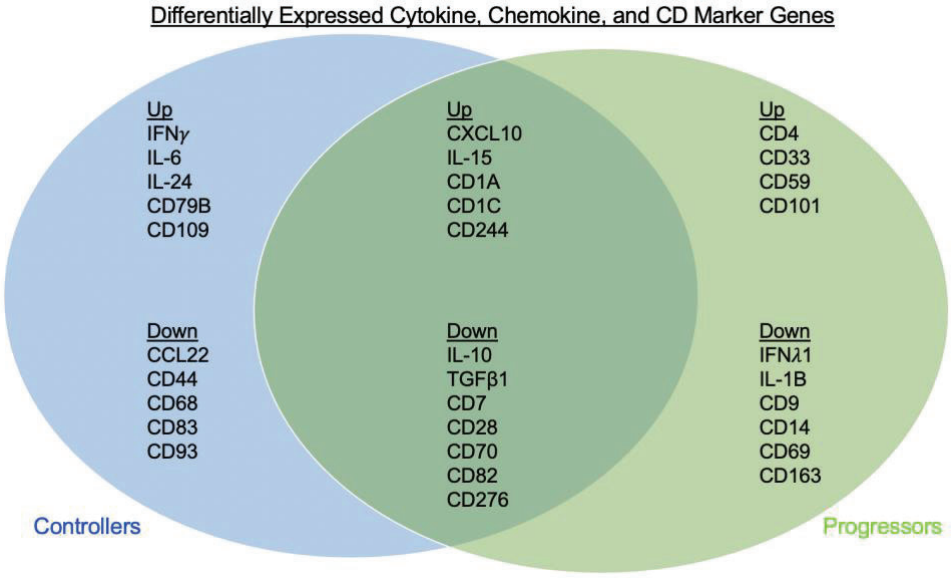

Figure 15: Shared and unique differentially expressed immune biomarkers between infected monkeys that can control parasitemia and infected monkeys with rising parasitemia.

Differentially expressed genes related to cytokine, chemokine, and CD marker expression compared between controller (blue) and progressor (green) samples. While both groups had a downregulated T_H2 profile, controllers balanced this with upregulated T_H1 and T_H2 responses, while progressors downregulated the T_H1 response.

monkeys. Downregulated genes in controller monkeys included the T-cell activator CCL22.

Progressors on the other hand only showed a downregulated T_H1 response, with IFNλ1 and IL-1B gene expression both down regulated in progressor monkeys.

CD markers can serve as immune biomarkers, both by suggesting differences in cell composition associated with parasitemia control or as membrane bound cell targets. While controller monkeys had upregulated CD79B and CD109 gene expression, both T-cell activators, they also had downregulated gene expression associated with lymphocyte, macrophage, and complement activation: CD44, CD68, CD83, and CD93 gene expression was downregulated in controller monkeys. These markers are also associated with dendritic cell inhibition.

CD marker gene expression upregulated in progressor monkeys were CD4, CD33, CD59, and CD101, all associated with T-cell activation as well as complement and monocyte inhibition. Progressor monkeys had downregulated gene expression of CD9, CD14, CD69, and CD163, markers associated with T cell inhibition, as well as monocyte, natural killer cell, and dendritic cell activation.

Multi-variate analysis was used to uncover which of these immune biomarkers were most associated with which group: uninfected, controller, or progressor. Between group analysis of gene expression between samples revealed strong separation of controller, progressor,

and uninfected monkeys along two main BGA discrimination axes (Figure 17B). The two main BGA discrimination axes provides coordinate data associated with sample clustering. By overlaying this coordinate data of the samples over the clustering of gene expression, genes found at the ends of the main BGA discrimination axes represent upregulated genes most associated with groups: controllers, progressors, or uninfected monkeys (Figure 17A). The top 20 genes associated with parasitemia control were identified along these main BGA discrimination axes. From this analysis, upregulation of IFNγ, CD1C, CD226, CD70, CD40LG,

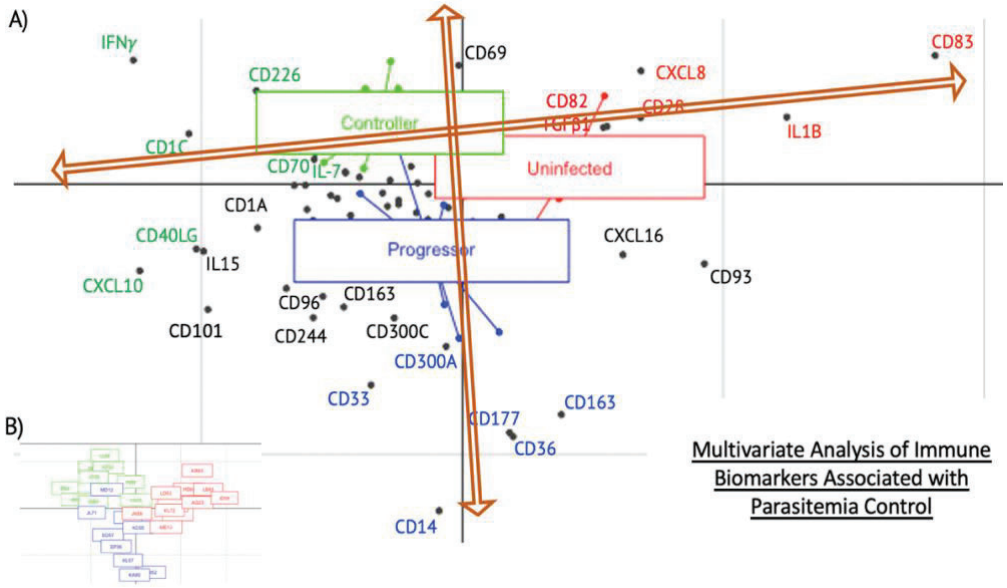

Figure 16: Between group analysis of cytokine, chemokine, and CD marker gene expression counts between uninfected monkeys (red), infected monkeys that could control parasitemia (green), and infected monkeys with rising parasitemia (blue).

Between group analysis showing their separation on the BGA discrimination axes along two lines of differentiation: infected vs uninfected (A). Clustering of samples used to create the BGA discrimination axes are shown in the inset (B). Black dots represent individual genes, colored dots and lines represent monkey samples, and the BGA discrimination axes are colored orange. Gene names are colored based on which group upregulation of the gene is predictive of.

CXCL10 and IL-7 gene expression were most associated with controller monkeys, whereas upregulation of CD14, CD36, CD177, CD33, CD300A, and CD163 gene expression were associated with progressor monkeys.

Identification of Protein Biomarkers Associated with Parasitemia Control

Differentially expressed genes not associated with immune biomarker expression were queried in the SPRomeDB database, a database of known human secreted proteins. Differentially expressed genes can represent differentially produced proteins that serve as candidate biomarkers of parasitemia control that are measurable in blood. Genes identified in the SPRomeDB database were further queried in the Human Protein Atlas (proteinatlas.org)[192] to condense the list into the best biomarker candidates: secreted proteins or transmembrane proteins expressed on specific immune cells with evidence of detection in blood by immunoassay and a high fold change of gene expression.

Among controller monkeys, 16 blood secreted proteins, 15 membrane proteins, and 7 intracellular proteins (**Table 7**) were identified. Of the 16 blood secreted proteins, 8 have been detected in blood by immunoassay, representing proteins most likely to be found and measurable in blood; 4 upregulated genes: apolipoprotein D (APOD), nucleobindin 2 (NUCB2), prepronociceptin (PNOC), protein S (PROS1) and 4 downregulated genes: lymphotoxin alpha (LTA), C1q and TNF

related 1 (C1QTNF1), HtrA serine peptidase 1 (HTRA1), oncostatin M (OSM). Eight additional secreted proteins were identified: inter-alpha-trypsin inhibitor heavy chain 2 (ITIH2), HtrA serine peptidase 4 (HTRA4), chondroadherin (CHAD), complement factor properdin (CFP), cartilage associated protein (CRTAP), cathepsin B (CTSB), transforming growth factor beta induced (TGFBI), and syndecan 4 (SDC4). Secreted proteins with the highest fold change have a good chance of being biomarkers of parasitemia control; among infected monkeys that could control parasitemia, these include upregulation of ITIH2 (Fold Change = 18.14) and downregulation of SDC4 (Fold Change = 0.25). Transmembrane proteins expressed on specific cell types also have a good chance of being biomarkers of parasitemia control. Among infected monkeys that could control parasitemia, immune cell specific transmembrane proteins with the largest fold changes included leucine rich repeat neuronal 3 (LRRN3) upregulated on $CD4^+$ T-cells and $CD8^+$ T-cells (Fold Change = 13.42), desmoglein 2 (DSG2) upregulated on basophils (Fold Change = 9.48), glycoprotein Ib platelet subunit alpha (GP1BA) upregulated on basophils (Fold Change = 2.76), and carboxypeptidase M (CPM) downregulated on dendritic cells and monocytes (Fold Change = 0.20).

Sixty-seven biomarker candidates were found differentially expressed among infected monkeys with rising parasitemia, 27 secreted proteins, 20 transmembrane proteins, and 20 intracellular proteins. Of the 27 secreted proteins, 8 have been detected in blood by immunoassay,

representing proteins most likely to be found and measurable in blood; upregulated platelet derived growth factor subunit B (PDGFB), upregulated von Willebrand factor (VWF), upregulated pro-platelet basic protein (PPBP), upregulated galanin GMAP prepropeptide (GAL), downregulated growth arrest specific 6 (GAS6), downregulated TIMP metallopeptidase inhibitor 1 (TIMP1), downregulated vascular endothelial growth factor A (VEGFA), and downregulated gremlin 1 DAN family BMP antagonist (GREM1). Secreted proteins with the highest fold change have a chance of being biomarkers of parasitemia control; among infected monkeys with rising parasitemia, these include upregulated latent transforming growth factor beta binding protein 1 (LTBP1), upregulated WNT inhibitory factor 1 (WIF1), upregulated coiled-coil glutamate rich protein 2 (CCER2), upregulated programmed cell death 1 ligand 2 (PDCD1LG2), and downregulated glycoprotein hormones alpha polypeptide (CGA). Transmembrane proteins expressed on specific cell types also have a good chance of being biomarkers of parasitemia control. Among infected monkeys with rising parasitemia, immune cell specific transmembrane proteins with the largest fold changes included integrin subunit alpha 2b upregulated on basophils (ITGA2B), inducible T cell costimulatory downregulated on T_{reg} cells (ICOS), and leucine rich repeat containing 32 downregulated on T_{reg} cells (LRRC32).

Table 6: Candidate protein biomarkers associated with infected monkeys that can control parasitemia

Gene Name	Fold Change	Description	Predicted Location	Immune Cell Specificity	Detected in Blood by Immunoassay
APOD	2.14	apolipoprotein D	Secreted	B-Cells	Yes
NUCB2	1.82	nucleobindin 2	Secreted	No	Yes
PNOC	1.71	prepronociceptin	Secreted	B-Cells, Dendritic Cells	Yes
PROS1	1.5	protein S	Secreted	No	Yes
LTA	0.59	lymphotoxin alpha	Secreted	No	Yes
C1QTNF1	0.46	C1q and TNF related 1	Secreted	No	Yes
HTRA1	0.34	HtrA serine peptidase 1	Secreted	No	Yes
OSM	0.1 control I7	oncostatin M	Secreted	Neutrophil, Basophils	Yes

ITIH2	18.14	inter-alpha-trypsin inhibitor heavy chain 2	Secreted	No	No
HTRA4	1.98	HtrA serine peptidase 4	Secreted	No	No
CHAD	1.54	chondroadherin	Secreted	B-Cells	No
CFP	0.64	complement factor properdin	Secreted	Dendritic Cells, Monocytes	No
CRTAP	0.63	cartilage associated protein	Secreted	Monocyte	No
CTSB	0.59	cathepsin B	Secreted	Dendritic Cells, Monocytes, Basophils	No
TGFBI	0.36	transforming growth factor beta induced	Secreted	Dendritic Cells, Monocytes	No
SDC4	0.25	syndecan 4	Secreted	No	No

LRRN3	13.42	leucine rich repeat neuronal 3	Membrane	CD4+ T-Cells, CD8+ T-Cells	No
DSG2	9.48	desmoglein 2	Membrane	Basophil	No
GYPA	3.64	glycophorin A (MNS blood group)	Membrane	No	No
GP1BA	2.76	glycoprotein Ib platelet subunit alpha	Membrane	Basophil	No
CD300LG	2.23	CD300 molecule like family member g	Membrane	No	No
SLC15A2	2.2	solute carrier family 15 member 2	Membrane	No	No
DLK1	2.09	delta like non-canonical Notch ligand 1	Membrane	No	No
SEMA4B	1.57	semaphorin 4B	Membrane	B-Cells, Neutrophils	No
NETO2	1.55	neuropilin and tolloid like 2	Membrane	No	No

ERN1	0.66	endoplasmic reticulum to nucleus signaling 1	Membrane	Basophil	No
SIRPA	0.64	signal regulatory protein alpha	Membrane	Dendritic Cells, Monocytes, Eosinophils, Neutrophils	No
NDRG1	0.63	N-myc downstream regulated 1	Membrane	No	No
SLC8B1	0.61	solute carrier family 8 member B1	Membrane	No	No
APLP2	0.57	amyloid beta precursor like protein 2	Membrane	Monocyte	No
CPM	0.2	carboxypeptidase M	Membrane	Dendritic Cells, Monocytes	No

MUC19	3.94	mucin 19, oligomeric	Intracellular	No	No
PIKFYVE	1.67	phosphoinositide kinase, FYVE-type zinc finger containing	Intracellular	No	No
CACNB1	1.62	calcium voltage-gated channel auxiliary subunit beta 1	Intracellular	No	No
MDN1	1.61	midasin AAA ATPase 1	Intracellular	No	No
NPC2	0.49	NPC intracellular cholesterol transporter 2	Intracellular	Dendritic Cells, Monocytes, Basophils, Neutrophils	No
RIN2	0.13	Ras and Rab interactor 2	Intracellular	Monocyte	No

B4GALNT1	0.04	beta-1,4-N-acetyl-galactosaminyltransferase 1	Intracellular	No	No

Table 7: Candidate protein biomarkers associated with monkeys infected with rising parasitemia

Gene Name	Fold Change	Description	Predicted Location	Immune Cell Specificity	Detected in Blood by Immunoassay
PDGFB	3.15	platelet derived growth factor subunit B	Secreted	T-cells	Yes
VWF	2.88	von Willebrand factor	Secreted	No	Yes
PPBP	2.73	pro-platelet basic protein	Secreted	Neutrophils, Basophils	Yes
GAL	1.52	galanin and GMAP prepropeptide	Secreted	No	Yes
GAS6	0.6	growth arrest specific 6	Secreted	Dendritic Cells	Yes
TIMP1	0.4	TIMP metallopeptidase inhibitor 1	Secreted	No	Yes
VEGFA	0.16	vascular endothelial growth factor A	Secreted	No	Yes
GREM1	0.06	gremlin 1, DAN family BMP antagonist	Secreted	No	Yes
LTBP1	4.94	latent transforming growth factor beta binding protein 1	Secreted	Basophils	No
WIF1	2.63	WNT inhibitory factor 1	Secreted	No	No
CCER2	2.42	coiled-coil glutamate rich protein 2	Secreted	No	No
PDCD1LG2	2.31	programmed cell death 1 ligand 2	Secreted	No	No
DNASE1	2.27	deoxyribonuclease 1	Secreted	No	No

CGREF1	2.22	cell growth regulator with EF-hand domain 1	Secreted	No	No
PSPN	2.12	persephin	Secreted	No	No
SERPINI 1	2.05	serpin family I member 1	Secreted	No	No
SPINT1	1.97	serine peptidase inhibitor, Kunitz type 1	Secreted	No	No
MZB1	1.84	marginal zone B and B1 cell specific protein	Secreted	Dendritic Cells, B-Cells	No
SFRP5	1.81	secreted frizzled related protein 5	Secreted	CD8+ T-Cells	No
LGALS3 BP	1.77	galectin 3 binding protein	Secreted	No	No
PI16	1.7	peptidase inhibitor 16	Secreted	Treg-Cells	No
SMPDL3 A	1.69	sphingomyelin phosphodiesterase acid like 3A	Secreted	Basophil s	No
PLOD3	1.68	procollagen-lysine,2-oxoglutarate 5-dioxygenase 3	Secreted	No	No
WFIKKN 1	1.57	WAP, follistatin/kazal, immunoglobulin, kunitz and netrin domain containing 1	Secreted	No	No
NOTUM	0.66	notum, palmitoleoyl-protein carboxylesterase	Secreted	No	No
CHI3L2	0.65	chitinase 3 like 2	Secreted	No	No
CGA	0.17	glycoprotein hormones, alpha polypeptide	Secreted	No	No
PKHD1L 1	2.96	PKHD1 like 1	Membra ne	No	No
SDK2	2.93	sidekick cell adhesion molecule 2	Membra ne	No	No
ITGA2B	2.85	integrin subunit alpha 2b	Membra ne	Basophil s	No
SELPLG	2.24	selectin P ligand	Membra ne	No	No
GP9	2.23	glycoprotein IX platelet	Membra ne	Neutroph ils,	No

				Basophils	
TTYH2	2.22	tweety family member 2	Membrane	Dendritic Cells, Monocytes	No
DCBLD2	2.07	discoidin, CUB and LCCL domain containing 2	Membrane	No	No
SIGLEC1	2	sialic acid binding Ig like lectin 1	Membrane	Monocyte	No
DHRS9	1.98	dehydrogenase/reductase 9	Membrane	Neutrophils, Basophils, Eosinophils	No
PCDH1	1.98	protocadherin 1	Membrane	No	No
BTN3A1	1.89	butyrophilin subfamily 3 member A1	Membrane	No	No
BRI3BP	1.89	BRI3 binding protein	Membrane	Eosinophils	No
ADAM10	1.73	ADAM metallopeptidase domain 10	Membrane	No	No
THY1	1.66	Thy-1 cell surface antigen	Membrane	No	No
TAPBP	1.54	TAP binding protein	Membrane	No	No
SARAF	0.65	store-operated calcium entry associated regulatory factor	Membrane	No	No
ICAM1	0.49	intercellular adhesion molecule 1	Membrane	No	No
SEMA4C	0.29	semaphorin 4C	Membrane	No	No
ICOS	0.18	inducible T cell costimulator	Membrane	Treg-Cells	No
LRRC32	0.13	leucine rich repeat containing 32	Membrane	Treg-Cells	No
CDH13	6.22	cadherin 13	Intracellular	Monocyte	No

OAS2	4.16	2'-5'-oligoadenylate synthetase 2	Intracellular	No	No
ANK1	3.39	ankyrin 1	Intracellular	B-Cells	No
PTGS1	2.48	prostaglandin-endoperoxide synthase 1	Intracellular	Basophils	No
GGH	1.94	gamma-glutamyl hydrolase	Intracellular	Dendritic Cells	No
TRIM47	1.87	tripartite motif containing 47	Intracellular	No	No
TXNDC15	1.86	thioredoxin domain containing 15	Intracellular	No	No
AHCYL1	1.72	adenosylhomocysteinase like 1	Intracellular	No	No
FUCA1	1.64	alpha-L-fucosidase 1	Intracellular	No	No
POGLUT1	1.57	protein O-glucosyltransferase 1	Intracellular	No	No
PPT2	1.54	palmitoyl-protein thioesterase 2	Intracellular	CD8+ T-Cells	No
SPATS2L	1.54	spermatogenesis associated serine rich 2 like	Intracellular	Basophils	No
TPST2	1.52	tyrosylprotein sulfotransferase 2	Intracellular	No	No
CNPY2	1.5	canopy FGF signaling regulator 2	Intracellular	No	No
SRSF3	0.64	serine and arginine rich splicing factor 3	Intracellular	No	No
UTP4	0.63	UTP4 small subunit processome component	Intracellular	No	No
ZNF821	0.54	zinc finger protein 821	Intracellular	B-cells, Treg-Cells	No
SDF2	0.52	stromal cell derived factor 2	Intracellular	No	No
DNAJB9	0.45	DnaJ heat shock protein family (Hsp40) member B9	Intracellular	No	No
PUS3	0.4	pseudouridine synthase 3	Intracellular	No	No

Discussion

To identify biomarkers associated with parasitemia control, transcriptomes of PBMCs from chronically infected monkeys with controlled parasitemia and transcriptomes of PBMCS from chronically infected monkeys with rising parasitemia were compared to uninfected samples. In this way, the immune response described in Aim 1 could be broken down into necessary molecules for parasite control, and any molecules potentially overexpressed or underexpressed in blood in infected monkeys able to control parasitemia and infected monkeys unable to control parasitemia could be identified. These molecules can serve has readily measurable biomarkers of parasitemia control in blood of infected hosts, providing prognostic targets of disease progression.

Due to the complex network of the immune system, it is unlikely that a single molecule can suffice as an immune biomarker of parasitemia control. Multivariate analysis allowed for the incorporation of multiple markers to test which markers are most predictive of ability to control parasitemia. Through this we were able to determine that a combination of upregulated IFNγ, CXCL10, IL-7, CD1C, CD226, CD70, and CD40LG could predict controller group status. Both IFNγ and CD40 have been suggested as biomarkers for disease progression previously[179]; however, our results suggest that these markers are predictive of controller status, not just overall infection. CXCL10 is generally upregulated in response to IFNγ; therefore, it makes sense that

upregulation of CXCL10 and IFNγ could predict the same group. IFNγ, CXCL10, IL-7, and CD40L can all be found as soluble molecules, meaning they can be measured in circulation. CD40L can also be found as a transmembrane protein, in addition to transmembrane proteins CD1C, CD226, and CD70. CD40L is a marker for activated CD4+ T-cells and CD1C is expressed on dendritic cells, suggesting that upregulation of these cell types could also serve as prognostic markers of parasitemia control. Expression of CD70 is highly regulated and transiently expressed by activated immune cells.[193] Polarization of CD70 expression could serve as a sensitive biomarker of controller status. The combination of upregulated cell surface markers CD14, CD177, CD36, CD33, CD300A, and CD163 could predict progressor status. CD14 and CD163 can both be found in soluble or transmembrane form expressed by monocytes and macrophages, making these likely targets for detection in blood; whereas CD177 is expressed on neutrophils and CD36, CD33, CD163, and CD14 expressed on monocytes and dendritic cells.

Many of the differentially expressed genes found in infected monkeys that could control parasitemia and infected monkeys that had rising parasitemia lead to expression of secreted proteins which could be measured in blood, acting as biomarkers predictive of ability to control parasitemia. We queried all non-immune biomarkers in the SPRomeDB, a free database of human classical secretory proteins, and the Human Protein Atlas to determine which differentially expressed genes lead to

expression of likely protein biomarker candidates. Interesting biomarker candidates expressed by infected monkeys that could control parasitemia were APOD, NUCB2, PNOC, PROS1, LTA, C1QTNF1, HTRA1, OSM, ITIH2, LRRN3, DSG2, and CPM. An isoform fragment of APOD, APOA1, has been proposed as a biomarker of Chagas disease treatment effectiveness[194], our work identifying over expression of APOD in infected monkeys that could control parasitemia suggests that perhaps targeting the whole gene or alternative isoforms may be more informative as a marker for disease progression. Polymorphisms in the LTA gene have been associated with chronic Chagas cardiomyopathy, yet the downregulated LTA protein we identified as a potential biomarker of infected monkeys that could control parasite has not been explored as a biomarker[195]. Six genes expressed secreted proteins that have been identified in blood using immunoassays: NUCB2, PNOC, and PROS1 were over-expressed in infected monkeys that could control parasitemia and C1QTNF1, HTRA1, and OSM were under-expressed in infected monkeys that could control parasitemia. Our work suggests that these would be optimum proteins for future functional studies as the tools exists to detect protein expression of NUCB2, PNOC, PROS1, C1QTNF1, HTRA1, and OSM easily from blood samples usually collected during routine examinations. ITIH2 had an 18.14 fold change in gene expression among infected monkeys with controlled parasitemia, the largest of all secreted proteins, suggesting this protein could be easily detected as a

biomarker of parasitemia control. Differentially expressed genes in infected monkeys that could control parasitemia that express cell surface markers included LRRN3, DSG2, and CPM. LRRN3 was previously found upregulated in monocytes[196], yet its expression on CD4+ T cells and CD8+ T cells have only been explored as a biomarker of HIV infection progression[197] and not as a biomarker of *T. cruzi* parasitemia control despite the high fold change in gene expression found among infected monkeys that could control parasitemia. DSG2, highly over expressed on basophils in infected monkeys that could control parasitemia, has been explored as a biomarker in various cancers[198] suggesting its prognostic role in other diseases. PDGFB, VWF, PPBP, GAL, GAS6, TIMP1, VEGFA, and GREM1 are all likely candidates as biomarkers of infected monkeys with rising parasitemia, as proteins expressed by these genes were likely to be secreted proteins in blood detectable by immunoassay. Both VEGFA and GREM1 were over 5 times under expressed in infected monkeys with rising parasitemia, suggesting differential expression could be large enough to provide prognostic value. Two transmembrane proteins, ICOS, LRRC32, both underexpressed on T_{reg} cells, could represent unique biomarkers for infected monkeys with rising parasitemia due to their expression on a unique population of T cells and the large fold change of expression.

In conclusion, we were able to identify biomarkers associated with parasitemia control in infected monkeys using PBMC transcriptome data

from infected monkeys able to control parasitemia and infected monkeys with rising parasitemia. Immune biomarkers upregulated in infected monkeys able to control parasitemia include IFNγ, CXCL10, IL-7, CD1C, CD226, CD70, and CD40LG whereas immune biomarkers upregulated in infected monkeys with rising parasitemia include CD14, CD177, CD36, CD33, CD300A, and CD163. We were also able to identify an additional 78 candidate protein biomarkers for parasitemia control, future studies can use this list as a starting point for functional biomarker studies, as many of the candidate proteins have been detected in blood using immunoassays.

X. Aim 2B: Characterize the Immune Response of Infected Monkeys with Parasite Diversity

Background

Nearly all parasite strains have resulted in human disease[43] but the relationship between *T. cruzi* strains and Chagas disease pathology is unclear. Both host and parasite traits can affect disease progression and outcomes:[74] experiments have shown that different parasite strains can elicit different pathologies in the same host,[74,95,199] exhibit different tissue tropisms,[86,200] and have different responses to anti-Trypanosoma drugs.[201]

Next-generation sequencing and new genetic markers, alongside the DTU classification system, have improved the ability to associate strains and pathology. Experimental infections with different pairs of parasite DTUs suggest differences in disease severity, pathology, and drug susceptibility among pairs[43,48,79,201-208]; however, these associations are difficult to generalize because laboratory experiments are restricted to culture adapted strains and limited number of strain combinations.

Recently, a study in natural infections found hosts infected with a high parasite genetic diversity could control parasitemia better than hosts infected with a low parasite genetic diversity.[3] Many non-exclusive theories have been suggested for this including competition between strains for resources or a more broad and diverse immune response against the infection. It is likely that competition between parasite strains

is occuring[3]; however, the host immune response to parasite diversity has yet to be explored, particularly in the context of natural infections.

We will compare the transcriptomes of PBMCs taken from naturally infected monkeys with high and low parasite genotype diversity, characterizing the immune response in each group. With this information, we can explore or confirm the theory that increasing parasite diversity results in a balanced and diverse immune response against the infection.

Results

Samples

Differential expression of significant genes from infected monkeys displayed distinct heterogeneity, clustering into three groups with similar gene expression patterns (**Figure 20**) suggesting another covariate could further help explain differences in the immune response.

To investigate if parasite diversity could explain this clustering within infected monkeys, samples with similar gene expression profiles were categorized by cluster. No differences in age, duration of infection, or sex were found between clusters. Infected monkeys from Aim 2A had been previously genotyped.[3] The average number of parasite genotypes were significantly different between clusters of gene expression (**Figure 21**). Monkeys in gene expression cluster 3 had a significantly higher number of parasite DTUs compared to those in cluster 1 with 3.38

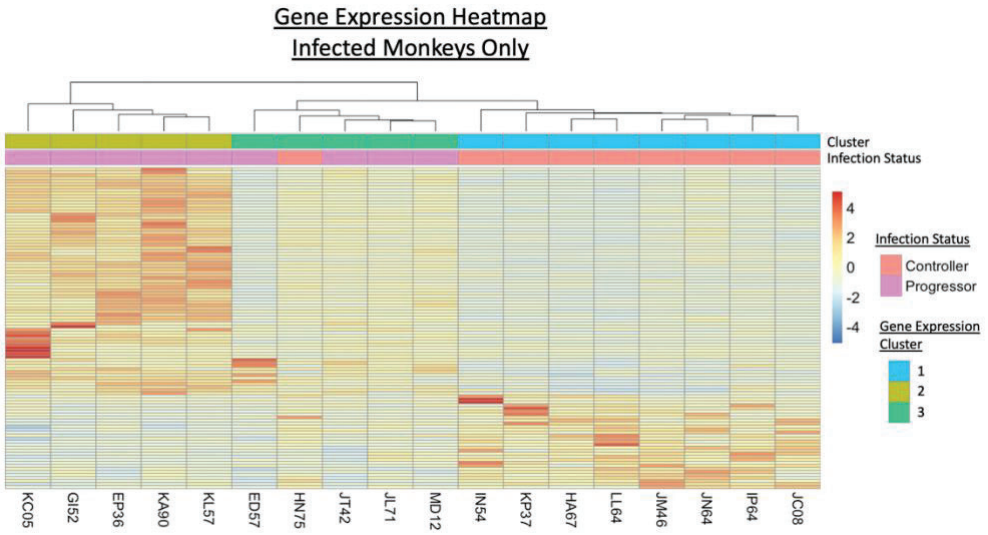

Figure 17: Comparative gene expression between infected monkeys.

Heatmap of differential gene expression among infected monkeys compared to uninfected monkeys. Infected monkeys appear to cluster into 3 groups ("Gene Expression Cluster", Blue/Yellow/Light Green). Distribution of infection status (Controllers, Peach and Progressors, Pink) is also displayed

DTUs/monkey in gene expression cluster 3 and 2 DTUs/monkey in gene expression cluster 1. Monkeys in gene expression cluster 2 had 2.6 DTUs/monkey, and while non-significantly different between cluster 1 and 2, potentially represent an in-between state between the two.

Only controller monkeys were found in gene expression cluster 1, both controller monkeys and progressor monkeys were found in gene expression cluster 2, and only progressor monkeys were found in gene expression cluster 3.

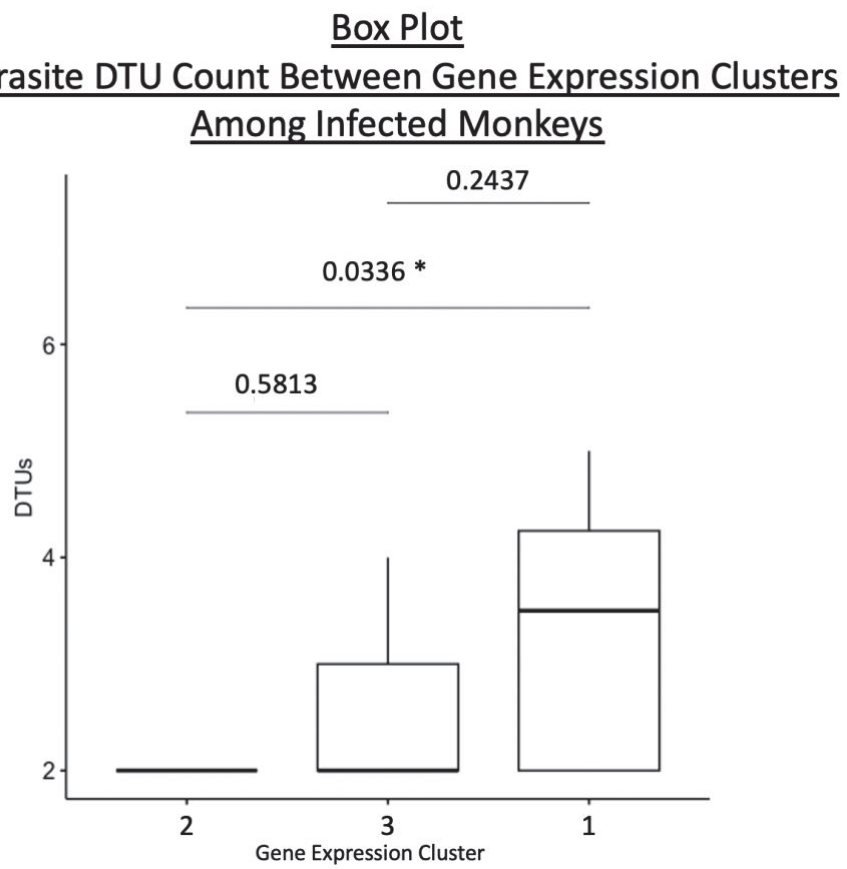

Figure 18:Gene expression clusters contain significantly different rates of parasite diversity

Within infected monkeys, gene expression clustered into three groups. There was a statistically significant difference in parasite diversity between gene expression cluster 1 and 2 (mean 3.38 DTUs/ sample and 2 DTUs/sample, Tukey test p-value = 0.0336). No parasite diversity difference could be found between gene expression cluster 1 and 3 or gene expression cluster 2 and 3.

Functional Response

The gene expression profile from each gene expression cluster was compared to uninfected monkeys to determine immune system changes associated with parasite diversity. Functional pathways and signaling molecules were explored as in Aim 1 and Aim 2A.

Monkeys infected with a high diversity of parasite strains had far more downregulated immune system pathways over-represented than

monkeys infected with a low diversity of parasite strains. All downregulated immune system pathways overrepresented in monkeys infected with a low diversity of parasite strains were found in downregulated immune system pathways over-represented in monkeys with a high diversity of parasite strains. Monkeys infected with a medium diversity of parasite strains had no downregulated pathways over-represented. None of the groups had any upregulated pathways over-represented.

All downregulated pathways over-represented in monkeys infected with a low diversity of parasite strains were also downregulated in monkeys infected with a high diversity of parasite strains. These pathways found in both monkeys infected with a high diversity of strains and monkeys infected with a low diversity of strains were related to T cell activity: T cell activation, T cell proliferation, and cell-cell adhesion.

Monkeys infected with a high diversity of parasite strains had downregulated pathways involved in both overall immune system processes as well as intracellular processes (**Table 7**). Immune system processes downregulated were T cell activation and proliferation, specifically $CD4^+$ T cells, IL-2, IL-10, and IL-4 production, tolerance induction, and the adaptive immune response. Downregulation of these pathways suggests an anti-inflammatory response, both T_H1 and T_H2, in monkeys infected with high diversity of parasite strains specifically. Monkeys infected with a high diversity of parasite strains also had

downregulation of intracellular processes: cellular response to external stressors, metabolism, energy consumption, and protein folding and expression, indicating that monkeys infected with a high diversity of parasite strains had dysregulated immune cells, focused on lymphocytes specifically $CD4^+$ T cells.

Table 8: Pathways over-enriched from genes differentially downregulated in infected monkeys with high diversity of parasite compared to uninfected monkeys.

Name	GO/KEGG ID	FDR p-value
adaptive immune response	GO:0002250	0.0238
adaptive immune response based on somatic recombination of immune receptors built from immunoglobulin superfamily domains	GO:0002460	0.0272
alpha-beta T cell activation	GO:0046631	0.0146
alpha-beta T cell differentiation	GO:0046632	0.0163
apoptotic signaling pathway	GO:0097190	0.0034
CD4-positive, alpha-beta T cell activation	GO:0035710	0.0464
cell activation	GO:0001775	0.0067
cell-cell adhesion	GO:0098609	0.0043

cellular response to biotic stimulus	GO:0071216	0.0032
cellular response to external stimulus	GO:0071496	0.0114
cellular response to extracellular stimulus	GO:0031668	0.0273
cellular response to glucose starvation	GO:0042149	0.0238
cellular response to lipid	GO:0071396	0.0094
cellular response to lipopolysaccharide	GO:0071222	0.0032
cellular response to molecule of bacterial origin	GO:0071219	0.0050
cellular response to nutrient levels	GO:0031669	0.0325
cellular response to oxygen-containing compound	GO:1901701	0.0191
cellular response to starvation	GO:0009267	0.0387
cellular response to topologically incorrect protein	GO:0035967	0.0423
cellular response to unfolded protein	GO:0034620	0.0236
cranial skeletal system development	GO:1904888	0.0438
cytokine production	GO:0001816	0.0031
DNA damage response, signal transduction by p53 class mediator	GO:0030330	0.0104
endoplasmic reticulum unfolded protein response	GO:0030968	0.0114

establishment of protein localization to organelle	GO:0072594	0.0120
hematopoietic or lymphoid organ development	GO:0048534	0.0003
hemopoiesis	GO:0030097	0.0004
I-kappaB kinase/NF-kappaB signaling	GO:0007249	0.0135
immune effector process	GO:0002252	0.0214
immune response-regulating signaling pathway	GO:0002764	0.0391
immune system development	GO:0002520	0.0002
inflammatory response	GO:0006954	0.0039
interleukin-2 production	GO:0032623	0.0070
interleukin-4 production	GO:0032633	0.0024
intrinsic apoptotic signaling pathway	GO:0097193	0.0126
leukocyte activation	GO:0045321	0.0024
leukocyte cell-cell adhesion	GO:0007159	0.0001
leukocyte differentiation	GO:0002521	0.0004
leukocyte proliferation	GO:0070661	0.0204
lymphocyte activation	GO:0046649	0.0002
lymphocyte differentiation	GO:0030098	0.0031
lymphocyte proliferation	GO:0046651	0.0095
mononuclear cell differentiation	GO:1903131	0.0029
mononuclear cell proliferation	GO:0032943	0.0095

mRNA metabolic process	GO:0016071	0.0449
mucopolysaccharide metabolic process	GO:1903510	0.0418
myeloid cell differentiation	GO:0030099	0.0025
myeloid dendritic cell activation	GO:0001773	0.0431
myeloid leukocyte differentiation	GO:0002573	0.0043
negative regulation of cell migration	GO:0030336	0.0449
negative regulation of cell-cell adhesion	GO:0022408	0.0298
negative regulation of cellular protein metabolic process	GO:0032269	0.0062
negative regulation of cytokine production	GO:0001818	0.0344
negative regulation of gene expression	GO:0010629	0.0056
negative regulation of NF-kappaB transcription factor activity	GO:0032088	0.0492
negative regulation of protein metabolic process	GO:0051248	0.0141
negative regulation of response to biotic stimulus	GO:0002832	0.0080
osteoclast differentiation	GO:0030316	0.0236
positive regulation of catabolic process	GO:0009896	0.0034
positive regulation of cell activation	GO:0050867	0.0070

positive regulation of cell adhesion	GO:0045785	0.0009
positive regulation of cell death	GO:0010942	0.0470
positive regulation of cell differentiation	GO:0045597	0.0060
positive regulation of cell-cell adhesion	GO:0022409	0.0013
positive regulation of cellular catabolic process	GO:0031331	0.0067
positive regulation of cytokine production	GO:0001819	0.0060
positive regulation of developmental process	GO:0051094	0.0223
positive regulation of gene expression	GO:0010628	0.0023
positive regulation of hemopoiesis	GO:1903708	0.0033
positive regulation of immune system process	GO:0002684	0.0024
positive regulation of interleukin-10 production	GO:0032733	0.0267
positive regulation of interleukin-2 production	GO:0032743	0.0114
positive regulation of interleukin-4 production	GO:0032753	0.0267
positive regulation of leukocyte activation	GO:0002696	0.0062

positive regulation of leukocyte cell-cell adhesion	GO:1903039	0.0003
positive regulation of leukocyte differentiation	GO:1902107	0.0033
positive regulation of lymphocyte activation	GO:0051251	0.0029
positive regulation of lymphocyte differentiation	GO:0045621	0.0141
positive regulation of mononuclear cell migration	GO:0071677	0.0354
positive regulation of myeloid cell differentiation	GO:0045639	0.0033
positive regulation of NF-kappaB transcription factor activity	GO:0051092	0.0267
positive regulation of programmed cell death	GO:0043068	0.0492
positive regulation of Ras protein signal transduction	GO:0046579	0.0354
positive regulation of reactive oxygen species metabolic process	GO:2000379	0.0238
positive regulation of small GTPase mediated signal transduction	GO:0051057	0.0354
positive regulation of T cell activation	GO:0050870	0.0024

positive regulation of T cell differentiation	GO:0045582	0.0070
protein import	GO:0017038	0.0395
protein localization to nucleus	GO:0034504	0.0449
protein localization to organelle	GO:0033365	0.0492
regulation of autophagy	GO:0010506	0.0272
regulation of catabolic process	GO:0009894	0.0050
regulation of cell activation	GO:0050865	0.0031
regulation of cell adhesion	GO:0030155	0.0008
regulation of cell migration	GO:0030334	0.0189
regulation of cell motility	GO:2000145	0.0416
regulation of cell-cell adhesion	GO:0022407	0.0001
regulation of cellular catabolic process	GO:0031329	0.0024
regulation of cellular component movement	GO:0051270	0.0323
regulation of cytokine production	GO:0001817	0.0029
regulation of DNA-binding transcription factor activity	GO:0051090	0.0287
regulation of hemopoiesis	GO:1903706	0.0004
regulation of I-kappaB kinase/NF-kappaB signaling	GO:0043122	0.0303
regulation of immune response	GO:0050776	0.0431
regulation of interleukin-2 production	GO:0032663	0.0070

regulation of interleukin-4 production	GO:0032673	0.0024
regulation of leukocyte activation	GO:0002694	0.0023
regulation of leukocyte cell-cell adhesion	GO:1903037	0.0001
regulation of leukocyte differentiation	GO:1902105	0.0024
regulation of leukocyte proliferation	GO:0070663	0.0055
regulation of lymphocyte activation	GO:0051249	0.0002
regulation of lymphocyte differentiation	GO:0045619	0.0141
regulation of lymphocyte proliferation	GO:0050670	0.0033
regulation of mononuclear cell proliferation	GO:0032944	0.0033
regulation of myeloid cell differentiation	GO:0045637	0.0024
regulation of myeloid leukocyte differentiation	GO:0002761	0.0216
regulation of protein modification by small protein conjugation or removal	GO:1903320	0.0366
regulation of regulatory T cell differentiation	GO:0045589	0.0063
regulation of T cell activation	GO:0050863	0.0001
regulation of T cell differentiation	GO:0045580	0.0039
regulation of T cell proliferation	GO:0042129	0.0024
regulatory T cell differentiation	GO:0045066	0.0086
response to bacterium	GO:0009617	0.0051

response to dsRNA	GO:0043331	0.0128
response to endoplasmic reticulum stress	GO:0034976	0.0043
response to lipid	GO:0033993	0.0024
response to lipopolysaccharide	GO:0032496	0.0023
response to molecule of bacterial origin	GO:0002237	0.0033
response to muramyl dipeptide	GO:0032495	0.0449
response to nitrogen compound	GO:1901698	0.0024
response to organic cyclic compound	GO:0014070	0.0155
response to organonitrogen compound	GO:0010243	0.0095
response to oxygen-containing compound	GO:1901700	0.0025
response to peptide	GO:1901652	0.0354
response to starvation	GO:0042594	0.0492
signal transduction by p53 class mediator	GO:0072331	0.0288
signal transduction in response to DNA damage	GO:0042770	0.0128
T cell activation	GO:0042110	0.0002
T cell differentiation	GO:0030217	0.0035
T cell proliferation	GO:0042098	0.0056
tolerance induction	GO:0002507	0.0141

vasculogenesis	GO:0001570	0.0325
viral process	GO:0016032	0.0492

Table 9: Pathways over-enriched from genes differentially downregulated in infected monkeys with low diversity of parasite compared to uninfected monkeys.

Name	GO/KEGG ID	FDR p-value
RNA processing	GO:0006396	0.0002
regulation of T cell activation	GO:0050863	0.0035
regulation of leukocyte cell-cell adhesion	GO:1903037	0.0035
leukocyte cell-cell adhesion	GO:0007159	0.0140
positive regulation of leukocyte cell-cell adhesion	GO:1903039	0.0140
T cell activation	GO:0042110	0.0179
positive regulation of T cell activation	GO:0050870	0.0185
mRNA metabolic process	GO:0016071	0.0216
protein import	GO:0017038	0.0220
regulation of cell-cell adhesion	GO:0022407	0.0238
positive regulation of cell-cell adhesion	GO:0022409	0.0318
mRNA processing	GO:0006397	0.0318
positive regulation of leukocyte activation	GO:0002696	0.0318
positive regulation of lymphocyte activation	GO:0051251	0.0318
positive regulation of cell activation	GO:0050867	0.0342
regulation of lymphocyte activation	GO:0051249	0.0421

regulation of T cell proliferation	GO:0042129	0.0421
T cell proliferation	GO:0042098	0.0421

Cytokine Inflammatory Profile

To identify the pro-inflammatory/anti-inflammatory profile of infected monkeys with high parasite diversity and infected monkeys with low parasite diversity, cytokine gene expression was investigated.

The profile of monkeys infected with high diversity of parasite showed a balanced T_H1/T_H2 response based on cytokine gene expression (**Figure 19A**). Gene expression of T_H1 activation cytokines, IL-15 and IFGγ, were upregulated, whereas the T_H2 activation cytokine gene expression IL-24 was also upregulated. Monkeys infected with a high diversity of parasite also had a downregulation of anti-inflammatory TGFβ1 gene expression.

The profile of monkeys infected with low diversity of parasite had a largely T_H1 skewed response with upregulated gene expression of T_H1 activation cytokine IL-15. Monkeys infected with low diversity of parasite had downregulated anti-inflammatory cytokine TGFβ1 and downregulated T_H1 activation cytokine IL-16; however, downregulation of IL-16 did not achieve statistical significance.

Immune Cell Activation

To determine cell trafficking and cell activation profiles associated with increasing parasite diversity, gene expression of chemokines and

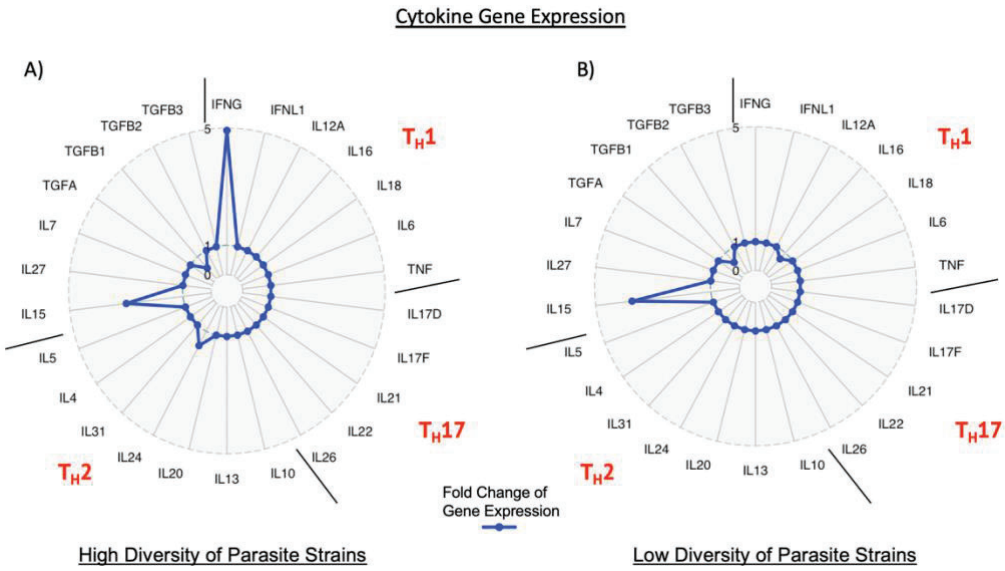

Figure 19: Fold change of cytokine gene expression

Fold change of cytokine gene expression visualized using a radar plot to compare the response between infected monkey PBMCs with high parasite diversity (A) and infected monkey PBMCs with low parasite diversity (B) compared to uninfected monkeys. Arrows indicate genes that were significantly different in expression as called by DESeq2 analysis. Arrows are colored to indicate the direction of expression change in infected monkeys compared to uninfected monkeys: up (green) or down (red).

CD markers were investigated in infected monkeys with high parasite diversity and infected monkeys with low parasite diversity.

Monkeys infected with a high parasite diversity had upregulation of CXCL10 gene expression, a chemokine associated with T-cell trafficking (**Figure 20A**). Monkeys infected with a high parasite diversity had slight downregulation of CCL22, a chemokine associated with T-cell and monocyte/macrophage trafficking. CD marker gene expression in infected monkeys with a high parasite diversity showed a balanced profile of immune cell activation (**Figure 21A**). T-cell activation markers such as CD109 gene expression were upregulated in infected monkeys with high parasite diversity, alongside downregulated T-cell activation marker gene

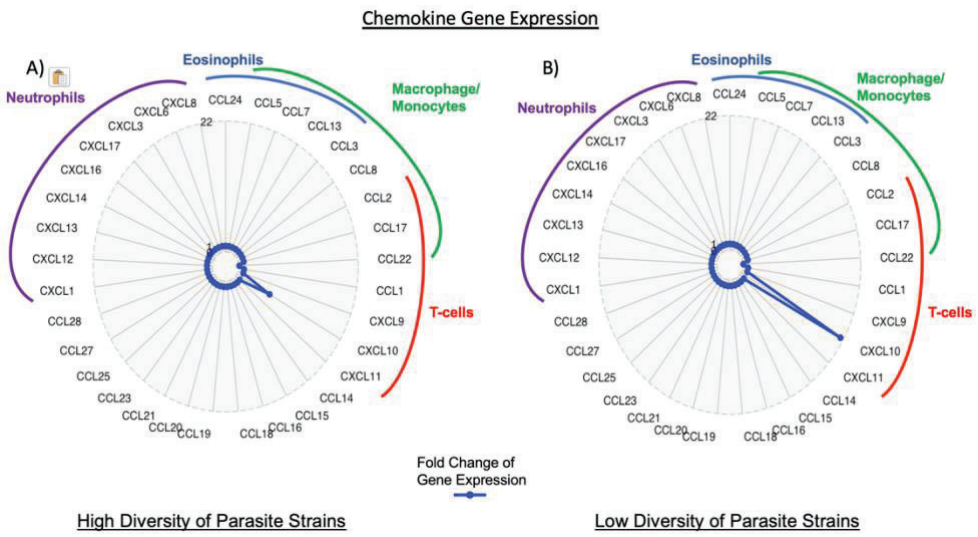

Figure 20: Fold change of chemokine gene expression

Fold change of chemokine gene expression visualized using a radar plot to compare the response between infected monkey PBMCs with high parasite diversity (A) and infected monkey PBMCs with low parasite diversity (B) compared to uninfected monkeys. Arrows indicate genes that were significantly different in expression as called by DESeq2 analysis. Arrows are colored to indicate the direction of expression change in infected monkeys compared to uninfected monkeys: up (green) or down (red).

expression of CD28, CD5, CD6, and CD7. The monocyte/macrophage activation marker CD14 gene expression was downregulated in infected monkeys with high parasitemia. Gene expression of CD1A, CD1C, CD244, CD38, CD79B, and CD84 was upregulated in infected monkeys with high parasite diversity, alongside downregulated gene expression of CD83, CD82, CD63, CD68, and CD44.

Monkeys infected with low parasite diversity had large upregulation of CXCL10 gene expression, nearly 20 times fold change in gene expression, a chemokine associated with T-cell trafficking (**Figure 20B**). Monkeys infected with low parasite diversity had slight

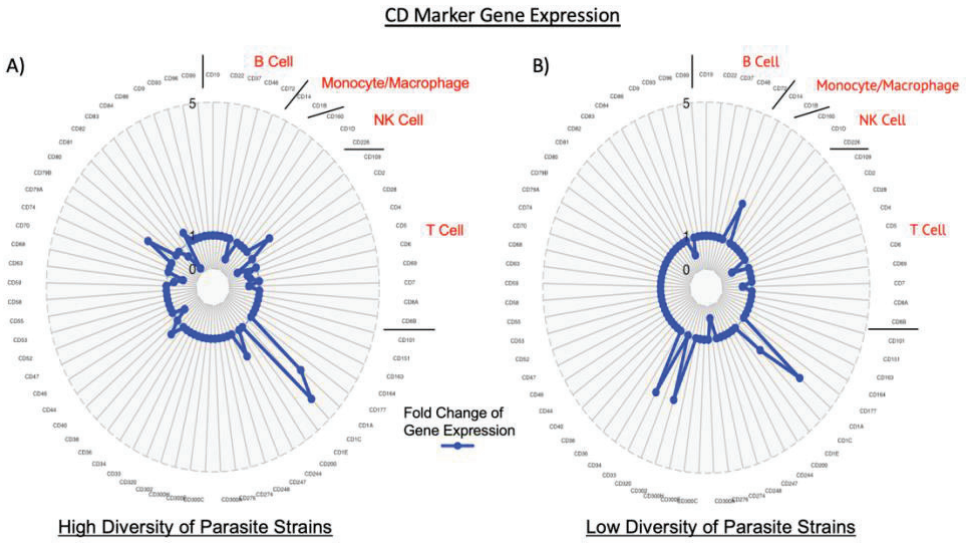

Figure 21: Fold change of CD marker gene expression

Fold change of CD marker gene expression visualized using a radar plot to compare the response between infected monkey PBMCs with high parasite diversity (A) and infected monkey PBMCs with low parasite diversity (B) compared to uninfected monkeys. Arrows indicate genes that were significantly different in expression as called by DESeq2 analysis. Arrows are colored to indicate the direction of expression change in infected monkeys compared to uninfected monkeys: up (green) or down (red).

downregulation of CCL22, a chemokine associated with T-cell and monocyte/macrophage trafficking. Monkeys infected with low parasite diversity had upregulated CD14 gene expression, a marker of monocyte/macrophage activation (**Figure 21B**). Monkeys infected with low parasite diversity had downregulated gene expression of CD28 and CD7, both T-cell activation markers. CD markers CD1A, CD1C, CD300H, and CD33 gene expression were upregulated in monkeys infected with low parasite diversity, alongside downregulation of CD9 and CD276 gene expression.

Multivariate Analysis

Multi-variate analysis was used to uncover which immune biomarker overexpression were most associated with which group:

uninfected monkeys, infected monkeys with high parasite diversity, or infected monkeys with low parasite diversity. Between group analysis of gene expression between samples revealed strong separation of infected monkeys with low parasite diversity, infected monkeys with high parasite diversity, and uninfected monkeys along two main BGA discrimination axes (Figure 22B). The two main BGA discrimination axes provides coordinate data associated with sample clustering. By overlaying this coordinate data of the samples over the clustering of gene expression, genes found at the ends of the main BGA discrimination axes represent upregulated genes most associated with groups: infected monkeys with low parasite diversity, infected monkeys with high parasite diversity, and uninfected monkey (Figure 22A). The top 27 genes associated with parasite diversity were identified along these main BGA discrimination axes. From this analysis, upregulation of IFNγ, CD40LG, CD1C, CD226, CD109, CD224, and IL-15 gene expression were most associated with infected monkeys with high parasite diversity whereas upregulation of

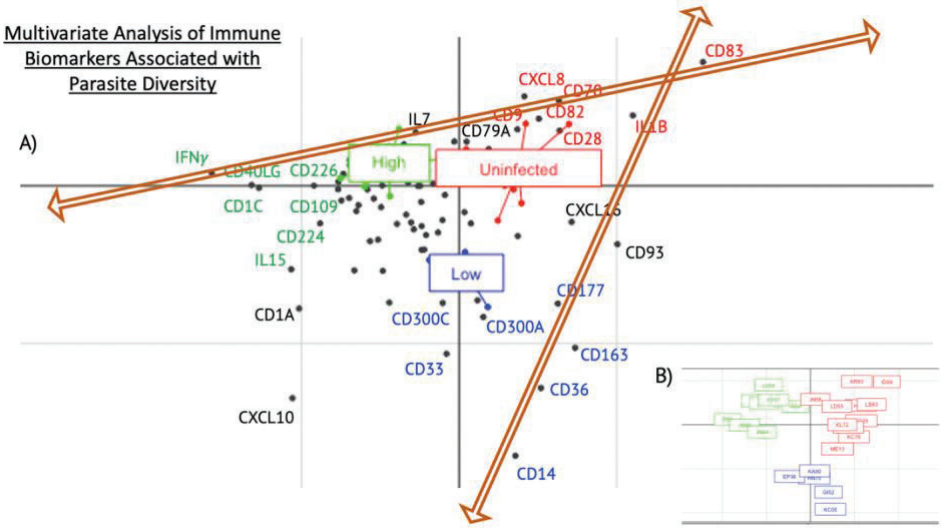

Figure 22: Between group analysis of cytokine, chemokine, and CD marker gene expression counts between uninfected monkeys (red), infected monkeys with high parasite diversity (green), and infected monkeys with low parasite diversity (blue).

Between group analysis of immune biomarker expression between infected monkeys with high parasite diversity (green), infected monkeys with low parasite diversity (blue), and uninfected monkeys (red). Between group analysis showing their separation on the BGA discrimination axes along two lines of differentiation (A). Clustering of samples used to create the BGA discrimination axes are shown in the inset (B). Black dots represent individual genes, colored dots and lines represent monkey samples, and the BGA discrimination axes are colored orange. Gene names are colored based on which group upregulation of the gene is predictive of.

CD14, CD36, CD33, CD300C, CD300A, CD163, and CD177 were most associated with infected monkeys with low parasite diversity.

Discussion

We identified distinct immune profiles associated with parasite diversity during natural chronic *T. cruzi* infections. We compared the transcriptomes of PBMCs taken from infected monkeys with high parasite diversity and infected monkeys with low parasite diversity, finding that monkeys with a balanced T_H1/T_H2 response and diverse cell activation profile tended to be infected with a high parasite diversity, while monkeys infected with a low parasite diversity had a T_H1 skewed response and

activated monocytes/macrophages with no specific markers of T-cell activation.

Nearly twice as many CD marker genes were differentially expressed in infected monkeys with high parasite diversity compared to infected monkeys with low parasite diversity, suggesting that cell activity was much more regulated in infected monkeys with high parasite diversity. Altogether, it appeared that infected monkeys with high parasite diversity expressed genes indicating varying levels of immune cell activation and immune cell inhibition, whereas infected monkeys with low parasite diversity expressed skewed CD marker genes. For example, infected monkeys with high parasite diversity had upregulated and downregulated CD markers genes associated with T-cell activation, while infected monkeys with low parasite diversity had only downregulated CD markers associated with T-cell activation. In addition, infected monkeys with low parasite diversity had upregulated CD marker genes for monocyte/macrophage activation, while infected monkeys with high parasite diversity had upregulated and downregulated CD markers for monocyte/macrophage activation. Next steps should focus on how immune cell populations, potentially with the use of cell deconvolution algorithms, change as parasite diversity increases.

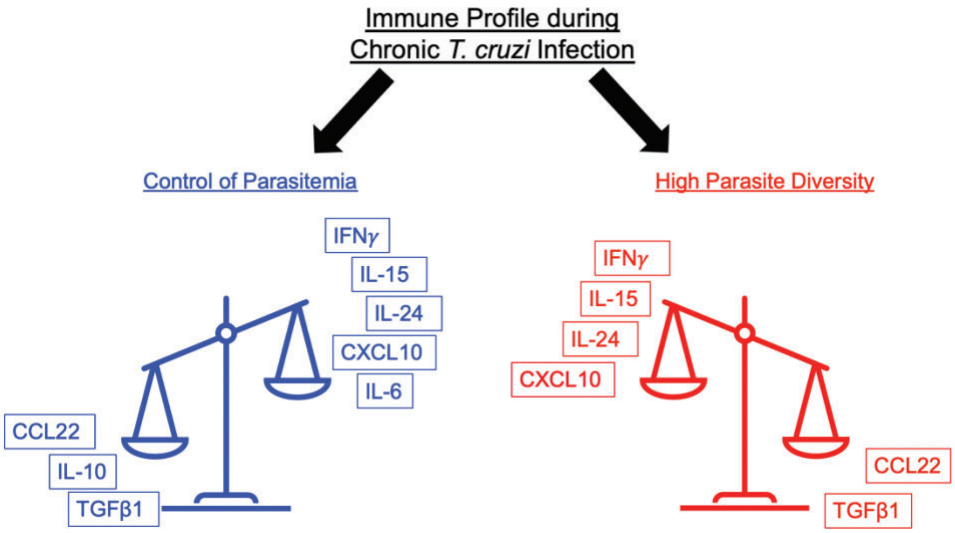

Figure 23: Cartoon representation of important cytokine and chemokine expression during states of chronic *T. cruzi* infection.

Upregulated and downregulated cytokine and chemokine genes found in chronically infected monkeys that could control parasitemia (Blue) and upregulated and downregulated cytokine and chemokine genes found in chronically infected monkeys with high parasite diversity (Red) showed very similar profiles.

The balanced immune response seen in monkeys infected with high parasite diversity was nearly identical to the immune response seen in monkeys that could control parasitemia (**Figure 23**), suggesting that the host immune response is more effective against infections with high parasite diversity. Important cytokines for parasitemia control, IFNγ and IL-24, were upregulated only in monkeys infected with high parasite diversity. T-cell marker gene expression in infected monkeys with low parasite diversity was strikingly downregulated; CD28 and CD7 gene expression, markers of naïve and mature T-cells respectively, were both downregulated in infected monkeys with low parasite diversity, suggesting any CXCL10 T-cell migration was occurring with inhibited T-

cell populations, like infected monkeys with rising parasitemia. Multivariate analysis was able to shed light on this relationship between parasite diversity and parasite control, allowing us to compare immune biomarkers associated with categorized groups of infected monkeys. Here we saw that both infected monkeys with high parasite diversity and monkeys that could control parasitemia were associated with upregulation of IFNγ, CD1C, CD40LG, and CD226; however, monkeys that could control parasitemia were associated with CD70, CXCL10, and IL7 expression while infected monkeys with high parasite diversity were associated with CD109, CD224, and IL-15 expression. Monkeys infected with low parasite diversity shared nearly all immune biomarkers associated with infected monkeys with rising parasitemia; CD14, CD163, CD177, CD300A, CD33, and CD36 expression were associated with infected monkeys with rising parasitemia and monkeys infected with low parasite diversity.

We can reconsider theories for why hosts infected with a high parasite genetic diversity could control parasitemia better than hosts infected with a low parasite genetic diversity.[3] Non-exclusive mechanisms likely involve both competition between strains for resources[3] and a more balanced and regulated host response. Future studies could explore this relationship.

In conclusion, we found that the host immune response was dependent on the *T. cruzi* parasite diversity. Infected monkeys with high

parasite diversity had a balanced and regulated immune response, with gene expression of both T_H1 and T_H2 cytokines alongside gene expression of an assortment of activation and inhibition markers expressed on multiple immune cells. Infected monkeys with low parasite diversity had a skewed immune response, with gene expression of T_H1 cytokines alongside upregulated gene expression of monocyte/macrophage activation markers and downregulated expression of T-cell markers of activation. This confirms that infections with parasite diversity largely benefit the host through parasite competition and control of parasitemia. Future work could build on this evidence that parasite diversity could serve as a prognostic tool for Chagas disease progression.

XI. Aim 3: Compare the DNA Methylation Patterns of Children Born to Chagasic and Uninfected Mothers

Disclosure Of Previous Publication

This work has been previously published[209].

Desale H, Buekens P, Alger J, Cafferata ML, Harville EW, Herrera C, Truyens C, Dumonteil E. Epigenetic signature of exposure to maternal Trypanosoma cruzi infection in cord blood cells from uninfected newborns. Epigenomics. 2022 Aug;14(15):913-927. doi: 10.2217/epi-2022-0153. Epub 2022 Aug 29. PMID: 36039408; PMCID: PMC9475499.

For all articles published in Epigenomics journals, copyright is retained by the authors and all co-authors agree to the inclusion of this material as part of this dissertation.

Background

Chagas disease, caused by the protozoan parasite *Trypanosoma cruzi* (*T. cruzi*), affects an estimated 8 million people throughout the Americas [210]. The best known morbi/mortality is associated with cardiac or digestive disease in Chagasic patients [211,212], which causes $627.46 million in annual health-care costs and has a burden of 806,170 Disease Adjusted Life Years (DALYs)[2]. This burden of disease is 7.5 times higher than malaria in the Americas [213].

Vertical transmission of the parasite occurs in about 5% of pregnancies from Chagasic women [214-216]. In the United States, an

estimated 63-315 babies acquire *T. cruzi* infection from their mother every year but most infections go undetected and untreated [76]. Infected newborns can develop chronic disease later in life; however, drug treatment is highly effective if congenital infections are detected early [159,217]. Thus, most work has focused on the timely detection of congenital transmission cases, and uninfected babies from Chagasic mothers have received limited attention. However, early life, including time *in utero*, has been identified as a critical period where alterations in the environment have particular significance for long-term health [218]. Developmental origins of health and disease (DOHaD) research has made us aware this can permanently influence the risks for adverse health outcomes in adulthood [219,220]. Such studies provide powerful evidence for life experiences affecting health and disease across the life course and generations, and how "life circumstances, health, and disease are linked at a molecular scale"[221]. Prenatal experiences influence health trajectories and contribute to adult health outcomes, including obesity, cancer, cardiovascular and metabolic diseases, asthma, and osteoporosis [6-8], and prenatal exposure to infectious agents is a risk factor for neurodevelopmental brain disorders, including schizophrenia [9,10], autism [11,12], and bipolar disorder [13,14].

Epigenetics provides a plausible mechanism by which risk factors might get "under the skin" to impact health across generations [222]. Indeed, epigenetic variation - most notably DNA methylation, contributes

to variation in gene expression [223,224]. Maternal infection may lead to fetal epigenetic reprogramming in response to maternal immune activation [225,226]. Animal studies indicate that prenatal infection can cause stable modifications in DNA methylation in offspring [227]. Prenatal maternal hepatitis B virus infection has been associated with alterations in DNA methylation of cord blood cells, including for genes associated with liver cancer and fatty acid oxidation [226], even in the absence of infant complications. Similarly, maternal infection with multiple bacteria [15], rubella virus [15], and Zika virus [16] can result in differential DNA methylation patterns in newborns compared to those born to uninfected mothers. Most recently, uterine exposure to SARS-Cov-2 was suggested to result in abnormal fetal DNA methylation.[15] Epigenetic changes and health outcomes of uninfected newborns from Chagasic mothers may thus have been overlooked.

Indeed, *in utero* exposure to maternal *T. cruzi* infection was found to induce changes in cord blood cell composition in uninfected newborns [228], and they present a significant polarization of their immune response towards pro-inflammatory cytokines at birth and following immunization with standard childhood vaccines [229]. As a key step to further assess the effects of *in utero* exposure to maternal *T. cruzi* infection, we performed an Epigenome-Wide Association Study (EWAS) to compare the DNA methylation patterns of cord blood cells from uninfected children born to

Chagasic and uninfected mothers. Such epigenetic changes may have important implications for long-term health outcomes of the newborns.

Methods

Participants

We used a cohort derived from a previous multi-centric study aiming to evaluate the congenital transmission of *T. cruzi* in Argentina, Honduras and Mexico [216]. The study was approved by Tulane IRB. We included archived umbilical cord blood samples collected from *T. cruzi* infected and uninfected women enrolled at delivery from two hospitals in Honduras (Hospital Enrique Aguilar Cerrato, La Esperanza, Intibuca and Hospital Santa Barbara Integrado, Santa Barbara), and two hospitals in Mexico (Hospital Materno Infantil, Merida, Yucatan and Hospital General de Valladolid, Valladolid, Yucatan). Eligible women were 18 years or older and had a live birth and uninfected women were recruited immediately after each *T. cruzi* infected case in each hospital. Newborn *in utero* exposure to maternal *T. cruzi* infection was assessed through two rapid tests (Stat-Pak, Chembio, Medford, NY, and *Trypanosoma*-Detect (T-Detect), InBios, Seattle, WA) and one enzyme-linked immunosorbent assay (Chagatest ELISA recombinant, version 3.0; Wiener, Rosario, Argentina) performed on umbilical cord blood [216]. Indeed, cord blood has been found to accurately reflect venous blood to identify maternal infection [230]. Exposed newborns presented at least two reactive serological tests in cord blood, and unexposed control newborns

were negative for all rapid tests and ELISA in cord blood. *T. cruzi* infection of mothers was further confirmed using a venous blood samples for serological testing as above as well as two conventional PCR and one qPCR assay [216]. Infected mothers were reactive with at least two serological tests and/or PCR positive for *T. cruzi* in at least one PCR assay. Parasite burden in maternal venous blood was 4.5 ± 0.9 parasites eq/ml blood. Congenital *T. cruzi* infection of the exposed newborns was defined as one or more of the following criteria: presence of parasites in cord blood (parasitological exam with positive PCR), presence of parasites in infant's blood at 4-8 weeks of age (parasitological exam), and persistence of *T. cruzi*-specific antibodies at 10 months, as measured by at least two tests [216]. None of the newborns from this cohort presented *T. cruzi* congenital infection.

DNA extraction and methylation array

Cord blood samples were mixed with equal volumes of 6M guanidine-HCl 0.2 M EDTA shortly following collection, and stored at 4ºC. DNA was extracted from 300 µL of blood/guanidine mixtures using an automated Maxwell® RSC Instrument (Promega Benelux, Leiden, The Netherlands), as described.[216] DNA methylation was characterized using the Illumina Infinium EPIC Array probing 850,000 methylation sites over the genome [231]. The Illumina EPIC array measures the ratio of

methylation versus non-methylation intensity at each probe for every sample. This ratio is referred to as a β-value.

Data analysis

All analyses were performed using R version 4.1.0 [171]. Available maternal demographics (age, parity, newborn birth weight, gestational age, maternal education level, delivery method, sex of newborns) were compared for differences between exposed and unexposed groups using bivariate analyses: 2 tailed t-test for continuous variables and Chi squared for categorical variables at p-value = 0.05 significance level.

Differential Methylation Analysis

Samples were normalized to correct for type-I and type-II probes distribution followed by batch effect correction and quality control (Q/C) using the Bioconductor R package Chip Analysis Methylation Pipeline (ChAMP) [232,233]. Samples with 10% failed probes on the EPIC array were removed from differential methylation analysis. Data was normalized to correct for type-I and type-II probes distribution and corrected for sample group, array, and slide batch effects using ChAMP. Corrected, normalized β-values were used to conduct differential methylation analysis.

Tensor Composition Analysis (TCA) [234] was used to detect differential methylation between exposed and unexposed newborns across all CpG sites by fitting all β-values to the TCA model under a joint test of significance. Quantile-Quantile (Q-Q) plots were used to plot the

distribution of observed (negative log transformed) p-values for each site versus what would be expected if exposure status had no effect on DNA methylation. Q-Q plots revealed substantial inflation of significant p-values, suggesting that additional covariates affected differential methylation. Because maternal *T. cruzi* infection has been shown to affect cord blood cell composition[235], the TCA *ReFACTor()*[236] function, which creates a set of principle components that can capture and adjust for the variation in methylation due to cell composition [234], was used to deconvolute heterogeneous cell-type-specific DNA methylation signals. These cell subtype fractions were inferred using the Bioconductor R package EpiDISH[237] in conjunction with the EPIC Cord Blood Reference Panel[238], which is a freely available reference panel of DNA methylation from sorted immune cells (CD4T, CD8T, Natural Killer, Granulocytes, Monocytes, and B cells) taken from human cord blood characterized with the Infinium EPIC array. Significant CpGs were called using a two-step approach: a joint test of significance to test CpGs across all cell types followed by a marginal conditional test for the effect of each cell type separately for significance. The joint test tends to be more effective than the marginal conditional test for the detection of CpG level associations because the joint test combines signals from all cell types [234]. The marginal conditional test allows for the attribution of CpG level hits to the specific cell types driving the association [234]. The two-step approach is rather conservative because the joint test corrects for the number of

hypotheses using the number of sites in the data, whereas the marginal conditional test considers the same number of hypothesis for each cell type [234]. CpGs with a Bonferroni correction adjusted for multiple testing p-value less than 0.05 were considered significant. Multi-dimensional plots and dendrograms were created using ChAMP [233]. The TCA package was used to create Q-Q plots [234].

Genes and pathways associated with significant differentially methylated probes were identified using champ.DMR [233] and methylGSA [239] incorporating significant CpGs as a covariate in logistic regression and linking this information to gene identifiers in the EPIC probe annotations dataframe found in ChAMP [233] and NCBI Gene Ontology knowledgebase. The following information was gleaned from the knowledge base for each CpG: chromosome containing the CpG (*CHR*), chromosomal coordinates of the CpG (*MAPINFO*), region of the gene (*Feature*: TSS200 = 200 bases upstream of the translation start site, 5'UTR = within the 5' untranslated region, Body = between the start and stop codon, IGR = intergenic region), proximity to a CpG dense region of the genome known as an island (*Cgi*: shore = 0–2 kb from island, shelf = 2–4 kb from island, opensea = rest of genome), and gene name. Functional role of the differentially methylated genes was investigated by gene ontology, pathway analysis and protein-protein interaction networks using the STRING database [240].

Results

Characteristics of Samples Included in the Study

The study included umbilical cord blood samples from a cohort of uninfected newborns exposed or unexposed to maternal *T. cruzi* infection. There were no significant differences in sociodemographic variables between the mothers from both groups (**Table 9**). In total, 63 samples passed Q/C: 31 from cord blood taken from mothers infected with *T. cruzi* (Exposed) and 32 from cord blood taken from mothers without infection (Unexposed), and one sample from an infected mother was excluded from further analysis for not passing Q/C analysis. A total of 715,343 probes targeting CpG sites across the genome were used for differential methylation analysis between the two groups.

Table 10: Sociodemographic data for subjects stratified by exposed and unexposed groups for EWAS study

	Group status		p-value
	Exposed (n = 33)	Unexposed (n = 33)	
Birth weight (g)	3140 ± 422	3254 ± 407	0.27
Gestational age at delivery (weeks)	38.9 ± 1.1	38.8 ± 1.3	0.70
Mother's age (years)			0.14
– 18–19	10	3	
– 20–24	6	14	
– 25–29	7	5	
– 30–34	6	5	
– 35–39	3	3	
– >40	1	3	
Parity (number)			0.79
– 0	8	10	
– 1	9	7	
– 2+	16	16	
Education			0.96
None, illiterate	3	2	
None, literate	1	1	
Primary	12	11	
Secondary	16	17	
Tertiary/university	1	2	
Delivery method			0.82
Vaginal, spontaneous	16	15	
Vaginal, assisted	5	7	
Caesarean section	12	11	
Sex of baby			0.81
Male	16	18	
Female	17	15	

Data are presented as mean ± standard deviation or counts.

Differential Methylation Analysis

β values were fit to the TCA model comparing differential methylation between exposed and unexposed newborns under a joint test of significance. Q-Q plots revealed sizeable inflation among transformed p-values (**Figure 25**), indicating covariates clouding the effect of exposure to *T. cruzi* infection.

Cell Fraction Estimation

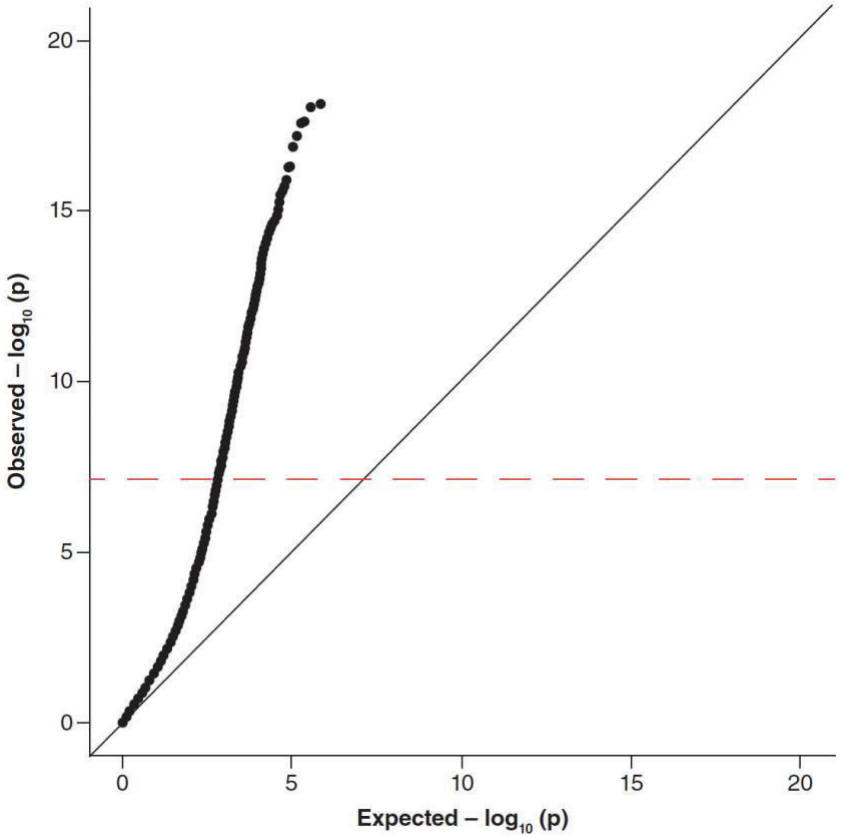

Figure 24:Quantile–quantile plot of the negative log-transformed p-values for CpG-level differential methylation between exposed and unexposed newborns.

Samples were analyzed using a joint test for significance across all CpGs. Observed versus expected p-value f Observed versus expected p-value for significant differential methylation at each CpG is plotted with black dots. The black line represents the ideal distribution from a perfectly specified model. The dashed red horizontal line represents significance threshold adjusted for multiple testing.

Estimated cell subtypes found granulocytes to be the predominant immune cell type among both exposed and unexposed subjects (Figure 2). Except for monocytes, there were significantly different proportions of each cell type in cord blood comparing exposed and unexposed newborns (**Figure 26**). The proportion of B cells, CD4 T cells, CD8 T cells, and Natural Killer cells were reduced in cord blood from exposed

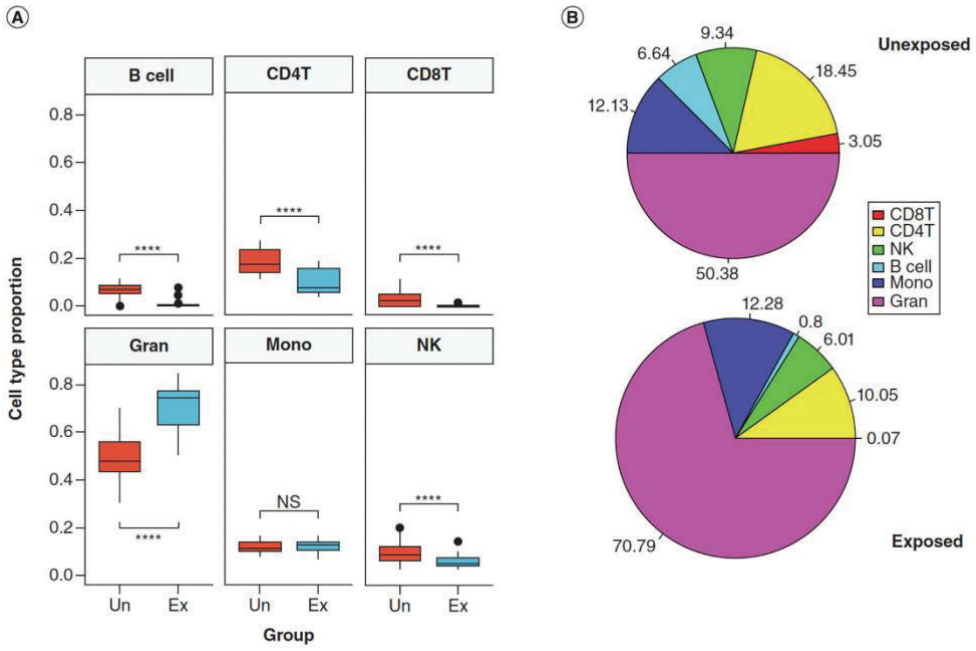

Figure 25:Estimated cord blood cell fractions among unexposed and exposed newborns.

(A) Cell proportions for unexposed ('Un', red) and exposed ('Ex', blue) newborns cord blood were determined. Proportions of all cell subtypes except monocytes were significantly different between the groups. (B) Average proportion of each cell subtype for unexposed and exposed newborns. ****p < 0.001. CD4T: CD4+ T cells; CD8T: CD8+ T cells; Ex: Exposed; Gran: Granulocytes; Mono: Monocytes; NK: Natural killer cells; NS: Nonsignificant; Un: Unexposed.

newborns, whereas granulocytes were reduced in cord blood from unexposed newborns.

Detection of Significant Cell-Type Methylation

ReFactor adjustment using the estimated cell fraction was able to reduce the inflation seen after refitting β values to the TCA model comparing differential methylation between exposed and unexposed newborns under a joint test of significance (**Figure 27**). After adjustment

over all cell types, 12 CpGs yielded experiment wide level of significance when combining the effects of all cell types.

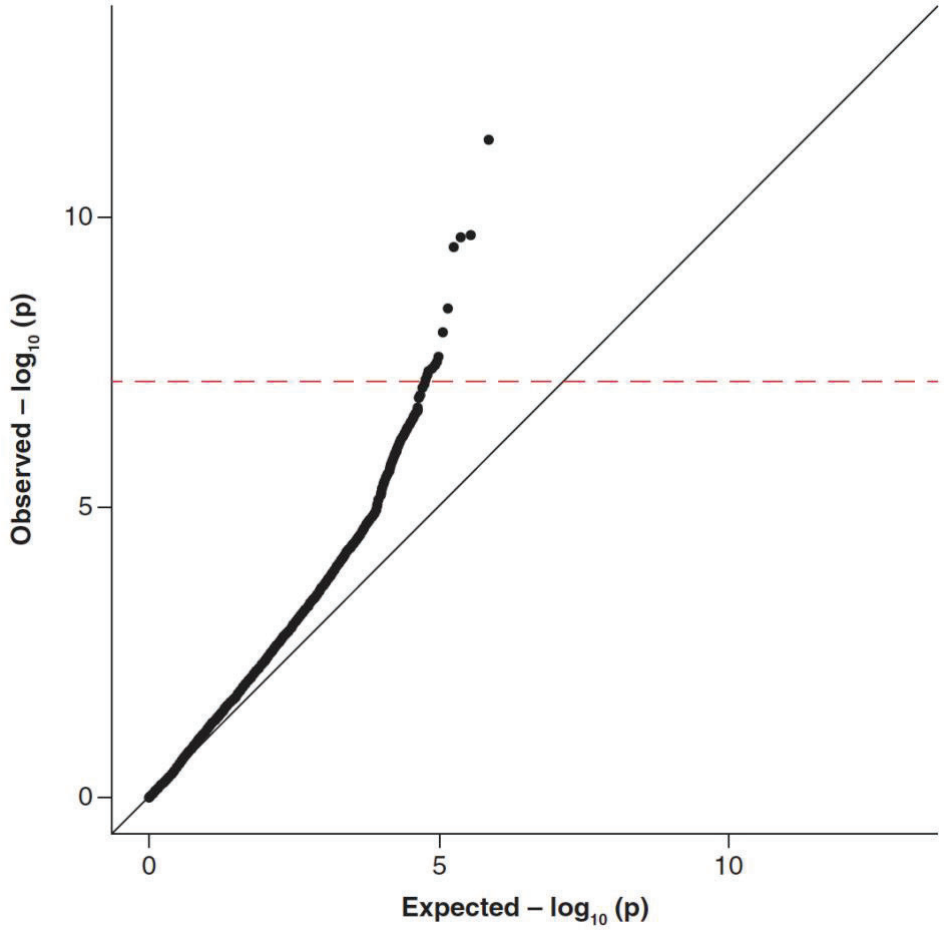

Figure 26:Quantile–quantile plot of the negative log-transformed p-values for CpG-level differential methylation between exposed and unexposed newborns after adjustment for cell composition.

Differential methylation was analyzed using a joint test for significance across all CpGs after ReFACTor adjustment for cell type heterogeneity. Observed versus expected p-value for significant differential methylation at each CpG is plotted with black dots. The black line represents the ideal distribution from a perfectly specified model. The dashed red horizontal line represents significance threshold adjusted for multiple testing.

Adjusted β values were further analyzed under a marginal conditional test of significance (**Figure 28**) to determine cell-specific

differential methylation. In total, 21 CpGs were predicted to have cell-type level differential methylation with group status exposed versus unexposed. Of these 21 CpGs, 7 were predicted to have CD4+ T cell-specific differential methylation and 14 were predicted to have B cell-specific differential methylation. No cell-specific differential methylation was predicted to be associated with CD8+ T cells, granulocytes,

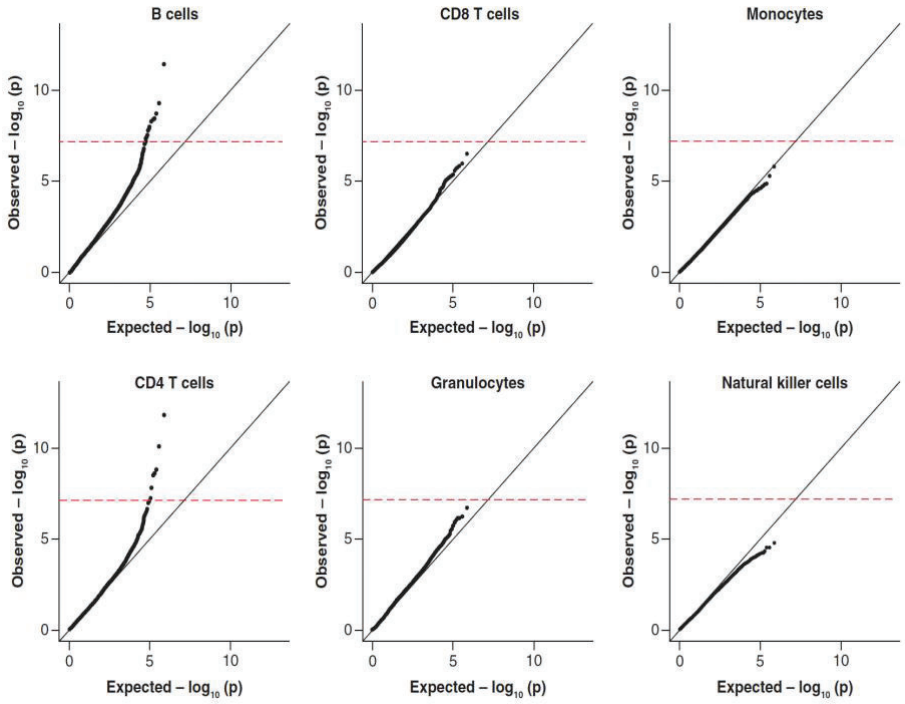

Figure 27:Quantile–quantile plots of the negative log-transformed p-values for CpG-level differential methylation between exposed and unexposed newborns for individual cell types.

Differential methylation was analyzed using a marginal conditional test for significance across CpGs from individual cell types after ReFACTor adjustment for cell type heterogeneity. Observed versus expected p-value for significant differential methylation at each CpG is plotted with black dots. The black line represents the ideal distribution from a perfectly specified model. The dashed red horizontal line represents significance threshold adjusted for multiple testing.

monocytes, or natural killer cells.

Using this information, we were able to determine the role of each cell type in the 12 significant CpGs found using the joint test of significance. Of these 12, 9 were associated with differential methylation among B cells and 3 associated with CD4+ T cells (**Table 10**).

Multi-dimensional and dendrogram plots found samples clustered based on the similarity of methylation among the 12 significant CpGs identified using the joint test (**Figure 29**). While unexposed samples clustered in one group (except one potential outlier), exposed samples clustered separately. Interestingly, a subgroup of exposed samples clustered further apart, suggesting some greater heterogeneity in the DNA methylation pattern of exposed newborns. Clustering of samples

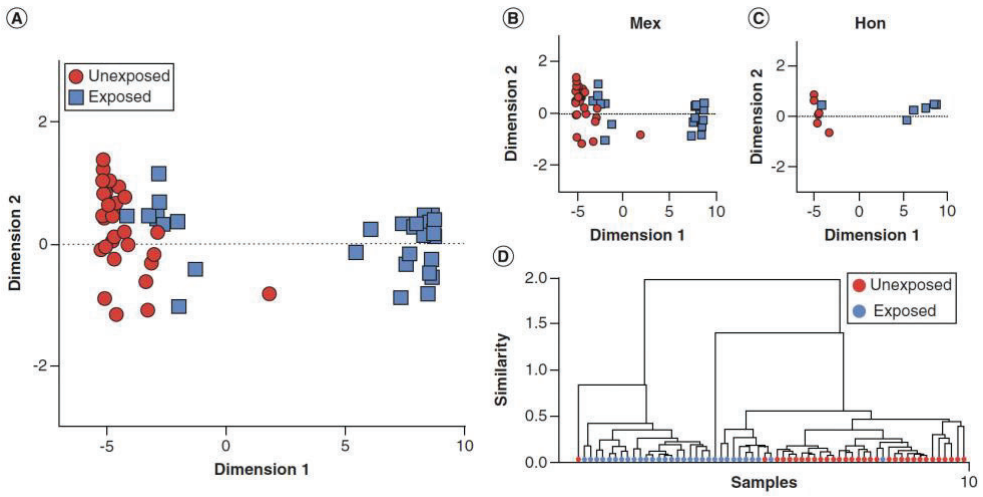

Figure 28:Similarity clustering of exposed and unexposed newborns based on differentially methylated CpGs from cord blood.

Sample clustering was performed based on the 12 significant CpGs identified through differential methylation analysis. Exposed (blue) samples clustered separately from unexposed (red) samples based on (A–C) multidimensional plot and (D) dendrogram analysis. Hon: Honduras; Mex: Mexico.

was independent from the country of origin (Mexico vs Honduras), and

differential methylation in response to maternal infection was observed in

Table 11: Differentially methylated CpGs associated with in utero exposure to maternal Trypanosoma cruzi infection

CpG	Cell type	Chr	MAPINFO	Gene name	Feature	Cgi	Full gene name
cg01396799	B cells	4	40195070	*RHOH*	TSS200	Opensea	Ras homolog family member H
cg06288316		15	35502313		IGR	Opensea	
cg06545968		14	32553698	*ARHGAP5*	5' UTR	Opensea	Rho GTPase activating protein 5
cg08135852		3	119049717	*ARHGAP31*	Body	Opensea	Rho GTPase activating protein 31
cg08800200		12	6484868	*SCNN1A*	5' UTR	Opensea	Sodium channel epithelial 1 subunit α
cg14078913		7	139144308	*KLRG2*	Body	Opensea	Killer cell lectin like receptor G2
cg17364772		5	132184001		IGR	Opensea	
cg19902050		1	150531110	*ADAMTSL4*	Body	Shore	ADAMTS like 4
cg21958394		2	145425418		IGR	Opensea	
cg10017394	$CD4^+$ T cells	9	74334857	*CEMIP2*	Body	Opensea	Cell migration inducing hyaluronidase 2
cg22398226		4	155662217		IGR	Shore	
cg25556035		19	13127873	*NFIX*	Body	Shelf	Nuclear factor IX

Cgi: CpG islands; Chr: Chromosome; IGR: Intergenic region.

both countries.

Identifying Differentially Methylated Genes

The human genomic information of the 12 significant differentially methylated CpGs was identified (**Table 10**). B cell differentially methylated CpGs were found on chromosomes 1, 2, 3, 4, 5, 7, 12, 14, and 15. $CD4^+$ T cell differentially methylated CpGs on chromosomes 4, 9, and 19. The majority of CpGs maped to opensea regions with 9. Of the rest, 2 mapped to methylation shores, and 1 to shelf regions. Of the 12 significant CpGs, 5 mapped to gene body regions, 2 in the 5' untranslated regions, 1 in the translation start site, and 4 in the intergenic region. The 8 CpGs not found in intergenic regions were associated with protein coding genes.

We then evaluated the biological function of these genes, and most are involved in multiple protein-protein interactions suggesting key

functional roles (**Figure 30**). Indeed, most have been associated with

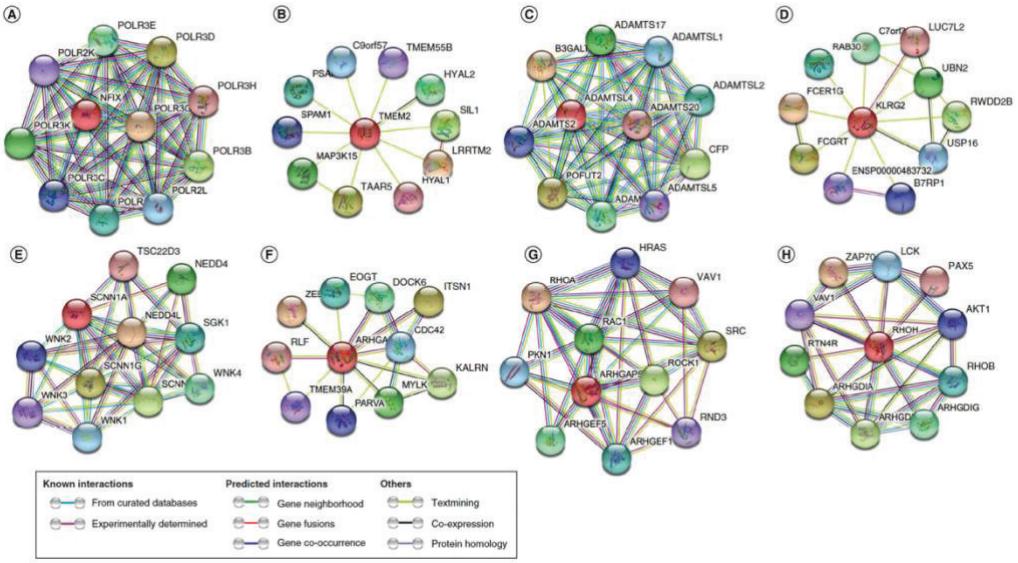

Figure 29:Protein–protein interaction networks of proteins encoded by differentially methylated genes.

Protein–protein interactions were examined for proteins encoded by differentially methylated genes to assess their potential functional networks and participation in biological processes and functions. (A) NFIX. (B) CEMIP2. (C) ADAMTSL4. (D) KLRG2. (E) SCNN1G. (F) ARHGAP31. (G) ARHGAP5. (H) RHOH. Edges between nodes are color-coded based on the type of information describing the interactions as indicated in the box.

major biological processes and some with diseases (**Table 11**). RHOH, ARHGAP5 and CDGAP are GTP-binding proteins involved in multiple signaling pathways. RHOH plays a key role in hematopoietic cell differentiation and immune response, and has also been associated with cancer. ARHGAP5 has also been implicated in multiple types of cancer, while CDGAP is linked to Adams-Oliver syndrome, a developmental disorder of the skin and limbs. SCNN1A is an ion channel playing an essential role in electrolyte and blood pressure homeostasis, and in airway surface liquid homeostasis. It has been associated with

phenotypes dominated by renal disease and hypertensive syndromes

Table 12: Gene function and ontogeny.

Gene	GO Function	KEGG pathway	Disease-gene association	Biological role
NFIX	GO:0003676 Nucleic acid binding GO:0003899 DNA-directed 5-3 RNA polymerase activity	hsa03020 RNA polymerase hsa04623 Cytosolic DNA-sensing pathway		
CEMIP2	GO:0030214 Hyaluronan catabolic process GO:0004415 Hyaluronoglucosaminidase activity GO:0004553 Hydrolase activity, hydrolyzing o-glycosyl compounds	hsa00531 Glycosaminoglycan degradation hsa04142 Lysosome	DOID:0050809 Mucopolysaccharidosis ix DOID:3211 Lysosomal storage disease	
ADAMTSL4	GO:0004222 Metalloendopeptidase activity GO:0008233 Peptidase activity GO:0031012 Extracellular matrix		DOID:0080201 Peters plus syndrome DOID:0050475 Weill-Marchesani syndrome DOID:0111148 Isolated ectopia lentis DOID:0111243 Acromicric dysplasia DOID:0111724 Geleophysic dysplasia	ADAMTS-like proteins reside in the extracellular matrix and regulate its assembly
KLRG2				Killer cell lectin-like receptor subfamily g member 2
SCNN1A	GO:1903288 Positive regulation of potassium ion import across plasma membrane GO:0070294 Renal sodium ion absorption GO:0015280 Ligand-gated sodium channel activity GO:0017081 Chloride channel regulator activity	hsa04960 Aldosterone-regulated sodium reabsorption hsa04742 Taste transduction	DOID:0050477 Liddle syndrome DOID:0111607 Distal arthrogryposis type 3 DOID:0060855 Autosomal dominant pseudohypoaldosteronism type 1	Amiloride-sensitive sodium channel subunit alpha; Plays an essential role in electrolyte and blood pressure homeostasis, but also in airway surface liquid homeostasis, which is important for proper clearance of mucus. Controls the reabsorption of sodium in kidney, colon, lung and eccrine sweat glands. Also plays a role in taste perception
ARHGAP31	GO:0030027 Lamellipodium GO:0031252 Cell leading edge		DOID:0060227 Adams-Oliver syndrome	Rho GTPase-activating protein, Required for cell spreading, polarized lamellipodia formation and cell migration
ARHGAP5	GO:0071803 Positive regulation of podosome assembly GO:0051894 Positive regulation of focal adhesion assembly GO:0043149 Stress fiber assembly GO:0045453 Bone resorption	hsa05219 Bladder cancer hsa04670 Leukocyte transendothelial migration hsa04370 VEGF signaling pathway hsa04611 Platelet activation	DOID:162 Cancer	Rho GTPase-activating protein
RHOH	GO:0031295 T cell costimulation GO:0007266 Rho protein signal transduction GO:0030217 T cell differentiation GO:0050870 Positive regulation of t cell activation GO:0001772 Immunological synapse	hsa05340 Primary immunodeficiency hsa04660 T cell receptor signaling pathway hsa04722 Neurotrophin signaling pathway hsa05235 PD-L1 expression and PD-1 checkpoint pathway in cancer	DOID:162 Cancer	Rho-related GTP-binding protein is a hematopoietic system-specific GTPase; Negative regulator of hematopoietic progenitor cell proliferation, survival and migration. Critical regulator of thymocyte development and T-cell antigen receptor signaling

including systemic pseudohypoaldosteronism type I and Liddle syndrome. Defects in the NFIX gene have been implicated in Sotos syndrome and Marshall-Smith syndrome, which are developmental disorders that can result in overgrowth, advanced bone age, macrocephaly, and dysmorphic facial features. TMEM2 has catalytic

functions associated with lysosomal activity, and has been linked with lysosome storage disease. ADAMTSL4 is an extracellular matrix protein playing a role in matrix assembly, and it has been implicated in hearing loss and vision defects. KLRG2 is a lectin receptor on killer cells, involved in the immune response.

Discussion

Epigenetic changes due to *in utero* exposure to maternal infection can be a mechanism leading to altered health outcomes later in life. Nonetheless, most studies on the impact of maternal *T. cruzi* infection have focused on the vertical transmission of the parasite to the newborn, as this can lead to chronic Chagas disease if untreated, and uninfected newborns have received much less attention as they are assumed to be healthy. Thus, we aimed here to investigate the differential DNA methylation patterns between uninfected neonates exposed to *T. cruzi* infection *in utero* versus those unexposed, to identify potential epigenetic effects that may have been overlooked.

Our analysis indicated important differences in umbilical cord blood cell composition between *T. cruzi* exposed and unexposed groups, with a marked increase in the proportion of granulocytes, while $CD4^+$ T cells, $CD8^+$ T cells, B Cells, and natural killer cells were reduced in exposed newborns. Altered cord blood cell composition associated with maternal *T. cruzi* infection has been observed before [228], as well as with maternal infections with other pathogens including *Plasmodium* [241],

Schistosoma [242], cytomegalovirus (CMV) [243] or HIV [244]. These effects of maternal infection suggest changes in the maturation and polarization of the immune response at birth [245], which may be maintained during infancy. Indeed, significant differences in infant responses to childhood vaccines has been observed in association with their exposure to maternal HIV infection [246]. Similarly, uninfected infants from *T. cruzi*-infected mothers present a more polarized type 1 response to PPD after BCG vaccination [229]. All these observations are in agreement with animal studies showing that maternal immune activation (which mimics the response to a viral infection) during pregnancy leads to long-lasting changes in immune response and cytokine levels of offsprings [247,248], and maternal *T. cruzi* infection may mediate such alterations in uninfected newborns. The mechanisms underlying the effect of maternal infection on newborn immune response are unclear, but epigenetic changes may be involved. For example, in mouse models of *Schistosoma* maternal infection, polarized T cell differentiation of offspring is modulated by epigenetic changes [249].

In agreement with this hypothesis, our analysis of umbilical cord blood DNA methylation patterns further indicated significant differences between *T. cruzi* exposed and unexposed newborns. To our knowledge, this suggests for the first time an epigenetic effect of maternal *T. cruzi* infection on newborns, even in the absence of parasite transmission. Indeed, confounding factors such as maternal socioeconomic level,

gestational age or newborn birth weight, which have been found to be associated with DNA methylation signatures [250-253] followed very similar distributions in our exposed and unexposed groups, and thus could not account for these differences. This finding adds to the growing list of factors influencing fetal development *in utero* through epigenetic mechanisms, which includes smoking [254,255], diabetes [256], hypertension [257], and others [258].

Differential CpG methylation affected specific genes in a cell-specific manner, namely in B cells and CD4 T cells. These genes differ from those affected by *in utero* infection with HBV [226] or HIV [259], suggesting some pathogen-specific alterations. Functional analysis revealed that several of the differentially methylated genes participate in hematopoietic cell differentiation and the immune response, with appears in agreement with the observations of immune polarization in exposed newborns discussed above. Thus, future studies should investigate the links between epigenetic changes and the immune system maturation and polarization in newborns exposed to maternal *T. cruzi* infection, and their potential sustainable effects during childhood and later in life. Indeed, these epigenetic changes may lead to increased susceptibility to some pathogens, or other immune disorders, as proposed before [260].

We also detected the differential methylation of additional genes, involved in several developmental disorders and syndromes, as well as with susceptibility genes associated with cancer, hypertension, and

degenerative diseases that may develop later in life. Because our study focused only on cord blood cells, we cannot exclude that still other genes may be differentially methylated in other cell types. For example, maternal immune activation in mice induces changes in brain DNA methylation of adult offspring, which has been associated with neurodevelopmental disorders, suggesting that long-term epigenetic changes caused by maternal infection may occur multiple tissues beyond cord blood [225].

It is unclear at this stage if uninfected newborns from Chagasic mothers present significant immune disorders or other pathologies or syndromes, as they are usually not followed and considered healthy. However, our findings indicate clear epigenetic alterations that may lead to changes in gene expression and potential long-term effects. It will be critical to validate our results in additional cohorts of newborns from *T. cruzi*-infected mothers, and investigate the potential phenotypic manifestations of these epigenetic changes on the health of these newborns and infants. In that respect, the pathologies associated with some of the genes identified here as differentially methylated provide a good framework to select phenotypic traits to be investigated.

In conclusion, our epigenome-wide association study identified cell-specific differential DNA methylation signatures of fetal exposure to maternal *T. cruzi* infection, in the absence of vertical transmission of the parasite. A total of 12 CpG sites were found differentially methylated in

umbilical cord blood B and CD4 T cells, corresponding to 8 protein coding genes. These genes participate in hematopoietic cell differentiation and the immune response and may be involved in immune disorders. They also have been associated with several developmental disorders and syndromes, as well as with susceptibility to diseases. These results warrant further studies focusing on the health outcomes of uninfected newborns from Chagasic mothers, to assess short and long-term effects.

XII. Global Discussion

In conclusion, our work provides novel insights into the mechanisms of Chagas disease pathology and progression. Through bioinformatics analysis combining information from chronically infected hosts and their infecting parasite strains, these studies validated our current understanding of the immune response to chronic *T. cruzi* infection, identified how this immune response changes depending on the diversity of the parasite strains, and identified important biomarkers associated with an effective immune response against the infections using bulk RNA sequencing of PBMCs taken from naturally chronically *T. cruzi* infected monkeys. We confirmed the hypothesis that chronic *T. cruzi* infection results in a skewed T_H1 inflammatory response, and that hosts that could control parasitemia responded to infection with a balanced T_H1/T_H2 response. Through our non-targeted approach, we were able to discover these responses were driven by a specific cytokine and chemokine gene expression; some such as IFN-γ and CXCL10 have been identified in clinical samples, and others such as the necessary expression of CCL22 for parasitemia control newly discovered in our analysis. Additionally, we identified significant differences in umbilical cord blood DNA methylation patterns between *T. cruzi* exposed and unexposed newborns through epigenetic analyses of fetal blood. This work has important public health implications, suggesting genetic alterations in the developing fetus in the absence of parasite transmission as well as providing the foundation for new prognostic markers for Chagas disease progression and tools for identifying those highest at risk of severe disease.

Because gene expression represents the first step to protein expression and phenotypic response, future research can expand on this work, for example, exploring these prognostic markers functionally or through immunoassay detection to design new molecular tests. In addition, follow up observational studies of children exposed to *T. cruzi* infection *in utero* can help associate any phenotypic results to epigenetic pathology from infection. In this way, our work provides valuable jump off points for future steps while adding to our current knowledge of Chagas disease.

XIII. References

1. Koh CC, Neves EGA, de Souza-Silva TG, et al. Cytokine Networks as Targets for Preventing and Controlling Chagas Heart Disease. Pathogens 2023;12.
2. Lee BY, Bacon KM, Bottazzi ME, Hotez PJ. Global economic burden of Chagas disease: a computational simulation model. Lancet Infect Dis 2013;13:342-8.
3. Dumonteil E, Desale H, Tu W, et al. Intra-host parasite strain dynamics, biomarkers and disease progression in Rhesus macaques with natural chronic Trypanosoma cruzi infection [Manuscript submitted for publication], Department of Tropical Medicine, Tulane University School of Public Health and Tropical Medicine 2023.
4. Jones KM, Poveda C, Versteeg L, Bottazzi ME, Hotez PJ. Preclinical advances and the immunophysiology of a new therapeutic Chagas disease vaccine. Expert Rev Vaccines 2022;21:1185-203.
5. Dumonteil E, Herrera C. The Case for the Development of a Chagas Disease Vaccine: Why? How? When? Trop Med Infect Dis 2021;6.
6. Sly PD. The early origins of asthma: who is really at risk? Curr Opin Allergy Clin Immunol 2011;11:24-8.
7. Duijts L, Reiss IK, Brusselle G, de Jongste JC. Early origins of chronic obstructive lung diseases across the life course. Eur J Epidemiol 2014;29:871-85.
8. Koletzko B, Decsi T, Molnár D, Hunty A. Early nutrition programming and health outcomes in later life: Obesity and beyond: Springer Science & Business Media; 2009.
9. Brown AS, Derkits EJ. Prenatal infection and schizophrenia: a review of epidemiologic and translational studies. Am J Psychiatry 2010;167:261-80.
10. Miller BJ, Culpepper N, Rapaport MH, Buckley P. Prenatal inflammation and neurodevelopment in schizophrenia: a review of human studies. Prog Neuropsychopharmacol Biol Psychiatry 2013;42:92-100.
11. Atladottir HO, Henriksen TB, Schendel DE, Parner ET. Autism after infection, febrile episodes, and antibiotic use during pregnancy: an exploratory study. Pediatrics 2012;130:e1447-54.
12. Brown AS, Sourander A, Hinkka-Yli-Salomaki S, McKeague IW, Sundvall J, Surcel HM. Elevated maternal C-reactive protein and autism in a national birth cohort. Mol Psychiatry 2014;19:259-64.
13. Parboosing R, Bao Y, Shen L, Schaefer CA, Brown AS. Gestational influenza and bipolar disorder in adult offspring. JAMA Psychiatry 2013;70:677-85.
14. Canetta SE, Bao Y, Co MD, et al. Serological documentation of maternal influenza exposure and bipolar disorder in adult offspring. Am J Psychiatry 2014;171:557-63.
15. Bhagirath AY, Medapati MR, de Jesus VC, et al. Role of Maternal Infections and Inflammatory Responses on Craniofacial Development. Frontiers in Oral Health 2021;2.

16. Anderson D, Neri J, Souza CRM, et al. Zika Virus Changes Methylation of Genes Involved in Immune Response and Neural Development in Brazilian Babies Born With Congenital Microcephaly. J Infect Dis 2021;223:435-40.
17. Parasites - American Trypanosomiasis (also known as Chagas Disease). (Accessed 08/06, 2022, at https://www.cdc.gov/parasites/chagas/.)
18. Franco-Paredes C, Bottazzi ME, Hotez PJ. The unfinished public health agenda of chagas disease in the era of globalization. PLoS Negl Trop Dis 2009;3:e470.
19. Chagas disease (also known as American trypanosomiasis). (Accessed 08/06, 2022, at https://www.who.int/news-room/fact-sheets/detail/chagas-disease-(american-trypanosomiasis).)
20. Yamagata Y, Nakagawa J. Control of Chagas disease. Adv Parasitol 2006;61:129-65.
21. Nunes MC, Dones W, Morillo CA, Encina JJ, Ribeiro AL, Council on Chagas Disease of the Interamerican Society of C. Chagas disease: an overview of clinical and epidemiological aspects. J Am Coll Cardiol 2013;62:767-76.
22. Hotez PJ, Bottazzi ME, Franco-Paredes C, Ault SK, Periago MR. The neglected tropical diseases of Latin America and the Caribbean: a review of disease burden and distribution and a roadmap for control and elimination. PLoS Negl Trop Dis 2008;2:e300.
23. Manne-Goehler J, Umeh CA, Montgomery SP, Wirtz VJ. Estimating the Burden of Chagas Disease in the United States. PLoS Negl Trop Dis 2016;10:e0005033.
24. Franco-Paredes C, Von A, Hidron A, et al. Chagas disease: an impediment in achieving the Millennium Development Goals in Latin America. BMC Int Health Hum Rights 2007;7:7.
25. Chagas' disease--an epidemic that can no longer be ignored. Lancet 2006;368:619.
26. Moncayo A. Chagas disease: current epidemiological trends after the interruption of vectorial and transfusional transmission in the Southern Cone countries. Mem Inst Oswaldo Cruz 2003;98:577-91.
27. Acevedo GR, Girard MC, Gomez KA. The Unsolved Jigsaw Puzzle of the Immune Response in Chagas Disease. Front Immunol 2018;9:1929.
28. Irish A, Whitman JD, Clark EH, Marcus R, Bern C. Updated Estimates and Mapping for Prevalence of Chagas Disease among Adults, United States. Emerg Infect Dis 2022;28:1313-20.
29. Costa J, Dale C, Galvao C, Almeida CE, Dujardin JP. Do the new triatomine species pose new challenges or strategies for monitoring Chagas disease? An overview from 1979-2021. Mem Inst Oswaldo Cruz 2021;116:e210015.
30. de Paiva VF, Belintani T, de Oliveira J, Galvao C, da Rosa JA. A review of the taxonomy and biology of Triatominae subspecies (Hemiptera: Reduviidae). Parasitol Res 2022;121:499-512.

31. Alevi KCC, de Oliveira J, da Silva Rocha D, Galvao C. Trends in Taxonomy of Chagas Disease Vectors (Hemiptera, Reduviidae, Triatominae): From Linnaean to Integrative Taxonomy. Pathogens 2021;10.
32. Chacon F, Bacigalupo A, Alvarez-Duhart B, Cattan PE, Solis R, Munoz-San Martin C. The Parasite Load of Trypanosoma cruzi Modulates Feeding and Defecation Patterns of the Chagas Disease Vector Triatoma infestans. Microorganisms 2022;10.
33. Dumonteil E, Pronovost H, Bierman EF, et al. Interactions among Triatoma sanguisuga blood feeding sources, gut microbiota and Trypanosoma cruzi diversity in southern Louisiana. Mol Ecol 2020;29:3747-61.
34. Curtis-Robles R, Hamer SA, Lane S, Levy MZ, Hamer GL. Bionomics and Spatial Distribution of Triatomine Vectors of Trypanosoma cruzi in Texas and Other Southern States, USA. Am J Trop Med Hyg 2018;98:113-21.
35. Fretes RE, Kemmerling U. Mechanism of Trypanosoma cruzi Placenta Invasion and Infection: The Use of Human Chorionic Villi Explants. J Trop Med 2012;2012:614820.
36. Jansen AM, Xavier S, Roque ALR. Landmarks of the Knowledge and Trypanosoma cruzi Biology in the Wild Environment. Front Cell Infect Microbiol 2020;10:10.
37. Jansen AM, Xavier SC, Roque AL. The multiple and complex and changeable scenarios of the Trypanosoma cruzi transmission cycle in the sylvatic environment. Acta Trop 2015;151:1-15.
38. Vieira CB, Praca YR, Bentes K, et al. Triatomines: Trypanosomatids, Bacteria, and Viruses Potential Vectors? Front Cell Infect Microbiol 2018;8:405.
39. Cavassin FB, Kuehn CC, Kopp RL, et al. Genetic variability and geographical diversity of the main Chagas' disease vector Panstrongylus megistus (Hemiptera: Triatominae) in Brazil based on ribosomal DNA intergenic sequences. J Med Entomol 2014;51:616-28.
40. Schmunis GA. Epidemiology of Chagas disease in non-endemic countries: the role of international migration. Mem Inst Oswaldo Cruz 2007;102 Suppl 1:75-85.
41. Lima Vdos S, Xavier SC, Maldonado IF, Roque AL, Vicente AC, Jansen AM. Expanding the knowledge of the geographic distribution of Trypanosoma cruzi TcII and TcV/TcVI genotypes in the Brazilian Amazon. PLoS One 2014;9:e116137.
42. Callejas-Hernandez F, Girones N, Fresno M. Genome Sequence of Trypanosoma cruzi Strain Bug2148. Genome Announc 2018;6.
43. Zingales B, Miles MA, Campbell DA, et al. The revised Trypanosoma cruzi subspecific nomenclature: rationale, epidemiological relevance and research applications. Infect Genet Evol 2012;12:240-53.
44. Roellig DM, Savage MY, Fujita AW, et al. Genetic variation and exchange in Trypanosoma cruzi isolates from the United States. PLoS One 2013;8:e56198.
45. Murray KO, Saldana MA, Gunter SM, et al. Diagnosis of Acute Chagas Disease in a Belizean Child with Evidence of a Multiclonal Trypanosoma cruzi Infection. Am J Trop Med Hyg 2022;107:992-5.

46. Polonio R, Lopez-Dominguez J, Herrera C, Dumonteil E. Molecular ecology of Triatoma dimidiata in southern Belize reveals risk for human infection and the local differentiation of Trypanosoma cruzi parasites. Int J Infect Dis 2021;108:320-9.
47. Yeo M, Mauricio IL, Messenger LA, et al. Multilocus sequence typing (MLST) for lineage assignment and high resolution diversity studies in Trypanosoma cruzi. PLoS Negl Trop Dis 2011;5:e1049.
48. Garcia MN, Burroughs H, Gorchakov R, et al. Molecular identification and genotyping of Trypanosoma cruzi DNA in autochthonous Chagas disease patients from Texas, USA. Infect Genet Evol 2017;49:151-6.
49. Dumonteil E, Desale H, Tu W, et al. Shelter cats host infections with multiple Trypanosoma cruzi discrete typing units in southern Louisiana. Vet Res 2021;52:53.
50. Dumonteil E, Elmayan A, Majeau A, et al. Genetic diversity of Trypanosoma cruzi parasites infecting dogs in southern Louisiana sheds light on parasite transmission cycles and serological diagnostic performance. PLoS Negl Trop Dis 2020;14:e0008932.
51. Herrera C, Majeau A, Didier P, Falkenstein KP, Dumonteil E. Trypanosoma cruzi diversity in naturally infected nonhuman primates in Louisiana assessed by deep sequencing of the mini-exon gene. Trans R Soc Trop Med Hyg 2019;113:281-6.
52. Herrera CP, Licon MH, Nation CS, Jameson SB, Wesson DM. Genotype diversity of Trypanosoma cruzi in small rodents and Triatoma sanguisuga from a rural area in New Orleans, Louisiana. Parasit Vectors 2015;8:123.
53. Hwang WS, Zhang G, Maslov D, Weirauch C. Infection rates of Triatoma protracta (Uhler) with Trypanosoma cruzi in Southern California and molecular identification of trypanosomes. Am J Trop Med Hyg 2010;83:1020-2.
54. Leiby DA, Nguyen ML, Proctor MC, Townsend RL, Stramer SL. Frequency of Trypanosoma cruzi parasitemia among infected blood donors with a potential association between parasite lineage and transfusion transmission. Transfusion 2017;57:1426-32.
55. Pronovost H, Peterson AC, Chavez BG, Blum MJ, Dumonteil E, Herrera CP. Deep sequencing reveals multiclonality and new discrete typing units of Trypanosoma cruzi in rodents from the southern United States. J Microbiol Immunol Infect 2020;53:622-33.
56. Ledezma AP, Blandon R, Schijman AG, Benatar A, Saldana A, Osuna A. Mixed infections by different Trypanosoma cruzi discrete typing units among Chagas disease patients in an endemic community in Panama. PLoS One 2020;15:e0241921.
57. Murillo-Solano C, Ramos-Ligonio A, Lopez-Monteon A, et al. Diversity of Trypanosoma cruzi parasites infecting Triatoma dimidiata in Central Veracruz, Mexico, and their One Health ecological interactions. Infect Genet Evol 2021;95:105050.
58. Herrera C, Truyens C, Dumonteil E, et al. Phylogenetic Analysis of Trypanosoma cruzi from Pregnant Women and Newborns from Argentina,

Honduras, and Mexico Suggests an Association of Parasite Haplotypes with Congenital Transmission of the Parasite. J Mol Diagn 2019;21:1095-105.
59. Joselin DV, Ignacio M, Angel RM, et al. Multiple Discrete Typing Units of Trypanosoma cruzi Infect Sylvatic Triatoma dimidiata and Panstrongylus rufotuberculatus in Southeast Mexico. Am J Trop Med Hyg 2021;105:1042-9.
60. Lopez-Cancino SA, Tun-Ku E, De la Cruz-Felix HK, et al. Landscape ecology of Trypanosoma cruzi in the southern Yucatan Peninsula. Acta Trop 2015;151:58-72.
61. Ramos-Ligonio A, Torres-Montero J, Lopez-Monteon A, Dumonteil E. Extensive diversity of Trypanosoma cruzi discrete typing units circulating in Triatoma dimidiata from central Veracruz, Mexico. Infect Genet Evol 2012;12:1341-3.
62. Rangel-Gamboa L, Lopez-Garcia L, Moreno-Sanchez F, et al. Trypanosoma cruzi infection associated with atypical clinical manifestation during the acute phase of the Chagas disease. Parasit Vectors 2019;12:506.
63. Rovirosa-Hernandez MJ, Lopez-Monteon A, Garcia-Orduna F, et al. Natural infection with Trypanosoma cruzi in three species of non-human primates in southeastern Mexico: A contribution to reservoir knowledge. Acta Trop 2021;213:105754.
64. Villanueva-Lizama L, Teh-Poot C, Majeau A, Herrera C, Dumonteil E. Molecular Genotyping of Trypanosoma cruzi by Next-Generation Sequencing of the Mini-Exon Gene Reveals Infections With Multiple Parasite Discrete Typing Units in Chagasic Patients From Yucatan, Mexico. J Infect Dis 2019;219:1980-8.
65. Ramirez JD, Hernandez C, Montilla M, et al. First report of human Trypanosoma cruzi infection attributed to TcBat genotype. Zoonoses Public Health 2014;61:477-9.
66. Lima-Cordon RA, Cahan SH, McCann C, et al. Insights from a comprehensive study of Trypanosoma cruzi: A new mitochondrial clade restricted to North and Central America and genetic structure of TcI in the region. PLoS Negl Trop Dis 2021;15:e0010043.
67. Marcili A, Lima L, Cavazzana M, et al. A new genotype of Trypanosoma cruzi associated with bats evidenced by phylogenetic analyses using SSU rDNA, cytochrome b and Histone H2B genes and genotyping based on ITS1 rDNA. Parasitology 2009;136:641-55.
68. Pinto CM, Kalko EK, Cottontail I, Wellinghausen N, Cottontail VM. TcBat a bat-exclusive lineage of Trypanosoma cruzi in the Panama Canal Zone, with comments on its classification and the use of the 18S rRNA gene for lineage identification. Infect Genet Evol 2012;12:1328-32.
69. Anez N, Crisante G. The tissue specific tropism in Trypanosoma cruzi. Is it true? Acta Trop 2021;213:105736.
70. Acosta-Serrano A, Almeida IC, Freitas-Junior LH, Yoshida N, Schenkman S. The mucin-like glycoprotein super-family of Trypanosoma cruzi: structure and biological roles. Mol Biochem Parasitol 2001;114:143-50.
71. Marin-Neto JA, Almeida Filho OC, Pazin-Filho A, Maciel BC. [Indeterminate form of Chagas' disease. Proposal of new diagnostic criteria and

perspectives for early treatment of cardiomyopathy]. Arq Bras Cardiol 2002;79:623-7.
72. Dias JC. The indeterminate form of human chronic Chagas' disease A clinical epidemiological review. Rev Soc Bras Med Trop 1989;22:147-56.
73. Herrera C, Guhl F, Falla A, et al. Genetic Variability and Phylogenetic Relationships within Trypanosoma cruzi I Isolated in Colombia Based on Miniexon Gene Sequences. J Parasitol Res 2009;2009.
74. Lo Presti MS, Esteves BH, Moya D, et al. Circulating Trypanosoma cruzi populations differ from those found in the tissues of the same host during acute experimental infection. Acta Trop 2014;133:98-109.
75. Coura JR, Borges-Pereira J. Chagas disease: 100 years after its discovery. A systemic review. Acta Trop 2010;115:5-13.
76. Bern C, Messenger LA, Whitman JD, Maguire JH. Chagas Disease in the United States: a Public Health Approach. Clinical microbiology reviews 2019;33.
77. Marin-Neto JA, Cunha-Neto E, Maciel BC, Simoes MV. Pathogenesis of chronic Chagas heart disease. Circulation 2007;115:1109-23.
78. Bonney KM, Luthringer DJ, Kim SA, Garg NJ, Engman DM. Pathology and Pathogenesis of Chagas Heart Disease. Annu Rev Pathol 2019;14:421-47.
79. Thompson JM, Habrun CA, Scully CM, et al. Locally Transmitted Trypanosoma cruzi in a Domestic Llama (Lama glama) in a Rural Area of Greater New Orleans, Louisiana, USA. Vector Borne Zoonotic Dis 2021;21:762-8.
80. Anez N, Carrasco H, Parada H, et al. Myocardial parasite persistence in chronic chagasic patients. Am J Trop Med Hyg 1999;60:726-32.
81. Lewis MD, Fortes Francisco A, Taylor MC, et al. Bioluminescence imaging of chronic Trypanosoma cruzi infections reveals tissue-specific parasite dynamics and heart disease in the absence of locally persistent infection. Cell Microbiol 2014;16:1285-300.
82. Buckner FS, Wilson AJ, Van Voorhis WC. Detection of live Trypanosoma cruzi in tissues of infected mice by using histochemical stain for beta-galactosidase. Infect Immun 1999;67:403-9.
83. Andrade ZA, Andrade SG, Sadigursky M. Enhancement of chronic Trypanosoma cruzi myocarditis in dogs treated with low doses of cyclophosphamide. Am J Pathol 1987;127:467-73.
84. Silva JS, Rossi MA. Intensification of acute Trypanosoma cruzi myocarditis in BALB/c mice pretreated with low doses of cyclophosphamide or gamma irradiation. J Exp Pathol (Oxford) 1990;71:33-9.
85. Okumura M, Mester M, Iriya K, Amato Neto V, Gama-Rodrigues J. Effects of immunosuppression and benzonidazole on Trypanosoma cruzi parasitism during experimental acute Chagas' disease. Transplant Proc 1994;26:1587-9.
86. Andrade LO, Machado CR, Chiari E, Pena SD, Macedo AM. Differential tissue distribution of diverse clones of Trypanosoma cruzi in infected mice. Mol Biochem Parasitol 1999;100:163-72.

87. Garcia S, Ramos CO, Senra JF, et al. Treatment with benznidazole during the chronic phase of experimental Chagas' disease decreases cardiac alterations. Antimicrob Agents Chemother 2005;49:1521-8.
88. Bahia MT, de Andrade IM, Martins TA, et al. Fexinidazole: a potential new drug candidate for Chagas disease. PLoS Negl Trop Dis 2012;6:e1870.
89. Andrade ZA, Andrade SG, Sadigursky M, Wenthold RJ, Jr., Hilbert SL, Ferrans VJ. The indeterminate phase of Chagas' disease: ultrastructural characterization of cardiac changes in the canine model. Am J Trop Med Hyg 1997;57:328-36.
90. Kaye PM, Rogers NJ, Curry AJ, Scott JC. Deficient expression of co-stimulatory molecules on Leishmania-infected macrophages. Eur J Immunol 1994;24:2850-4.
91. Fruth U, Solioz N, Louis JA. Leishmania major interferes with antigen presentation by infected macrophages. J Immunol 1993;150:1857-64.
92. Brodskyn CI, DeKrey GK, Titus RG. Influence of costimulatory molecules on immune response to Leishmania major by human cells in vitro. Infect Immun 2001;69:665-72.
93. Urban BC, Ferguson DJ, Pain A, et al. Plasmodium falciparum-infected erythrocytes modulate the maturation of dendritic cells. Nature 1999;400:73-7.
94. Luder CG, Walter W, Beuerle B, Maeurer MJ, Gross U. Toxoplasma gondii down-regulates MHC class II gene expression and antigen presentation by murine macrophages via interference with nuclear translocation of STAT1alpha. Eur J Immunol 2001;31:1475-84.
95. Franco DJ, Vago AR, Chiari E, Meira FC, Galvao LM, Machado CR. Trypanosoma cruzi: mixture of two populations can modify virulence and tissue tropism in rat. Exp Parasitol 2003;104:54-61.
96. Joiner K, Sher A, Gaither T, Hammer C. Evasion of alternative complement pathway by Trypanosoma cruzi results from inefficient binding of factor B. Proc Natl Acad Sci U S A 1986;83:6593-7.
97. Rimoldi MT, Sher A, Heiny S, Lituchy A, Hammer CH, Joiner K. Developmentally regulated expression by Trypanosoma cruzi of molecules that accelerate the decay of complement C3 convertases. Proc Natl Acad Sci U S A 1988;85:193-7.
98. Rimoldi MT, Tenner AJ, Bobak DA, Joiner KA. Complement component C1q enhances invasion of human mononuclear phagocytes and fibroblasts by Trypanosoma cruzi trypomastigotes. J Clin Invest 1989;84:1982-9.
99. Teixeira MM, Gazzinelli RT, Silva JS. Chemokines, inflammation and Trypanosoma cruzi infection. Trends Parasitol 2002;18:262-5.
100. dos Santos PV, Roffe E, Santiago HC, et al. Prevalence of CD8(+)alpha beta T cells in Trypanosoma cruzi-elicited myocarditis is associated with acquisition of CD62L(Low)LFA-1(High)VLA-4(High) activation phenotype and expression of IFN-gamma-inducible adhesion and chemoattractant molecules. Microbes Infect 2001;3:971-84.
101. Florez O, Martin J, Gonzalez CI. Genetic variants in the chemokines and chemokine receptors in Chagas disease. Hum Immunol 2012;73:852-8.

102. Higuchi Mde L, Gutierrez PS, Aiello VD, et al. Immunohistochemical characterization of infiltrating cells in human chronic chagasic myocarditis: comparison with myocardial rejection process. Virchows Arch A Pathol Anat Histopathol 1993;423:157-60.
103. Higuchi MD, Ries MM, Aiello VD, et al. Association of an increase in CD8+ T cells with the presence of Trypanosoma cruzi antigens in chronic, human, chagasic myocarditis. Am J Trop Med Hyg 1997;56:485-9.
104. de Diego J, Punzon C, Duarte M, Fresno M. Alteration of macrophage function by a Trypanosoma cruzi membrane mucin. J Immunol 1997;159:4983-9.
105. Cronemberger-Andrade A, Xander P, Soares RP, et al. Trypanosoma cruzi-Infected Human Macrophages Shed Proinflammatory Extracellular Vesicles That Enhance Host-Cell Invasion via Toll-Like Receptor 2. Front Cell Infect Microbiol 2020;10:99.
106. Amezcua Vesely MC, Rodriguez C, Gruppi A, Acosta Rodriguez EV. Interleukin-17 mediated immunity during infections with Trypanosoma cruzi and other protozoans. Biochim Biophys Acta Mol Basis Dis 2020;1866:165706.
107. Rodriguez-Angulo H, Marques J, Mendoza I, et al. Differential cytokine profiling in Chagasic patients according to their arrhythmogenic-status. BMC Infect Dis 2017;17:221.
108. Reis MM, Higuchi Mde L, Benvenuti LA, et al. An in situ quantitative immunohistochemical study of cytokines and IL-2R+ in chronic human chagasic myocarditis: correlation with the presence of myocardial Trypanosoma cruzi antigens. Clin Immunol Immunopathol 1997;83:165-72.
109. Abrahamsohn IA, Coffman RL. Cytokine and nitric oxide regulation of the immunosuppression in Trypanosoma cruzi infection. J Immunol 1995;155:3955-63.
110. Kierszenbaum F, Cuna WR, Beltz LA, Sztein MB. Trypanosomal immunosuppressive factor: a secretion product(s) of Trypanosoma cruzi that inhibits proliferation and IL-2 receptor expression by activated human peripheral blood mononuclear cells. J Immunol 1990;144:4000-4.
111. Natale MA, Minning T, Albareda MC, et al. Immune exhaustion in chronic Chagas disease: Pro-inflammatory and immunomodulatory action of IL-27 in vitro. PLoS Negl Trop Dis 2021;15:e0009473.
112. Laucella SA, Postan M, Martin D, et al. Frequency of interferon- gamma -producing T cells specific for Trypanosoma cruzi inversely correlates with disease severity in chronic human Chagas disease. J Infect Dis 2004;189:909-18.
113. Vitelli-Avelar DM, Sathler-Avelar R, Teixeira-Carvalho A, et al. Strategy to assess the overall cytokine profile of circulating leukocytes and its association with distinct clinical forms of human Chagas disease. Scand J Immunol 2008;68:516-25.
114. Talvani A, Rocha MO, Barcelos LS, Gomes YM, Ribeiro AL, Teixeira MM. Elevated concentrations of CCL2 and tumor necrosis factor-alpha in chagasic cardiomyopathy. Clin Infect Dis 2004;38:943-50.

115. Ramasawmy R, Cunha-Neto E, Fae KC, et al. The monocyte chemoattractant protein-1 gene polymorphism is associated with cardiomyopathy in human chagas disease. Clin Infect Dis 2006;43:305-11.
116. Curvo EO, Ferreira RR, Madeira FS, et al. Correlation of transforming growth factor-beta1 and tumour necrosis factor levels with left ventricular function in Chagas disease. Mem Inst Oswaldo Cruz 2018;113:e170440.
117. Rodriguez-Perez JM, Cruz-Robles D, Hernandez-Pacheco G, et al. Tumor necrosis factor-alpha promoter polymorphism in Mexican patients with Chagas' disease. Immunol Lett 2005;98:97-102.
118. Campelo V, Dantas RO, Simoes RT, et al. TNF microsatellite alleles in Brazilian Chagasic patients. Dig Dis Sci 2007;52:3334-9.
119. Sousa GR, Gomes JA, Fares RC, et al. Plasma cytokine expression is associated with cardiac morbidity in chagas disease. PLoS One 2014;9:e87082.
120. Guedes PM, Gutierrez FR, Silva GK, et al. Deficient regulatory T cell activity and low frequency of IL-17-producing T cells correlate with the extent of cardiomyopathy in human Chagas' disease. PLoS Negl Trop Dis 2012;6:e1630.
121. Cunha-Neto E, Dzau VJ, Allen PD, et al. Cardiac gene expression profiling provides evidence for cytokinopathy as a molecular mechanism in Chagas' disease cardiomyopathy. Am J Pathol 2005;167:305-13.
122. Sousa GR, Gomes JA, Damasio MP, et al. The role of interleukin 17-mediated immune response in Chagas disease: High level is correlated with better left ventricular function. PLoS One 2017;12:e0172833.
123. Magalhaes LM, Villani FN, Nunes Mdo C, Gollob KJ, Rocha MO, Dutra WO. High interleukin 17 expression is correlated with better cardiac function in human Chagas disease. J Infect Dis 2013;207:661-5.
124. Calzada JE, Nieto A, Beraun Y, Martin J. Chemokine receptor CCR5 polymorphisms and Chagas' disease cardiomyopathy. Tissue Antigens 2001;58:154-8.
125. Medeiros GA, Silverio JC, Marino AP, et al. Treatment of chronically Trypanosoma cruzi-infected mice with a CCR1/CCR5 antagonist (Met-RANTES) results in amelioration of cardiac tissue damage. Microbes Infect 2009;11:264-73.
126. Zafra G, Morillo C, Martin J, Gonzalez A, Gonzalez CI. Polymorphism in the 3' UTR of the IL12B gene is associated with Chagas' disease cardiomyopathy. Microbes Infect 2007;9:1049-52.
127. Costa GC, da Costa Rocha MO, Moreira PR, et al. Functional IL-10 gene polymorphism is associated with Chagas disease cardiomyopathy. J Infect Dis 2009;199:451-4.
128. Calzada JE, Beraun Y, Gonzalez CI, Martin J. Transforming growth factor beta 1 (TGFbeta1) gene polymorphisms and Chagas disease susceptibility in Peruvian and Colombian patients. Cytokine 2009;45:149-53.
129. Araujo-Jorge TC, Waghabi MC, Bailly S, Feige JJ. The TGF-beta pathway as an emerging target for Chagas disease therapy. Clin Pharmacol Ther 2012;92:613-21.

130. Saraiva RM, Waghabi MC, Vilela MF, et al. Predictive value of transforming growth factor-beta1in Chagas disease: towards a biomarker surrogate of clinical outcome. Trans R Soc Trop Med Hyg 2013;107:518-25.
131. Udoko AN, Johnson CA, Dykan A, et al. Early Regulation of Profibrotic Genes in Primary Human Cardiac Myocytes by Trypanosoma cruzi. PLoS Negl Trop Dis 2016;10:e0003747.
132. Gonzalez F, Villar S, D'Attilio L, et al. Dysregulated Network of Immune, Endocrine and Metabolic Markers is Associated to More Severe Human Chronic Chagas Cardiomyopathy. Neuroimmunomodulation 2018;25:119-28.
133. Truyens C, Angelo-Barrios A, Torrico F, Van Damme J, Heremans H, Carlier Y. Interleukin-6 (IL-6) production in mice infected with Trypanosoma cruzi: effect of its paradoxical increase by anti-IL-6 monoclonal antibody treatment on infection and acute-phase and humoral immune responses. Infect Immun 1994;62:692-6.
134. Gutierrez FR, Guedes PM, Gazzinelli RT, Silva JS. The role of parasite persistence in pathogenesis of Chagas heart disease. Parasite Immunol 2009;31:673-85.
135. de Araujo FF, Vitelli-Avelar DM, Teixeira-Carvalho A, et al. Regulatory T cells phenotype in different clinical forms of Chagas' disease. PLoS Negl Trop Dis 2011;5:e992.
136. Kimura A, Kishimoto T. IL-6: regulator of Treg/Th17 balance. Eur J Immunol 2010;40:1830-5.
137. Amatya N, Garg AV, Gaffen SL. IL-17 Signaling: The Yin and the Yang. Trends Immunol 2017;38:310-22.
138. Miyazaki Y, Hamano S, Wang S, Shimanoe Y, Iwakura Y, Yoshida H. IL-17 is necessary for host protection against acute-phase Trypanosoma cruzi infection. J Immunol 2010;185:1150-7.
139. Ma CS, Deenick EK, Batten M, Tangye SG. The origins, function, and regulation of T follicular helper cells. J Exp Med 2012;209:1241-53.
140. Okada M, Kitahara M, Kishimoto S, Matsuda T, Hirano T, Kishimoto T. IL-6/BSF-2 functions as a killer helper factor in the in vitro induction of cytotoxic T cells. J Immunol 1988;141:1543-9.
141. Diehl S, Rincon M. The two faces of IL-6 on Th1/Th2 differentiation. Mol Immunol 2002;39:531-6.
142. Gao W, Pereira MA. Interleukin-6 is required for parasite specific response and host resistance to Trypanosoma cruzi. Int J Parasitol 2002;32:167-70.
143. Van Overtvelt L, Vanderheyde N, Verhasselt V, et al. Trypanosoma cruzi infects human dendritic cells and prevents their maturation: inhibition of cytokines, HLA-DR, and costimulatory molecules. Infect Immun 1999;67:4033-40.
144. Gil-Jaramillo N, Motta FN, Favali CB, Bastos IM, Santana JM. Dendritic Cells: A Double-Edged Sword in Immune Responses during Chagas Disease. Front Microbiol 2016;7:1076.

145. Graefe SE, Jacobs T, Gaworski I, Klauenberg U, Steeg C, Fleischer B. Interleukin-12 but not interleukin-18 is required for immunity to Trypanosoma cruzi in mice. Microbes Infect 2003;5:833-9.
146. Kayama H, Takeda K. The innate immune response to Trypanosoma cruzi infection. Microbes Infect 2010;12:511-7.
147. Zuniga E, Motran C, Montes CL, Diaz FL, Bocco JL, Gruppi A. Trypanosoma cruzi-induced immunosuppression: B cells undergo spontaneous apoptosis and lipopolysaccharide (LPS) arrests their proliferation during acute infection. Clin Exp Immunol 2000;119:507-15.
148. Torrico F, Heremans H, Rivera MT, Van Marck E, Billiau A, Carlier Y. Endogenous IFN-gamma is required for resistance to acute Trypanosoma cruzi infection in mice. J Immunol 1991;146:3626-32.
149. Coelho PS, Klein A, Talvani A, et al. Glycosylphosphatidylinositol-anchored mucin-like glycoproteins isolated from Trypanosoma cruzi trypomastigotes induce in vivo leukocyte recruitment dependent on MCP-1 production by IFN-gamma-primed-macrophages. J Leukoc Biol 2002;71:837-44.
150. Reed SG, Brownell CE, Russo DM, Silva JS, Grabstein KH, Morrissey PJ. IL-10 mediates susceptibility to Trypanosoma cruzi infection. J Immunol 1994;153:3135-40.
151. Silva JS, Morrissey PJ, Grabstein KH, Mohler KM, Anderson D, Reed SG. Interleukin 10 and interferon gamma regulation of experimental Trypanosoma cruzi infection. J Exp Med 1992;175:169-74.
152. Matthews S, Tannis A, Puchner KP, et al. Estimation of the morbidity and mortality of congenital Chagas disease: A systematic review and meta-analysis. PLoS Negl Trop Dis 2022;16:e0010376.
153. Kemmerling U, Osuna A, Schijman AG, Truyens C. Congenital Transmission of Trypanosoma cruzi: A Review About the Interactions Between the Parasite, the Placenta, the Maternal and the Fetal/Neonatal Immune Responses. Front Microbiol 2019;10:1854.
154. Edwards MS, Montgomery SP. Congenital Chagas disease: progress toward implementation of pregnancy-based screening. Curr Opin Infect Dis 2021;34:538-45.
155. Kumar M, Saadaoui M, Al Khodor S. Infections and Pregnancy: Effects on Maternal and Child Health. Front Cell Infect Microbiol 2022;12:873253.
156. Megli CJ, Coyne CB. Infections at the maternal-fetal interface: an overview of pathogenesis and defence. Nat Rev Microbiol 2022;20:67-82.
157. Jash S, Sharma S. Pathogenic Infections during Pregnancy and the Consequences for Fetal Brain Development. Pathogens 2022;11.
158. Rios L, Campos EE, Menon R, Zago MP, Garg NJ. Epidemiology and pathogenesis of maternal-fetal transmission of Trypanosoma cruzi and a case for vaccine development against congenital Chagas disease. Biochim Biophys Acta Mol Basis Dis 2020;1866:165591.
159. Carlier Y, Sosa-Estani S, Luquetti AO, Buekens P. Congenital Chagas disease: an update. Mem Inst Oswaldo Cruz 2015;110:363-8.
160. Messenger LA, Bern C. Congenital Chagas disease: current diagnostics, limitations and future perspectives. Curr Opin Infect Dis 2018;31:415-21.

161. Messenger LA, Gilman RH, Verastegui M, et al. Toward Improving Early Diagnosis of Congenital Chagas Disease in an Endemic Setting. Clin Infect Dis 2017;65:268-75.
162. Oliveira AER, Grazielle-Silva V, Ferreira LRP, Teixeira SMR. Close encounters between Trypanosoma cruzi and the host mammalian cell: Lessons from genome-wide expression studies. Genomics 2020;112:990-7.
163. Lowe R, Shirley N, Bleackley M, Dolan S, Shafee T. Transcriptomics technologies. PLoS Comput Biol 2017;13:e1005457.
164. Libisch MG, Rego N, Díaz-Viraqué F, Robello C. Host-pathogen transcriptomics: Trypanosoma cruzi as a model for studying RNA contamination. J Proteomics 2020;223:103804.
165. Hart SN, Therneau TM, Zhang Y, Poland GA, Kocher JP. Calculating sample size estimates for RNA sequencing data. J Comput Biol 2013;20:970-8.
166. Stoler N, Nekrutenko A. Sequencing error profiles of Illumina sequencing instruments. NAR Genom Bioinform 2021;3:lqab019.
167. Dobin A, Davis CA, Schlesinger F, et al. STAR: ultrafast universal RNA-seq aligner. Bioinformatics 2013;29:15-21.
168. Zhang Y, Parmigiani G, Johnson WE. ComBat-seq: batch effect adjustment for RNA-seq count data. NAR Genom Bioinform 2020;2:lqaa078.
169. Love MI, Huber W, Anders S. Moderated estimation of fold change and dispersion for RNA-seq data with DESeq2. Genome Biol 2014;15:550.
170. Zhu A, Ibrahim JG, Love MI. Heavy-tailed prior distributions for sequence count data: removing the noise and preserving large differences. Bioinformatics 2019;35:2084-92.
171. R: A language and environment for statistical computing. 2021. at https://www.R-project.org/.)
172. Yu G, Wang LG, Han Y, He QY. clusterProfiler: an R package for comparing biological themes among gene clusters. OMICS 2012;16:284-7.
173. Ge SX, Jung D, Yao R. ShinyGO: a graphical gene-set enrichment tool for animals and plants. Bioinformatics 2020;36:2628-9.
174. Ashburner M, Ball CA, Blake JA, et al. Gene ontology: tool for the unification of biology. The Gene Ontology Consortium. Nat Genet 2000;25:25-9.
175. Gene Ontology C. The Gene Ontology resource: enriching a GOld mine. Nucleic Acids Res 2021;49:D325-D34.
176. Kanehisa M, Furumichi M, Sato Y, Ishiguro-Watanabe M, Tanabe M. KEGG: integrating viruses and cellular organisms. Nucleic Acids Res 2021;49:D545-D51.
177. Luo W, Brouwer C. Pathview: an R/Bioconductor package for pathway-based data integration and visualization. Bioinformatics 2013;29:1830-1.
178. Culhane AC, Thioulouse J, Perriere G, Higgins DG. MADE4: an R package for multivariate analysis of gene expression data. Bioinformatics 2005;21:2789-90.
179. Abel LC, Ferreira LR, Cunha Navarro I, et al. Induction of IL-12 production in human peripheral monocytes by Trypanosoma cruzi Is mediated by glycosylphosphatidylinositol-anchored mucin-like glycoproteins and

potentiated by IFN- gamma and CD40-CD40L interactions. Mediators Inflamm 2014;2014:345659.
180. Eickhoff CS, Vasconcelos JR, Sullivan NL, et al. Co-administration of a plasmid DNA encoding IL-15 improves long-term protection of a genetic vaccine against Trypanosoma cruzi. PLoS Negl Trop Dis 2011;5:e983.
181. Neves EGA, Koh CC, Souza-Silva TG, et al. T-Cell Subpopulations Exhibit Distinct Recruitment Potential, Immunoregulatory Profile and Functional Characteristics in Chagas versus Idiopathic Dilated Cardiomyopathies. Front Cardiovasc Med 2022;9:787423.
182. Barros JF, Waclawiak I, Pecli C, et al. Role of Chemokine Receptor CCR4 and Regulatory T Cells in Wound Healing of Diabetic Mice. J Invest Dermatol 2019;139:1161-70.
183. Abad Dar M, Holscher C. Arginase-1 Is Responsible for IL-13-Mediated Susceptibility to Trypanosoma cruzi Infection. Front Immunol 2018;9:2790.
184. Bermejo DA, Jackson SW, Gorosito-Serran M, et al. Trypanosoma cruzi trans-sialidase initiates a program independent of the transcription factors RORgammat and Ahr that leads to IL-17 production by activated B cells. Nat Immunol 2013;14:514-22.
185. Menezes CA, Rocha MO, Souza PE, Chaves AC, Gollob KJ, Dutra WO. Phenotypic and functional characteristics of CD28+ and CD28- cells from chagasic patients: distinct repertoire and cytokine expression. Clin Exp Immunol 2004;137:129-38.
186. Dutra WO, Martins-Filho OA, Cancado JR, et al. Chagasic patients lack CD28 expression on many of their circulating T lymphocytes. Scand J Immunol 1996;43:88-93.
187. Altcheh JM, Freilij H. Chagas Disease : A Clinical Approach. Birkhäuser Advances in Infectious Diseases,. 1st ed. Cham: Springer International Publishing : Imprint: Springer,; 2019:1 online resource (XII, 356 pages 48 illustrations, 34 illustrations in color.
188. Nohaile M. The biomarker is not the end. Drug Discov Today 2011;16:878-83.
189. Bustamante JM, Bixby LM, Tarleton RL. Drug-induced cure drives conversion to a stable and protective CD8+ T central memory response in chronic Chagas disease. Nat Med 2008;14:542-50.
190. Pinazo MJ, Thomas MC, Bustamante J, Almeida IC, Lopez MC, Gascon J. Biomarkers of therapeutic responses in chronic Chagas disease: state of the art and future perspectives. Mem Inst Oswaldo Cruz 2015;110:422-32.
191. Chen S, Zhou Y, Chen Y, Gu J. fastp: an ultra-fast all-in-one FASTQ preprocessor. Bioinformatics 2018;34:i884-i90.
192. Karlsson M, Zhang C, Mear L, et al. A single-cell type transcriptomics map of human tissues. Sci Adv 2021;7.
193. Nolte MA, van Olffen RW, van Gisbergen KP, van Lier RA. Timing and tuning of CD27-CD70 interactions: the impact of signal strength in setting the balance between adaptive responses and immunopathology. Immunol Rev 2009;229:216-31.

194. Ruiz-Lancheros E, Golizeh M, Ndao M. Apolipoprotein A1 and Fibronectin Fragments as Markers of Cure for the Chagas Disease. Methods Mol Biol 2019;1955:263-73.
195. Ramasawmy R, Fae KC, Cunha-Neto E, et al. Polymorphisms in the gene for lymphotoxin-alpha predispose to chronic Chagas cardiomyopathy. J Infect Dis 2007;196:1836-43.
196. Nisimura LM, Coelho LL, de Melo TG, et al. Trypanosoma cruzi Promotes Transcriptomic Remodeling of the JAK/STAT Signaling and Cell Cycle Pathways in Myoblasts. Front Cell Infect Microbiol 2020;10:255.
197. Chou JP, Ramirez CM, Wu JE, Effros RB. Accelerated aging in HIV/AIDS: novel biomarkers of senescent human CD8+ T cells. PLoS One 2013;8:e64702.
198. Kim J, Beidler P, Wang H, et al. Desmoglein-2 as a prognostic and biomarker in ovarian cancer. Cancer Biol Ther 2020;21:1154-62.
199. Alba Soto CD, Mirkin GA, Solana ME, Gonzalez Cappa SM. Trypanosoma cruzi infection modulates in vivo expression of major histocompatibility complex class II molecules on antigen-presenting cells and T-cell stimulatory activity of dendritic cells in a strain-dependent manner. Infect Immun 2003;71:1194-9.
200. Martins HR, Toledo MJ, Veloso VM, et al. Trypanosoma cruzi: Impact of dual-clone infections on parasite biological properties in BALB/c mice. Exp Parasitol 2006;112:237-46.
201. Ragone PG, Perez Brandan C, Monje Rumi M, et al. Experimental evidence of biological interactions among different isolates of Trypanosoma cruzi from the Chaco Region. PLoS One 2015;10:e0119866.
202. Sanchez-Guillen Mdel C, Bernabe C, Tibayrenc M, et al. Trypanosoma cruzi strains isolated from human, vector, and animal reservoir in the same endemic region in Mexico and typed as T. cruzi I, discrete typing unit 1 exhibit considerable biological diversity. Mem Inst Oswaldo Cruz 2006;101:585-90.
203. Anez N, Crisante G, da Silva FM, et al. Predominance of lineage I among Trypanosoma cruzi isolates from Venezuelan patients with different clinical profiles of acute Chagas' disease. Trop Med Int Health 2004;9:1319-26.
204. Messenger LA, Miles MA, Bern C. Between a bug and a hard place: Trypanosoma cruzi genetic diversity and the clinical outcomes of Chagas disease. Expert Rev Anti Infect Ther 2015;13:995-1029.
205. Barth E, Kundrotas L. Megacolon from Chagas disease in an ancient Texan. Diagnosis: Chagas disease causing mega-disease, in this case megacolon. Gastroenterology 2011;141:35-404.
206. del Puerto R, Nishizawa JE, Kikuchi M, et al. Lineage analysis of circulating Trypanosoma cruzi parasites and their association with clinical forms of Chagas disease in Bolivia. PLoS Negl Trop Dis 2010;4:e687.
207. Florez O, Esper J, Higuera S, et al. Chagasic megacolon associated with Trypanosoma cruzi I in a Colombian patient. Parasitol Res 2010;107:439-42.
208. Panesso-Gomez S, Pavia P, Rodriguez-Mantilla IE, et al. Trypanosoma cruzi Detection in Colombian Patients with a Diagnosis of Esophageal Achalasia. Am J Trop Med Hyg 2018;98:717-23.

209. Desale H, Buekens P, Alger J, et al. Epigenetic signature of exposure to maternal Trypanosoma cruzi infection in cord blood cells from uninfected newborns. Epigenomics 2022;14:913-27.
210. WHO. Chagas disease in Latin America: an epidemiological update based on 2010 estimates. Wkly Epidemiol Rec 2015;90:33-43.
211. Rassi A, Jr., Rassi A, Marin-Neto JA. Chagas disease. Lancet 2010;375:1388-402.
212. Pereira Nunes MC, Beaton A, Acquatella H, et al. Chagas cardiomyopathy: An update of current clinical knowledge and management. A scientific statement from the American Heart Association. Circulation 2018;138.
213. Bern C. Chagas' Disease. N Engl J Med 2015;373:456-66.
214. Howard EJ, Xiong X, Carlier Y, Sosa-Estani S, Buekens P. Frequency of the congenital transmission of Trypanosoma cruzi: a systematic review and meta-analysis. BJOG 2014;121:22-33.
215. Howard EJ, Buekens P, Carlier Y. Current treatment guidelines for Trypanosoma cruzi infection in pregnant women and infants. Int J Antimicrob Agents 2012;39:451-2.
216. Buekens P, Cafferata ML, Alger J, et al. Congenital Transmission of *Trypanosoma cruzi* in Argentina, Honduras, and Mexico: An Observational Prospective Study. The American journal of tropical medicine and hygiene 2018;98:478-85.
217. Carlier Y, Truyens C. Congenital Chagas disease as an ecological model of interactions between Trypanosoma cruzi parasites, pregnant women, placenta and fetuses. Acta Trop 2015;151:103-15.
218. Cameron N, Demerath EW. Critical periods in human growth and their relationship to diseases of aging. Am J Phys Anthropol 2002;Suppl 35:159-84.
219. Barker DJ. Fetal origins of coronary heart disease. BMJ (Clinical research ed) 1995;311:171-4.
220. Barker DJ, Eriksson JG, Forsen T, Osmond C. Fetal origins of adult disease: strength of effects and biological basis. International journal of epidemiology 2002;31:1235-9.
221. Penkler M, Hanson M, Biesma R, Muller R. DOHaD in science and society: emergent opportunities and novel responsibilities. J Dev Orig Health Dis 2019;10:268-73.
222. Francis DD. Conceptualizing child health disparities: a role for developmental neurogenomics. Pediatrics 2009;124 Suppl 3:S196-202.
223. Pepin ME, Drakos S, Ha CM, et al. DNA methylation reprograms cardiac metabolic gene expression in end-stage human heart failure. Am J Physiol Heart Circ Physiol 2019;317:H674-H84.
224. Glezeva N, Moran B, Collier P, et al. Targeted DNA Methylation Profiling of Human Cardiac Tissue Reveals Novel Epigenetic Traits and Gene Deregulation Across Different Heart Failure Patient Subtypes. Circ Heart Fail 2019;12:e005765.
225. Richetto J, Massart R, Weber-Stadlbauer U, Szyf M, Riva MA, Meyer U. Genome-wide DNA Methylation Changes in a Mouse Model of Infection-Mediated Neurodevelopmental Disorders. Biol Psychiatry 2017;81:265-76.

226. Cheng Q, Zhao B, Huang Z, et al. Epigenome-wide study for the offspring exposed to maternal HBV infection during pregnancy, a pilot study. Gene 2018;658:76-85.
227. Weber-Stadlbauer U. Epigenetic and transgenerational mechanisms in infection-mediated neurodevelopmental disorders. Transl Psychiatry 2017;7:e1113.
228. Neves SF, Eloi-Santos S, Ramos R, Rigueirinho S, Gazzinelli G, Correa-Oliveira R. In utero sensitization in Chagas' disease leads to altered lymphocyte phenotypic patterns in the newborn cord blood mononuclear cells. Parasite Immunol 1999;21:631-9.
229. Dauby N, Alonso-Vega C, Suarez E, et al. Maternal infection with Trypanosoma cruzi and congenital Chagas disease induce a trend to a type 1 polarization of infant immune responses to vaccines. PLoS Negl Trop Dis 2009;3:e571.
230. Sosa-Estani S, Gamboa-Leon MR, Del Cid-Lemus J, et al. Use of a rapid test on umbilical cord blood to screen for *Trypanosoma cruzi* infection in pregnant women in Argentina, Bolivia, Honduras, and Mexico. The American journal of tropical medicine and hygiene 2008;79:755-9.
231. Pidsley R, Zotenko E, Peters TJ, et al. Critical evaluation of the Illumina MethylationEPIC BeadChip microarray for whole-genome DNA methylation profiling. Genome Biol 2016;17:208.
232. Aryee MJ, Jaffe AE, Corrada-Bravo H, et al. Minfi: a flexible and comprehensive Bioconductor package for the analysis of Infinium DNA methylation microarrays. Bioinformatics 2014;30:1363-9.
233. Morris TJ, Butcher LM, Feber A, et al. ChAMP: 450k Chip Analysis Methylation Pipeline. Bioinformatics 2014;30:428-30.
234. Rahmani E, Schweiger R, Rhead B, et al. Cell-type-specific resolution epigenetics without the need for cell sorting or single-cell biology. Nat Commun 2019;10:3417.
235. Neves SPF, Elr i-Santos SM, Ramos RA, Rigueirinho S, Gazzinelli G, CorrÍa-Oliveira R. In utero sensitization in Chagas' disease leads to altered lymphocyte phenotypic patterns in the newborn cord blood mononuclear cells. Parasite Immunology 1999;21.
236. Rahmani E, Zaitlen N, Baran Y, et al. Sparse PCA corrects for cell type heterogeneity in epigenome-wide association studies. Nat Methods 2016;13:443-5.
237. Zheng SC, Breeze CE, Beck S, Teschendorff AE. Identification of differentially methylated cell types in epigenome-wide association studies. Nat Methods 2018;15:1059-66.
238. Lin X, Tan JYL, Teh AL, et al. Cell type-specific DNA methylation in neonatal cord tissue and cord blood: a 850K-reference panel and comparison of cell types. Epigenetics 2018;13:941-58.
239. Ren X, Kuan PF. methylGSA: a Bioconductor package and Shiny app for DNA methylation data length bias adjustment in gene set testing. Bioinformatics 2019;35:1958-9.

240. Szklarczyk D, Gable AL, Nastou KC, et al. The STRING database in 2021: customizable protein-protein networks, and functional characterization of user-uploaded gene/measurement sets. Nucleic Acids Res 2021;49:D605-D12.
241. Nouatin O, Gbedande K, Ibitokou S, et al. Infants' Peripheral Blood Lymphocyte Composition Reflects Both Maternal and Post-Natal Infection with Plasmodium falciparum. PLoS One 2015;10:e0139606.
242. da Paz VRF, Sequeira D, Pyrrho A. Infection by Schistosoma mansoni during pregnancy: Effects on offspring immunity. Life Sci 2017;185:46-52.
243. Jaime-Perez JC, Colunga-Pedraza JE, Monreal-Robles R, et al. Acute maternal cytomegalovirus infection is associated with significantly decreased numbers of CD34+ cells in umbilical cord blood. Blood Cells Mol Dis 2012;49:166-9.
244. Borges-Almeida E, Milanez HM, Vilela MM, et al. The impact of maternal HIV infection on cord blood lymphocyte subsets and cytokine profile in exposed non-infected newborns. BMC Infect Dis 2011;11:38.
245. Abioye AI, McDonald EA, Park S, et al. Maternal, placental and cord blood cytokines and the risk of adverse birth outcomes among pregnant women infected with Schistosoma japonicum in the Philippines. PLoS Negl Trop Dis 2019;13:e0007371.
246. Miles DJ, Gadama L, Gumbi A, Nyalo F, Makanani B, Heyderman RS. Human immunodeficiency virus (HIV) infection during pregnancy induces CD4 T-cell differentiation and modulates responses to Bacille Calmette-Guerin (BCG) vaccine in HIV-uninfected infants. Immunology 2010;129:446-54.
247. Rose DR, Careaga M, Van de Water J, McAllister K, Bauman MD, Ashwood P. Long-term altered immune responses following fetal priming in a non-human primate model of maternal immune activation. Brain Behav Immun 2017;63:60-70.
248. Mueller FS, Scarborough J, Schalbetter SM, et al. Behavioral, neuroanatomical, and molecular correlates of resilience and susceptibility to maternal immune activation. Mol Psychiatry 2021;26:396-410.
249. Klar K, Perchermeier S, Bhattacharjee S, et al. Chronic schistosomiasis during pregnancy epigenetically reprograms T-cell differentiation in offspring of infected mothers. Eur J Immunol 2017;47:841-7.
250. Alfano R, Guida F, Galobardes B, et al. Socioeconomic position during pregnancy and DNA methylation signatures at three stages across early life: epigenome-wide association studies in the ALSPAC birth cohort. Int J Epidemiol 2019;48:30-44.
251. Kupers LK, Monnereau C, Sharp GC, et al. Meta-analysis of epigenome-wide association studies in neonates reveals widespread differential DNA methylation associated with birthweight. Nat Commun 2019;10:1893.
252. de Goede OM, Lavoie PM, Robinson WP. Cord blood hematopoietic cells from preterm infants display altered DNA methylation patterns. Clin Epigenetics 2017;9:39.
253. Merid SK, Novoloaca A, Sharp GC, et al. Epigenome-wide meta-analysis of blood DNA methylation in newborns and children identifies numerous loci related to gestational age. Genome Med 2020;12:25.

254. Barcelona V, Huang Y, Brown K, et al. Novel DNA methylation sites associated with cigarette smoking among African Americans. Epigenetics 2019;14:383-91.
255. Hannon E, Schendel D, Ladd-Acosta C, et al. Variable DNA methylation in neonates mediates the association between prenatal smoking and birth weight. Philosophical transactions of the Royal Society of London Series B, Biological sciences 2019;374:20180120.
256. Haertle L, El Hajj N, Dittrich M, et al. Epigenetic signatures of gestational diabetes mellitus on cord blood methylation. Clin Epigenetics 2017;9:28.
257. Kazmi N, Sharp GC, Reese SE, et al. Hypertensive Disorders of Pregnancy and DNA Methylation in Newborns. Hypertension 2019;74:375-83.
258. Linner A, Almgren M. Epigenetic programming-The important first 1000 days. Acta Paediatr 2020;109:443-52.
259. Shiau S, Strehlau R, Wang S, et al. Distinct epigenetic profiles in children with perinatally-acquired HIV on antiretroviral therapy. Sci Rep 2019;9:10495.
260. Bermick J, Schaller M. Epigenetic regulation of pediatric and neonatal immune responses. Pediatr Res 2021.